Development of new signal analysis methods as preoperative predictors of the Cox-Maze procedure outcome in atrial fibrillation

Antonio Hernández Alonso

TUTOR: José Joaquín Rieta Ibáñez
COTUTOR: Raúl Alcaraz Martínez
COTUTOR: Fernando Hornero Sos

Valencia, July 2017
Doctoral Thesis

DEPARTMENT OF ELECTRONIC ENGINEERING
UNIVERSIDAD POLITÉCNICA DE VALENCIA

UNIVERSIDAD
POLITECNICA
DE VALENCIA

Abstract

Atrial Fibrillation (AF) is most commonly diagnosed cardiac arrhythmia in clinical practice, affecting up to 1% of the general population. Considering its prevalence with age, this arrhythmia affects up to 10% of the population older than 80. This arrhythmia is characterized by the uncoordinated atrial electrical activation, causing an irregular atrial contraction. As a consequence, the atria is unable to pump blood efficiently increasing the likelihood of developing blood clots in the atria, and therefore, the risk of thromboembolic events increases. As a result, AF is directly related to stroke, with an overall incidence of 20% per year of all strokes and an increase of 5 times the risk of the general population without AF.

Different hypotheses have been proposed to explain AF, however, the physiological mechanisms causing its initiation and maintenance are still not fully understood. To date, the most widely accepted theory to explain AF mechanisms is based on the continuous propagation of multiple wavelets wandering throughout the atria. The fractionation of the wave fronts as they propagate results in self-perpetuating independent wavelets called reentries. The number of simultaneous reentries depends on the refractory period, mass and conduction velocity along the atria. Therefore, structural and electrophysiological remodeling are directly related to its development and perpetuation. In consequence, its quantification its considered as a helpful clinical tool in AF assessment. Traditionally, clinicians have quantified indirectly the atrial remodeling by means of different clinical information. Nonetheless, there is a lack of studies that with the use of surface electrocardiogram (ECG) recordings are able to quantify atrial remodeling as well as to provide preoperative valuable clinical information in the study of AF treatments, such as the Cox-Maze surgery. Although alternative techniques, such as catheter ablation, have been introduced for the treatment of AF, Cox-Maze surgery is still the therapy with the highest success rate. Mid and long-term outcome prediction of this procedure based on clinical parameters has been studied in previous works. However, none of them made use of the surface ECG as a prediction tool and they all reported limited mid-term predictive ability. To this respect, simple and accurate mid-term predictive methods could avoid aggressive pharmacologic treatments in patients with positive AF-free prognostic. Moreover, it will also serve to anticipate electrical cardioversion in patients at high risk of AF recidivity, thus avoiding AF perpetuation.

In the present thesis, preoperative information from the surface ECG is analyzed to quantify electroanatomic remodeling in AF as well as to predict the patient's rhythm after Cox-Maze surgery at different follow up perdiods: discharge, three, six and twelve months after surgery. Three aspects have been studied: the dominant atrial frequency (DAF), the pattern repetitiveness in the atrial activity via sample entropy (SampEn) and the fibrillatory waves mean power (fWP). Furthermore, this information has been compared and combined, by means of developing prediction models, with patient's clinical information. Specifically with widely used clinical parameters such as age, AF duration and left atrial size (LA size) and, additionally, a common indicator of cardiac risk such as wight and BMI.

The reported results pointed that ECG analysis provided more useful information than the provided by the clinical parameters analysis. In fact, while all ECG indices reported statistically significant results, from clinical indices only AF duration found statistically significant differences between AF and normal sinus rhythm (NSR) groups. Additionally, ECG predictions were more accurate than the clinical predictions, where only AF duration exceeded 70% accuracy. Thus, despite being traditionally underused, ECG analysis could be useful to define a valuable tool to analyze AF and help to preditc the outcome of its surgical ablation. As a matter of fact, ECG analysis could provide new ways of quantifying the atrial remodelling and, in consequence, generate new methods to analyze AF causes and mechanisms.

On the other hand, through the generation of prediction models combining ECG and clinical information, accuracies over 90% were yielded in each follow up period.

In conclusion, this work has demonstrate that, by including the ECG information to the AF analysis, a reliable tool to predict preoperatively the Cox-Maze surgery outcome could be performed. In fact, the results yielded in this Thesis outperformed the current methods known which use clinical information. Furthermore, ECG analysis also could contribute to develop new ways to understand AF causes and mechanisms.

Resumen

La fibrilación auricular (FA) es la arritmia cardiaca más comúnmente encontrada en la práctica clínica diaria, afectando al 1% de la población global. Su prevalencia aumenta con la edad, llegando a ser del 10% en la población mayor de 80 años. Esta arritmia se caracteriza por una activación eléctrica descoordinada en las aurículas, causando que éstas se contraigan de manera irregular. Como resultado, la aurícula es incapaz de bombear sangre eficientemente, incrementando, de este modo, la probabilidad de que se produzcan coágulos y, por tanto, aumentando el riesgo de sufrir un accidente cerebrovascular. En consecuencia, la FA está relacionada directamente con el ictus, con una incidencia del 20% de los episodios anuales y multiplicando por 5 el riesgo de sufrirlo frente a la población sin FA.

Se han propuesto diferentes hipótesis para entender la FA, sin embargo, todavía no se comprenden completamente los mecanismos fisiológicos que causan el inicio y la perpetuación de la FA. Hasta la fecha, la teoría más aceptada para explicar los mecanismos de la FA se basa en la existencia de múltiples frentes de propagación que recorren el tejido auricular. La división de estos frentes mientras se propagan resultan en ondas independientes conocidas como reentradas. La cantidad de reentradas que se pueden propagar simultáneamente depende del periodo refractario, de la masa y de la velocidad de conducción de las aurículas. Por tanto, el remodelado estructural y electrofisiológico estaría directamente relacionado con la perpetuación de estas ondas, y por tanto de la FA. En consecuencia, la cuantificación del remodelado auricular es considerado como una herramienta útil en el estudio clínico de la FA. Tradicionalmente, los médicos han cuantificado indirectamente el remodelado auricular haciendo uso de diferente información clínica. Sin embargo, hay una falta de estudios que hagan uso de los registros electrocardiográficos (ECG) para cuantificar el remodelado auricular, así como, para obtener información valiosa en el estudio de los distintos tratamientos de la FA, como podría ser la cirugía Cox-Maze. A pesar de que se han introducido distintas técnicas, como la ablación por catéter, para el tratamiento de la FA, la cirugía Cox-Maze sigue siendo la terapia con mayor índice de éxito. Hay muchos estudios previous, enfocados en predecir el resultado de a cirugía Cox-Maze a medio y largo plazo analizando la información clínica. Por contra, pocos estudios se enfocan en un análisis consistente del ECG como herramienta de predicción.

En este sentido, una herramienta fácil de usar que proveyera predicciones precisas a medio plazo podría evitar tratamientos farmacológicos agresivos en pacientes con gran probabilidad de revertir la FA. Además, también serviría para preparar con antelación la electro cardioversión en pacientes con probabilidad de recaer en FA, reduciendo de esta manera, las posibilidades de mantener la FA.

En esta Tesis, se analiza información de ECG preoperatorios para cuantificar el remodelado auricular, así como para predecir el ritmo de los pacientes en diferentes periodos de evaluación: en el momento del alta, tres, seis y doce meses después de la cirugía. Para ello, se han analizado tres aspectos diferentes: la frecuencia auricular dominante (DAF), la repetitividad de la actividad auricular usando la entropía muestral (SampEn) y la potencia media de las ondas fibrilatorias (fWP). Adicionalmente, esta información se ha comparado y combinado, mediante el desarrollo de modelos de predicción, con la información clínica de los pacientes. Concretamente con parámetros clínicos ampliamente usados en el análisis de la FA como la edad, el tiempo en FA y el tamaño de la aurícula izquierda. Asimismo, se ha analizado también un indicador común de riesgo cardíaco como es el peso o Índice de Masa Corporal.

Los resultados obtenidos señalan que el análisis del ECG proporcionó información más útil que la obtenida al analizar los parámetros clínicos. De hecho, mientras todos los índices electrocardiográficos reportaron diferencias estadísticamente significativas, de los parámetros clínicos, solo la duración de la FA obtuvo diferencias estadísticamente significativas entre los grupos que mantuvieron la FA y los que recuperaron el ritmo sinusal normal. Además, las predicciones llevadas a cabo con el análisis del ECG fueron más precisas que las obtenidas con los índices clínicos, donde solo la duración de la FA superó el 70%. Por tanto, a pesar de haber sido tradicionalmente infrautilizado, el análisis del ECG sería útil para generar una herramienta valiosa a la hora de analizar la FA y ayudar a predecir preoperatoriamente el resultado de la ablación quirúrgica de ésta. De hecho, el análisis del ECG podría proporcionar nuevos maneras de cuantificar el remodelado auricular y, en consecuencia, proveer de nuevas vías de estudio para analizar las causas y mecanismos de la FA.

Por otro lado, el objetivo principal de esta Tesis doctoral se consiguió al combinar la información electrocardiográfica con la clínica mediante modelos de predicción. Dichos modelos sobrepasaron el 90% de precisión en sus predicciones en cada seguimiento analizado.

En conclusión, este trabajo ha demostrado que, incluyendo la información contenida en el ECG al análisis de la FA, se puede desarrollar una herramienta fiable a la hora de predecir preoperatoriamente el resultado de la cirugía Cox-Maze. De hecho, los resultados alcanzados en esta Tesis han superado los métodos usados tradicionalmente mediante el análisis de la información clínica del paciente. Además, el análisis del ECG también podría contribuir a desarrollar nuevas maneras de entender las causas y mecanismos de la FA.

Resum

La fibril·lació auricular (FA) és l'arítmia cardíaca més comunament trobada en la pràctica clínica diària, afectant el 1% de la població global. La seua prevalença augmenta amb l'edat, arribant a ser del 10% en la població major de 80 anys. Esta arítmia es caracteritza per una activació elèctrica descoordinada en les aurícules, causant que estes es contraguen de manera irregular. Com resultat, l'aurícula és incapaç de bombar sang eficientment, incrementant, d'esta manera, la probabilitat que es produïsquen coàguls i, per tant, augmentant el risc de patir un accident cerebrovascular. En conseqüència, la FA està relacionada directament amb l'ictus, amb una incidència del 20% dels episodis anuals i multiplicant per 5 el risc de patir-ho enfront de la població sense FA.

S'han proposat diferents hipòtesis per a entendre la FA, no obstant això, encara no es comprenen completament els mecanismes fisiològics que causen l'inici i la perpetuació de la FA. Fins a la data, la teoria més acceptada per a explicar els mecanismes de la FA es basa en l'existència de múltiples fronts de propagació que recorren el teixit auricular. La divisió d'estos fronts mentres es propaguen resulten en ones independents conegudes com reentrades. La quantitat de reentrades que es poden propagar simultàniament depén del període refractari, de la massa i de la velocitat de conducció de les aurícules. Per tant, el remodelat estructural i electrofisiològic estaria directament relacionat amb la perpetuació d'estes ones, i per tant de la FA. En conseqüència, la quantificació del remodelat auricular és considerat com una ferramenta útil en l'estudi clínic de la FA. Tradicionalment, els metges han quantificat indirectament el remodelat auricular fent ús de diferent informació clínica. No obstant això, hi ha una falta d'estudis que facen ús dels registres electrocardiogràfics (ECG) per a quantificar el remodelat auricular, així com, per a obtindre informació valuosa en l'estudi dels distints tractaments de la FA, com podria ser la cirurgia Cox-Maze. A pesar que s'han introduït distintes tècniques, com l'ablació per catèter, per al tractament de la FA, la cirurgia Cox-Maze continua sent la teràpia amb major índex d'èxit. Hi ha molts estudis previous, enfocats a predir el resultat de a cirurgia Cox-Maze a mitjà i llarg termini analitzant la informació clínica. Per contra, pocs estudis s'enfoquen en una anàlisi consistent de l'ECG com a ferramenta de predicció. En este sentit, una ferramenta fàcil d'usar que proveïra prediccions precises a mitjà termini podria evitar tractaments farmacològics agressius en pacients amb gran probabilitat de

revertir la FA. A més, també serviria per a preparar amb antelació l'electro cardioversió en pacients amb probabilitat de recaure en FA, reduint d'esta manera, les possibilitats de mantindre la FA.

En esta tesi, s'analitza informació d'ECG preoperatoris per a quantificar el remodelat auricular, així com per a predir el ritme dels pacients en diferents períodes d'avaluació: en el moment de l'alta, tres, sis i dotze mesos després de la cirurgia. Per a això, s'han analitzat tres aspectes diferents: la freqüència auricular dominant (DAF) , la repetitivitat de l'activitat auricular usant l'entropia mostral (SampEn) i la potència mitjana de les ones fibrilatories (fWP) . Addicionalment, esta informació s'ha comparat i combinat, per mitjà del desenrotllament de models de predicció, amb la informació clínica dels pacients. Concretament amb paràmetres clínics àmpliament usats en l'anàlisi de la FA com l'edat, el temps en FA i la grandària de l'aurícula esquerra. Així mateix, s'ha analitzat també un indicador comú de risc cardíac com és el pes o IMC.

Els resultats obtinguts assenyalen que l'anàlisi de l'ECG va proporcionar informació més útil que l'obtinguda a l'analitzar els paràmetres clínics. De fet, mentres tots els índexs electrocardiogràfics van reportar diferències estadísticament significatives, dels paràmetres clínics, només la duració de la FA va obtindre diferències estadísticament significatives entre els grups que van mantindre la FA i els que van recuperar el ritme sinusal normal. A més, les prediccions dutes a terme amb l'anàlisi de l'ECG van ser més precises que les obtingudes amb els índexs clínics, on només la duració de la FA va superar el 70%. Per tant, a pesar d'haver sigut tradicionalment infrautilitzat, l'anàlisi de l'ECG seria útil per a generar una ferramenta valuosa a l'hora d'analitzar la FA i ajudar a predir preoperatòriament el resultat de l'ablació quirúrgica d'esta. De fet, l'anàlisi de l'ECG podria proporcionar noves maneres de quantificar el remodelat auricular i, en conseqüència, proveir de noves vies d'estudi per a analitzar les causes i mecanismes de la FA.

D'altra banda, l'objectiu principal d'esta Tesi doctoral es va aconseguir al combinar la informació electrocardiográfica amb la clínica per mitjà de models de predicció. Els dits models van sobrepassar el 90% de precisió en les seues prediccions en cada seguiment analitzat.

En conclusió, este treball ha demostrat que, incloent la informació continguda en l'ECG a l'anàlisi de la FA, es pot desenrotllar una ferramenta fiable a l'hora de predir preoperatòriament el resultat de la cirurgia Cox-Maze. De fet, els resultats aconseguits en esta Tesi han superat els mètodes usats tradicionalment per mitjà de l'anàlisi de la informació clínica del pacient. A més, l'anàlisi de l'ECG també podria contribuir a desenrotllar noves maneres d'entendre les causes i mecanismes de la FA.

Agradecimientos

En estas líneas me gustaría expresar mi gratitud a todas aquellas personas que me han apoyado y ayudado a desarrollar el trabajo de esta tesis.

En primer lugar, me gustaría dar las gracias a mis directores de tesis José Joaquín Rieta, Raúl Alcaraz y Fernando Hornero por sus constantes consejos y por todo el esfuerzo y dedicación que han puesto para que esta tesis se haya podido terminar. Ha sido un placer poder desarrollar esta actividad investigadora en el futuro y espero que esta tesis abra nuevas puertas a futuros estudios y colaboraciones.

También me gustaría agradecer al personal de la Universidad Politécnica y en especial a Matilde Julián con quien tuve la oportunidad de compartir despacho y compartir ideas e hipótesis.

También me gustaría dar las gracias a mi familia que siempre me ha apoyado en cada paso de mis estudios que daba y me animaba a seguir más allá y especialmente a María, por estar constantemente animándome y ayudándome para que yo pudiera dedicarme a la tesis.

Gracias a todos por haber hecho posibe este trabajo.

Contents

Chapter 1

Motivation, hypothesis and objectives

1.1 Motivation

Atrial fibrillation (AF) is the most commonly diagnosed sustained arrhythmia in clinical practice and affects approximately 1-2% of the general population [1, 2] and in more than 6% of those patients older than 65 years of age [3]. As a consequence of aging the prevalence of AF is expected to double in the next 50 years[4]. During AF, the atria normal, organized electrical activity is replaced by several coexisting wavefronts called reentries, which continuously depolarize the atrial cells [5]. As a result, atrial activity (AA) is disorganized and, therefore, the atria are unable to be contracted in a regular rhythm. This unorganized rhythm makes that the ventricles beat irregularly and often rapidly. In consequence, AF is associated with increased rates of death, stroke and other thrombo-embolic events, heart failure and hospitalizations, degraded quality of life, reduced exercise capacity and left ventricular dysfunction [6]. Hence, there have been aggressive attempts to find a cure over the last decades.

AF may be treated with pharmacologic therapy or with non-pharmacologic therapy. Two pharmacological treatment approaches are used to manage patients with atrial fibrillation: (1) control of ventricular rate and anticoagulation; (2) restoration and maintaining of sinus rhythm by means of antiarrhythmic drugs [7].

Antiarrhythmic drugs form the mainstay of medical treatment but unfortunately suffer from significant recurrence rates in many cases [7, 8]. On the other hand, non-pharmacological approaches aims at resolving AF and restoring normal sinus rhythm (NSR). These techniques include include termination of the arrhythmia by applying controlled electrical impulses (electrical cardioversion or ECV) and the destruction of the cardiac tissue that triggers atrial fibrillation (ablation therapy). The ablation therapy could be done by catheterization or by surgery. The most effective procedure to eliminate AF is a surgical procedure known as Cox-Maze surgery, with a reported long term success rate higher than 90% [9].

Patients undergoing Cox-Maze are exposed to the risks and discomfort of open-heart surgery. Furthermore, the procedure is a a complex surgery which requires multiple atrial incisions and has the potential risk of postoperative morbidities. In consequence, this surgery is indicated for patients that have shown drug intolerance, arrhythmia intolerance, and recurrent embolic events [10]. In this sense, in order to avoid unnecessary risks, it is important to select the patients most suitable to recover NSR. For this purpose, clinicians have performed several studies looking for clinical information to identify predictors of failure [11]. However, the results should be improved in order to maximize the efficiency of the Cox-Maze procedure by performing a proper patient selection.

Regarding the postoperative treatment, all patients use to be treated with oral anticoagulants and antiarrhythmic drugs prior to discharge, independently of their post-surgery rhythm [12]. Furthermore, some hospitals treat post-surgery AF with chemical and electrical cardioversion (ECV) before discharge [13]. After discharge, patients are routinely evaluated at 3, 6 and 12 months; and then, every year. Until 3 months follow up, the drug treatment is maintained regardless of the presented rhythm at discharge: NSR or AF [12]. Clinicians follow this procedure because in the first months after the surgery, postablation AF may occur transiently [5]. In consequence, a blanking period of 3 months after the surgery has been defined before taking clinical decisions and reporting results [14]. If AF persists after the blanking period, electrical cardioversion (ECV) is applied to restore NSR [12]. In contrast, antiarrhythmic drugs are withdrawn if a stable NSR is recorded. Similarly, anticoagulant treatment is stopped in patients maintaining NSR 6 months after surgery [12]. Hence, preoperative prediction about patient's rhythm at follow up could be clinically relevant. For patients with high risk of AF, ECV could be planned before surgery without the need of waiting for a routine evaluation. In this way, clinical resources could be optimally managed and risks for the patient could be minimized by reducing postoperative AF duration and, therefore, the arrhythmia perpetuation probability [15]. Contrarily, an aggressive treatment with antiarrhythmic drugs could be avoided for those patients with a low risk of maintaining AF. Thus, clinical costs could be reduced and the patient's quality of life could be improved.

1.2 Initial hypothesis

AF occurs when the electrical impulses in the atria degenerate from their usual organized pattern into a rapid chaotic pattern. Consequently, AF is characterized by uncoordinated atrial activation [5]. On the electrocardiogram (ECG), AF is described by the replacement of consistent P waves by rapid oscillations or fibrillatory waves (f waves) that vary in size, shape, and timing [16] associated with an irregular ventricular response [5]. The most widely accepted theory to explain AF mechanisms is based on the continuous propagation of multiple wavelets wandering throughout the atria [5]. The fractionation of the wave fronts as they propagate results in self-perpetuating independent wavelets called reentries. The number of simultaneous reentries depends on the refractory period, mass and conduction velocity along the atria, and these parameters present severe inhomogeneities in AF [5].

Based on this theory, the Cox-Maze procedure is applied to terminate AF [10]. This procedure is an open-heart surgery, which consists of forming scar tissue in the atria by means of surgical incisions to block atrial conduction and interrupt the most common macro-reentrant circuits. Furthermore, at the same time, the sinus node impulse is directed to the atrioventricular node along a specified route [17, 7]. However, as any AF therapy, it is not 100% effective. AF recurrence depends, among other things, on the state of the atria, defined as atrial remodeling [18]. To this respect, in order to maximize the efficiency of the Cox-Maze procedure due to a proper patient selection, several studies analyzing clinical information to find predictors of recurrence have been carried out [19, 20, 13].

Regarding ECG analysis, despite that AF leaves recognizable traces on it, traditionally it has not received much attention to predict AF recurrence [21]. Only the f waves amplitude has been studied as a diagnostic tool since long time ago [22, 23]. The accuracy of the f waves amplitude to predict the Cox-Maze outcome was also studied. These studies related this feature to the amount of activated atrial tissue and, therefore, showed that it is affected by the progressive atrial structural remodeling produced by the AF. In consequence, coarse waves ($>$0.1 mV) were rather a sign of AF reversion, while fine oscillations were rather in favour of AF recurrence ($<$0.1 mV) [24, 25]. However, due to the difficulty of separating the AA and the ventricular activity no further analyses were performed.

Recently, with the development of signal processing techniques and electronic recordings, some validations comparing surface recordings with intra-atrial recordings were performed [26, 27]. These studies obtained similar results in the intra-atrial recordings and the surface recordings. In consequence, the importance of ECG analysis has began to increase and many studies using it to predict AF termination have been performed [28, 29, 24]. These studies mainly study the dominant frequency and the organization of the AA. Both characteristics are estimations of the number of coexisting wavelets in the atria [27, 30] and, in this

way, they are related with the electrical remodeling and likelihood of AF recurrence [31]. In consequence, it is highly likely that fibrillation of different origins or at different stages of progression, i.e. in different substrates, might manifest with different fingerprints in the ECG tracing [21]. However, such typical characteristics of ECGs in AF have not been considered potentially relevant for rendering more precise the clinical definition and treatment of AF in current international guidelines [5, 6]. Therefore, the hypothesis of the present thesis is that a more detailed ECG analysis could help to improve the preoperative predictions of the Cox-Maze outcome and could lead to a better understanding of the AF mechanisms.

On the other hand, this work also studies the possibility that the information provided by the clinical information and the electrocardiographic information could be complementary. Therefore, combining the indices, the prediction capability could be enhanced. For this purpose, the indices have been combined by means of different prediction models.

Finally, this kind of study could provide reliable information about the atrial substrate alteration and evolution in patients undergoing concomitant Cox-Maze surgery of AF. This kind of preoperative prognosis could lead to a better understanding of the atrial remodeling mechanisms.

1.3 Objectives

The objective of this research is to predict preoperatively the Cox-Maze outcome. This prediction is performed at different follow up. The most important one is the prediction 12 months after the surgery because the rhythm at this period allows to assess the procedure as effective or ineffective. In this way, these prediction would help to perform a better patient selection. On the other hand, predictions at different follow up periods such as at discharge and then 3 and 6 months after surgery were also performed. This analysis could provide reliable information about the atrial substrate alteration and evolution in patients undergoing concomitant Cox-Maze surgery of AF. This kind of preoperative prognosis could lead to a better understanding of the atrial remodeling mechanisms. Furthermore, it could also be used to modulate the patient's therapeutic window depending on the risk of maintaining mid-term AF. To this respect, several studies are speculating that AF treatment personalization would allow to reach high efficacy and safety in AF management by applying specific therapies to each patient [32].

In order to perform the main objective, some secondary objectives have been set. In one side, signal processing tools have been used to study preoperative ECG in order to obtain reliable information to predict the procedure outcome. Despite not being used for ablation predictions, this type of analysis has been used with reliable results to characterize AF in differen situations [28, 29]. Hence, this analysis has been performed following the hypothesis that it would provided

useful information in this situation also. On the other hand, clinical information about patients has been analyzed in order to identify which variables provided better predictions. To this respect, the variables used were selected according to previous studies [11].

Finally, the clinical and the electrocardiographic data have been combined using prediction models in order to enhance the prediction capability. Furthermore, in this way, the complementary information could be identified.

1.4 Thesis structure

This document is divided into six chapters:

- **Chapter 1.** In this chapter the clinical motivations for performing this work have been explained. Moreover, the initial hypothesis and the main proposed objectives have been briefly commented.
- **Chapter 2.** The heart anatomy and physiology will be commented in this chapter. Then, the measurement of the heart's electrical activity via surface electrocardiographic recordings is introduced. Next, some concepts about AF will be also explained, such as its definition, prevalence, incidence, etc. Finally, an explanation about Cox-Maze surgery and its evolution will be provided.
- **Chapter 3.** This chapter describes the methodology applied in this study. It starts by introducing the database used. Next, signal preprocessing and extraction of the atrial activity from the ECG are explained. Then, an explanation about the clinical and ECG indices studied is provided. Following, the prediction models generated are detailed. Finally, the statistical analysis carried out is detailed.
- **Chapter 4.** This chapter gathers the results obtained with the studies presented in Chapter 3. It shows the prediction capability of the individual indices and the classification models generated in the different follow up periods studied.
- **Chapter 5.** This chapter discusses analytically the results presented in Chapter 4, as well as their possible interpretations and clinical implications.
- **Chapter 6.** In this chapter, the concluding remarks of the preceding chapters will be summarized. Moreover, some possible future research lines are suggested. Finally, the contributions in scientific journals and conferences are enumerated.

Chapter 2

Heart physiology, Electrocardiography and Atrial Fibrillation

The aim of this chapter is to provide a general view of causes, mechanisms and treatment of atrial fibrillation. However, before that, in order to provide a better understanding on the subject, basic concepts of electrocardiography, heart anatomy and heart physiology are introduced.

2.1 Heart physiology

2.1.1 Heart anatomy

The human heart is a hollow muscular organ that weights between 250-300 g and it is about the size of a fist. It pumps blood continuously through the circulatory system to the whole boy. Blood brings needed nutrients and oxygen to tissue, and carries away metabolic waste and carbon dioxide for excretion through the kidneys and the lungs, respectively [33].

The heart lies in the center of the thoracic cavity between the lungs behind the sternum and above the diaphragm with its center located about 1.5 cm to the left of the midsagittal plane. Its shape is similar to a cone , with the base facing upwards, toward the right side and slightly backward while the tip is in contact with the chest wall in the fifth intercostal space. The heart is held in this position by its attachment to the great vessels and arteries and because it is surrounded by the pericardium, which is a is a double layered membrane with a layer around the heart and another which binds to the sternum, to the diaphragm and membrane chest. The space between these two layers is filled with serous fluid which protects the heart from any kind of external jerk or shock and also allows the heart to move freely during contraction and relaxation. Located above the heart are the great vessels: the superior and inferior vena cava, the pulmonary artery and vein, as well as the aorta. The aortic arch lies behind the heart. The esophagus and the spine lie further behind the heart [34, 35]. The location of the heart in the human body is depicted in Figure 2.1.

Figure 2.2 shows the structure of the heart. It consists of two upper chambers, called the left and right atria or auricles, and two lower chambers, called the left and right ventricles [33]. The heart is oriented so that the anterior aspect is the right ventricle while the posterior aspect shows the left atrium (see Figure 2.1). The atria are attached to the ventricles by fibrous, non-conductive tissue that keeps the ventricles electrically isolated from the atria [33]. This has special importance to the electric function of the heart, which will be discussed later. A thin membranous wall called the interatrial septum separates the left atrial chamber from the right while a thicker muscular wall called the interventricular septum separates the left ventricular chamber from the right. Additionally, the heart has four valves to regulate the blood flow between atria, ventricles and blood vessels by ensuring that blood flows only in the desired direction, preventing backflow [33]. Between the right atrium and ventricle lies the tricuspid valve, and between the left atrium and ventricle is the mitral valve. The pulmonary valve lies between the right ventricle and the pulmonary artery, while the aortic valve lies in the outflow tract of the left ventricle (controlling flow to the aorta) [35]. This valves are also represented in Figure 2.2.

The walls of the heart are composed of cardiac muscle, called myocardium. It also has striations similar to skeletal muscle. The cardiac muscle fibers are ori-

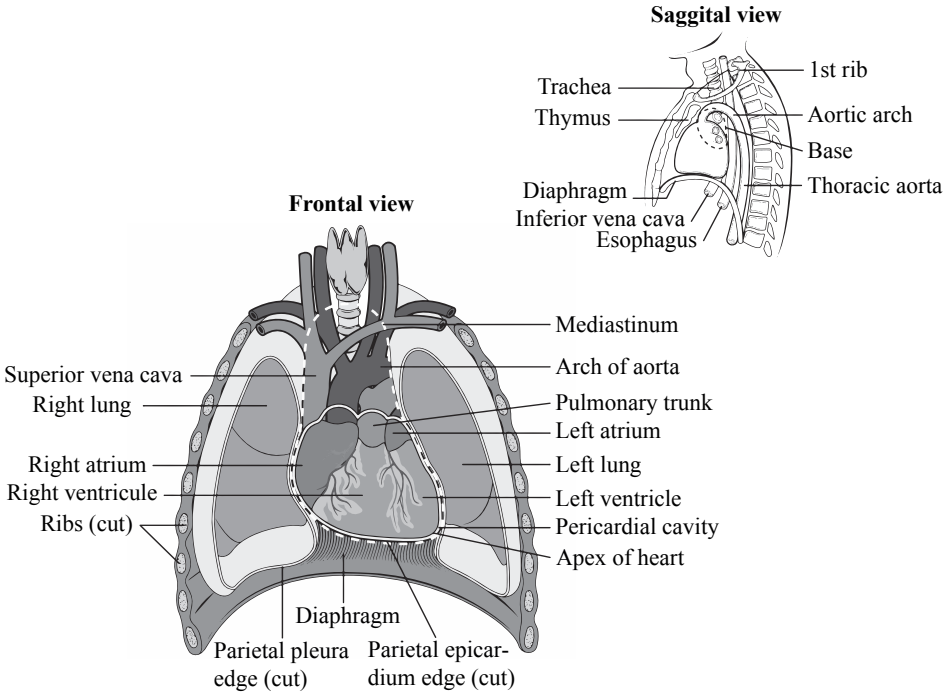

Figure 2.1. Heart location

ented spirally (see Figure 2.3) and are divided into four groups: Two groups of fibers wind around the outside of both ventricles (see Figure 2.3(a) and (b)). Beneath these fibers a third group winds around both ventricles(see Figure 2.3 (c)). Beneath these fibers a fourth group winds only around the left ventricle (see Figure 2.3 (d)) [36]. The fact that cardiac muscle cells are oriented more tangentially than radially, and that the resistivity of the muscle is lower in the direction of the fiber has importance in electrocardiography and magnetocardiography [37].

2.1.2 Cardiac cycle

Oxygen-poor blood returns to the heart after circulating through the body. It flows to the heart through veins and enters the right atrium. This chamber empties blood through the tricuspid valve into the right ventricle. The right ventricle pumps blood under low pressure through the pulmonary valve into the pulmonary artery. From there the blood goes to the lungs, where it gets fresh oxygen. Blood returns to the heart from the lungs via four pulmonary veins that enter the left atrium. From there it passes through the mitral valve and enters the left ventricle.

The left ventricle pumps the oxygen-rich blood through the aortic valve and

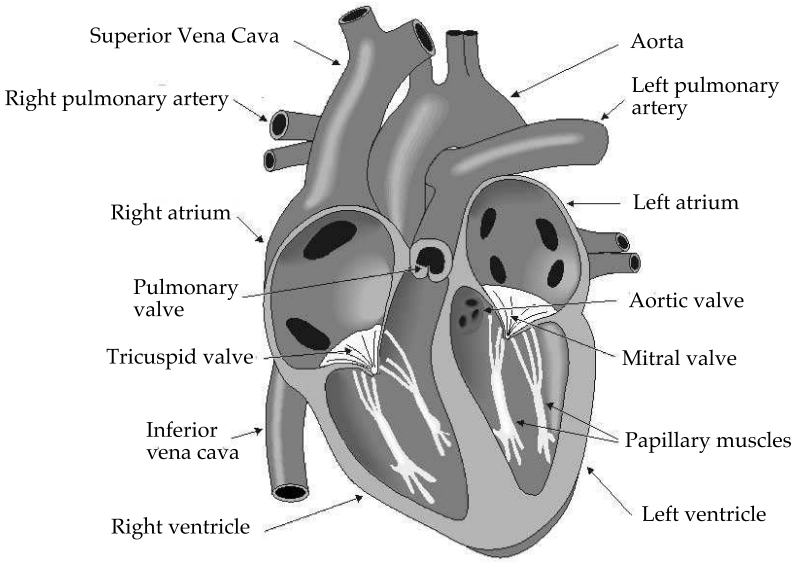

Figure 2.2. Anatomy of the heart, valves and vessels [36]

into a large artery called the aorta. The aorta takes blood from the heart to the rest of the body. Since the left ventricle pumps blood to the systemic circulation, it needs to generate higher pressure than the right ventricular wall, which pumps blood to the pulmonary circulation. In consequence, the left ventricular free wall and the septum are much thicker than the right ventricular wall [38]. Blood from the left ventricle is ejected across the aortic valve and into the aorta. While passing through the body, oxygen in the blood is distributed to the tissues. The cycle repeats as the blood flows back to the right atrium [35].

The heart performs to main phases to make possible the movement of the blood through the body: the diastole and systole. During the diastole, the atrioventricular valves open and the blood flow from the atria to the ventricles because of the pressure difference between both chambers. The last phase of the diastole is the atrial systole, where the atria contract to pump the remaining blood to the ventricles. Approximately, a 30% of the blood arriving to the ventricles enters during this phase [34].

On the other hand, the systole begins with an isometric ventricular contraction (that is, without a considerable volume variation) and at the same time, the atrioventricular valves close. The pressure in the ventricle raises until it opens the aortic and pulmonar valves. In this moment, the blood starts to flow to the body, emptying the ventricles. This phase represents 75% of the systole duration. When the pressure decreases, the blood keeps flowing due to the ventricular con-

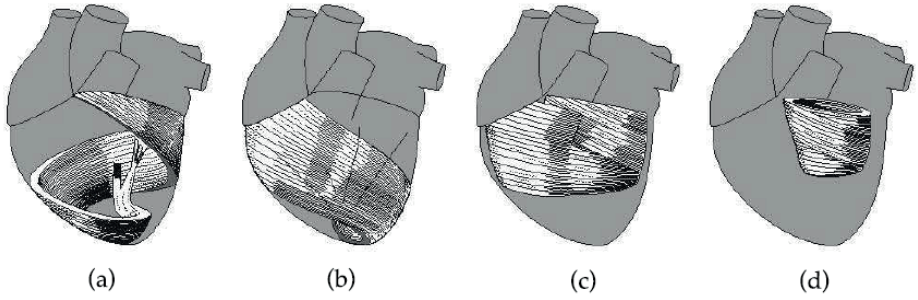

Figure 2.3. Orientation of cardiac muscle fibers [36]

traction. Finally, the ventricular fibres relax. Blood tends to return to the ventricles because the pressure is lower there that in the arteries, however, the closing of the valves prevents this. When the ventricular pressure is low enough, the atrioventricular valves open due to the difference in pressure (the atria have been filled of blood during the systole). In that way, the cycle is completed [34].

2.2 Electrical activity of the heart

The heart can be considered in a simplified description as a physiological organ that consists of two elements. The first element, already described, is the pump that impulses the blood through the body. The second element is the electric system that activates the pump, which includes an electric generator and a conduction system of electric pulses [39]. This system is described next.

2.2.1 Cardiac muscle cells

In the heart muscle cell, or myocyte, electric activation takes place by means of the same mechanism as in the nerve cell from the inflow of sodium ions across the cell membrane. This mechanism is known as depolarization and is produced when a trigger causes that the cell membrane becomes permeable and let the ions go through it, generating an ionic current flow [33]. Myocyte and nerve cell have also similar action potential amplitude, being about 100 mV. The duration of the cardiac muscle impulse, however, is two orders of magnitude longer than that in either nerve cell or skeletal muscle. Therefore, cardiac depolarization produces a very quick increment of the action potential. A plateau phase follows cardiac depolarization, and thereafter repolarization takes place. As in the nerve cell, repolarization is a consequence of the outflow of potassium ions to bring the ionic balance of the cell to its equilibrium state [38]. The duration of the action impulse is about 300 ms, as shown in Figure 2.4.

Associated with the electric activation of cardiac muscle cell is its mechanical

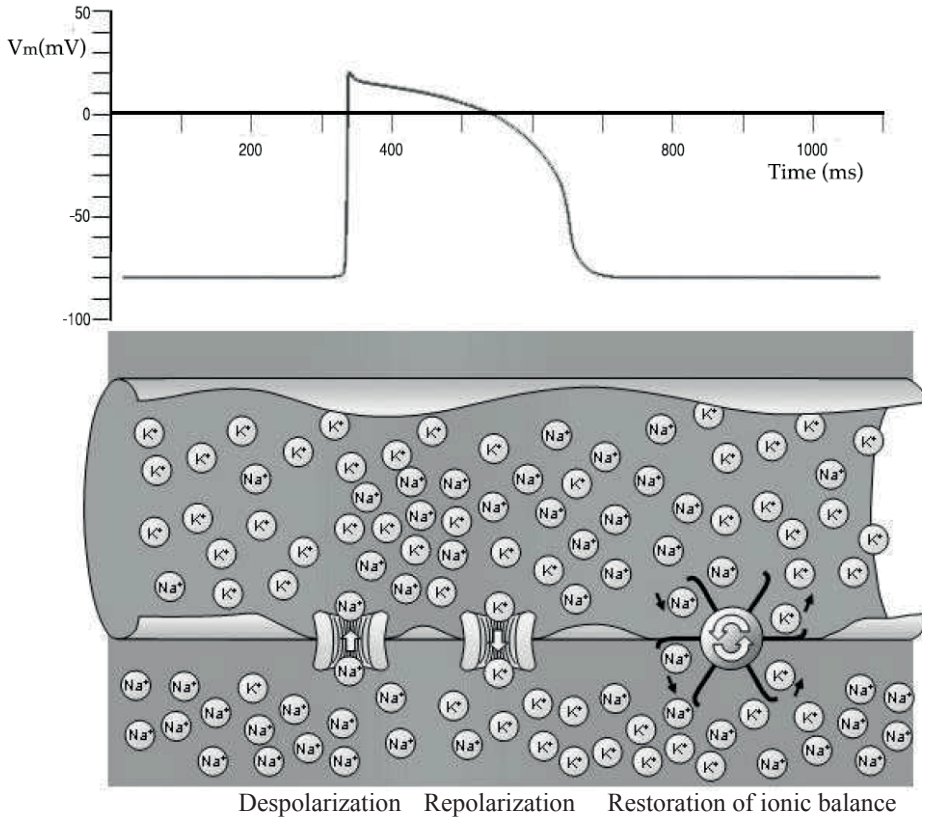

Figure 2.4. Electrophysiology of the cardiac muscle cell [36]

contraction, which occurs a little later. An important distinction between cardiac muscle tissue and skeletal muscle is that in cardiac muscle, activation can propagate from one cell to another in any direction. As a result, the activation wavefronts are of rather complex shape. The only exception is the boundary between the atria and ventricles, which the activation wave normally cannot cross except along a special conduction system, since a nonconducting barrier of fibrous tissue is present [36].

2.2.2 Cardiac electrical conduction system

Pumping is only efficient when the heart contracts in a coordinated manner. This coordination is achieved by an elaborate electrical conduction system that controls the precise timing for depolarizing the substantial mass of electrically excitable myocardium. This delicate control starts with an intrinsic self-excitable cardiac pacemaker which sets the rate at which the heart beats. The pacemaker spontaneously generates regular electrical impulses, which then spread through

the conduction system of the heart and initiate contraction of the myocardium. This pacemaker is called the sinus node (sinoatrial or SA node) node [33].

The SA node is located in the upper wall of the right atrium, near the entrance of the superior vena cava, as shown in Figure 2.5. The SA node in humans is in the shape of a crescent and is about 15 mm long and 5 mm wide (see Figure 2.5). It has the ability to spontaneously depolarize and generate an action potential at the rate of about 70 per minute that is propagated to the rest of the heart. This rate may be modulated by the balance of sympathetic and parasympathetic inputs, or by drugs. Sympathetic stimulation (from nerves connected to the brain) speeds up the rate of impulse generation while parasympathetic stimulation slows the rate. This variability in rate allows the heart to respond to demands for higher or lower cardiac output (i.e. faster or slower heart rate) [33].

The action potentials generated by the SA node spread throughout the atria primarily by cell-to-cell conduction. The conduction velocity of action potentials in the atrial muscle is about 0.5 m/sec. As the wave of action potentials depolarizes the atrial muscle, the cardiomyocytes contract by a process termed excitation-contraction coupling [36, 39]. All cells of the conduction system are capable to generate action potential, but the intrinsic activation rate of the SA node is the greatest, which obliges the rest of cells to follow its rhythm. In case of a SA node disfunction, other cells would replace it so that action potentials would be generated at a lower rate [36]. Typical intrinsic activation rates of the conduction system are also indicated if Figure 2.5.

From the SA node, electrical impulses propagate throughout the atria, stimulating its contraction. At the same time, the interatrial conduction tract (Bachman's Bundle) between the SA node and the left atrium carries the impulse quickly to the left atrium, spreading it through the left atrial myocardium so that the contraction of the left atrium occurs almost simultaneously with that of the right (see Figure 2.5) [33]. However, the electrical impulses cannot propagate directly across the boundary between atria and ventricles [37, 35]. In the healthy heart, the only pathway available for action potentials to enter the ventricles is through a specialized region of cells located in the boundary between the atria and ventricles. This region is known as atrioventricular node or AV node and is the gateway to the ventricular conduction system (see Figure 2.5). As showed in Figure 2.5, three internodal conduction tracts carry the impulses from the SA node to the VA node.

The AV node has an intrinsic frequency of about 50 pulses/min. However, if the AV node is triggered with a higher pulse frequency, it follows this higher frequency. In a normal heart, the AV node provides the only conducting path from the atria to the ventricles. Thus, under normal conditions, the latter can be excited only by pulses that propagate through it [37, 35] (see Figure 2.5). The AV node is a highly specialized conducting tissue that slows the impulse conduction considerably (to about 0.05 m/sec). This delay is to provide sufficient time for complete atrial depolarization and contraction and therefore, allow blood from the atria to fully fill the ventricles prior to ventricular depolarization and contraction [33].

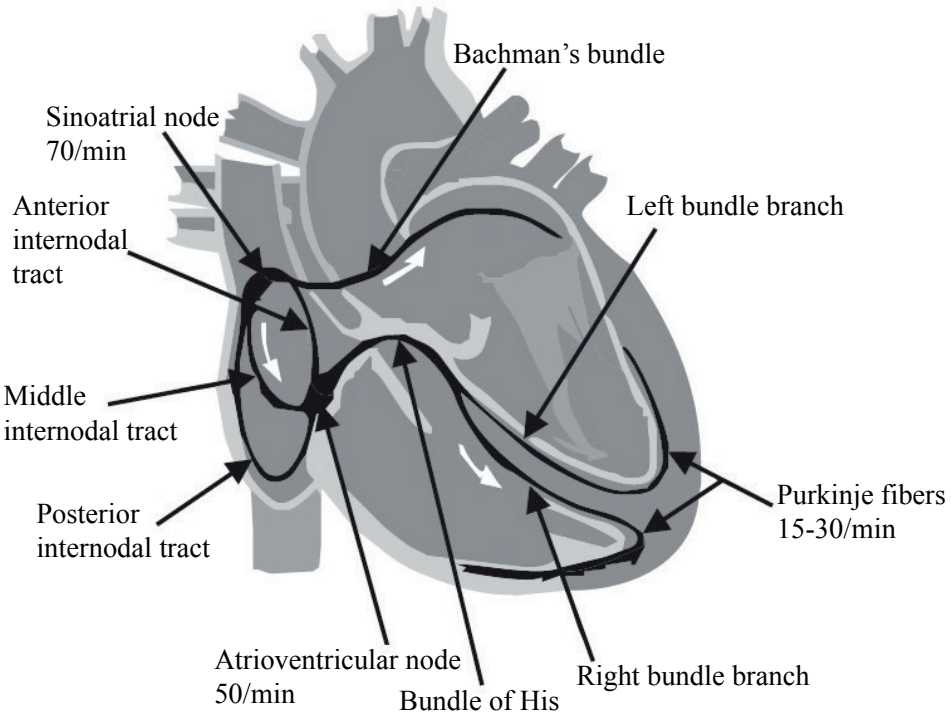

Figure 2.5. The conduction system of the heart

Propagation from the AV node to the ventricles is provided by a specialized conduction system. This system starts in a common bundle, called the bundle of His, which perforates the interventricular septum posteriorly. Within the septum, the bundle of His bifurcates into the left and right bundles. The bundle branches then divide into an extensive system of Purkinje fibers that conduct the impulses to the ventricular muscle (see Figure 2.5) [35, 39]. This results in depolarization of ventricular myocytes and therefore, in ventricular contraction.

From the inner side of the ventricular wall, the many activation sites cause the formation of a wavefront which propagates through the ventricular mass toward the outer wall. This process results from cell-to-cell activation. After each ventricular muscle region has depolarized, repolarization occurs. Repolarization is not a propagating phenomenon, and because the duration of the action impulse is much shorter at the epicardium (the outer side of the cardiac muscle) than at the endocardium (the inner side of the cardiac muscle), the termination of activity appears as if it were propagating from epicardium toward the endocardium [36]. Figure 2.6 shows the different waveforms generated by the specialized cells heart conduction system in a normal ECG and the resultant body surface potential.

Because the intrinsic rate of the sinus node is the greatest, it sets the activation frequency of the whole heart. If the connection from the atria to the AV node fails,

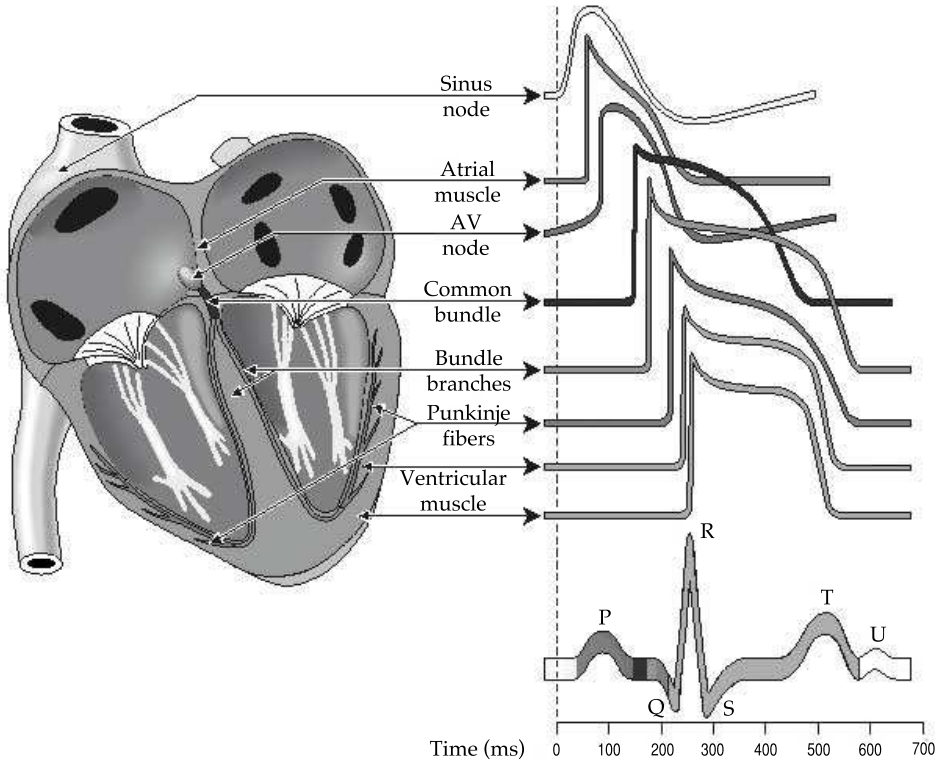

Figure 2.6. Electrophysiology of the heart. The different waveforms for each of the specific cells found in the heart are shown. The latency shown approximates that normally found in the healthy heart [36]

the AV node adopts its intrinsic frequency. If the conduction system fails at the bundle of His, the ventricles will beat at the rate determined by their own region that has the highest intrinsic frequency [39].

2.3 The electrocardiogram

The cardiac electrical events on an intracellular level may be recorded with a microelectrode, which is inserted inside a cardiac muscle cell. However, the ECG is a recording of the electrical potential, generated by the electrical activity of the heart, made from electrodes placed on the surface of the skin [40]. The first clinically important ECG measuring system was published in 1908 by Willem Einthoven. By using electrodes placed on the arms and legs, Einthoven described the tracings that can be observed during the cardiac cycle of a healthy subject and named the parts of the ECG as they are known today.

The body acts as a giant conductor of electrical currents. Any two points on

the body may be paired by two electrodes to register the electrical activity of the heart. Every pair of these electrodes placed on the body surface constitutes a lead. These electrode leads are connected to a device that measures potential differences between selected electrodes, and the resulting tracing is called an ECG [40]. The ECG describes the electrical activity of the heart at each time instant of the cardiac cycle and represents a summation in time and space of the action potentials generated in myocardial cells. Each group of cells which is simultaneously depolarizing can be represented as an equivalent current dipole source to which a vector is associated, describing the dipole's time-varying position, orientation and magnitude. According to this dipolar model, the recorded ECG can be interpreted as the projection of the heart vector on the lead vector defined by the exploring electrodes [36].

In summary, the ECG is a graphical recording of the electrical signals generated by the heart. The signals are generated when cardiac muscles depolarize in response to electrical impulses generated by pacemaker cells [33]. The ECG can reveal many things about the heart, including its rhythm, whether its electrical conduction paths are intact, whether certain chambers are enlarged, and even the approximate ischemic location in the event of a heart attack (myocardial infarction) [33].

2.3.1 Leads of the electrocardiogram

The standard ECG is composed by 12 beforehand fixed leads. There are two basic types of ECG leads: bipolar and unipolar. Bipolar leads utilize a single positive and a single negative electrode between which electrical potentials are measured. Unipolar leads (augmented leads and precordial leads) have a single positive recording electrode and utilize a combination of the other electrodes to serve as a composite negative electrode [40]. The classification of the 12 leads is described next.

Einthoven limb leads (bipolar)

The bipolar limb leads were the leads proposed by Einthoven in 1908. This measuring system consists of three bipolar ECG leads, namely leads I, II and III. By convention, Lead I has the positive electrode on the left arm, and the negative electrode on the right arm, and therefore measures the potential difference between the two arms. In the Lead II configuration, the positive electrode is on the left leg and the negative electrode is on the right arm. Lead III has the positive electrode on the left leg and the negative electrode on the left arm (see Figure 2.7). That is [36, 40]:

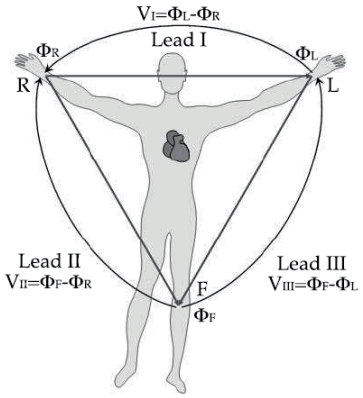

Figure 2.7. Einthoven limb leads and Einthoven triangle [36].

$$\begin{aligned} V_I &= \Phi_L - \Phi_R \\ V_{II} &= \Phi_F - \Phi_R \\ V_{III} &= \Phi_F - \Phi_L \end{aligned} \tag{2.1}$$

where V_I, V_{II} and V_{III} are the voltage of Lead I, Lead II and Lead III, respectively, and Φ_L, Φ_R and Φ_F are the potential at the left arm, right arm and left foot, respectively. Note that, according to the second Kirchhoff's law, V_{II}=V_I+V_{III}. The right leg potential is never used for obtaining the ECG. However, and electrode is placed there to set a ground reference and help the ECG recorder to reduce common mode interference.

These three bipolar limb leads roughly form an equilateral triangle (with the heart at the center) that is called Einthoven's triangle (see Figure 2.7) [40]. Whether the limb leads are attached to the end of the limb (wrists and ankles) or at the origin of the limb (shoulder or upper thigh) makes no difference in the recording because the limb can simply be viewed as a long wire conductor originating from a point on the trunk of the body.

Maximum positive ECG deflection will occur in Lead I when a wave of depolarization travels parallel to the axis between the right and left arms. Similar statements can be made for Leads II and III where the positive electrode is located on the left leg. For example, a wave of depolarization traveling towards the left leg will give a positive deflection in both Leads II and III because the positive electrode for both leads is on the left leg. A maximal positive deflection will be obtained in Lead II when the depolarization wave travels parallel to the axis between the right arm and left leg. Similarly, a maximal positive deflection will be obtained in Lead III when the depolarization wave travels parallel to the axis between the left arm and left leg [40].

If the three limbs of Einthoven's triangle (assumed to be equilateral) are broken apart, collapsed, and superimposed over the heart, then the positive electrode for Lead I is said to be at zero degrees relative to the heart (along the horizontal axis) (see Figure 2.8). Similarly, the positive electrode for Lead II will be $+60°$ relative to the heart, and the positive electrode for Lead III will be $+120°$ relative to the heart. This new construction of the electrical axis is called the Axial Reference System [40]. With this system, a wave of depolarization travelling at $+60°$ will produce the greatest positive deflection in Lead II. A wave of depolarization oriented $+90°$ relative to the heart will produce equally positive deflections in both Lead II and III. In this latter case, Lead I will show no net deflection because the wave of depolarization is heading perpendicular to the $0°$, or Lead I, axis.

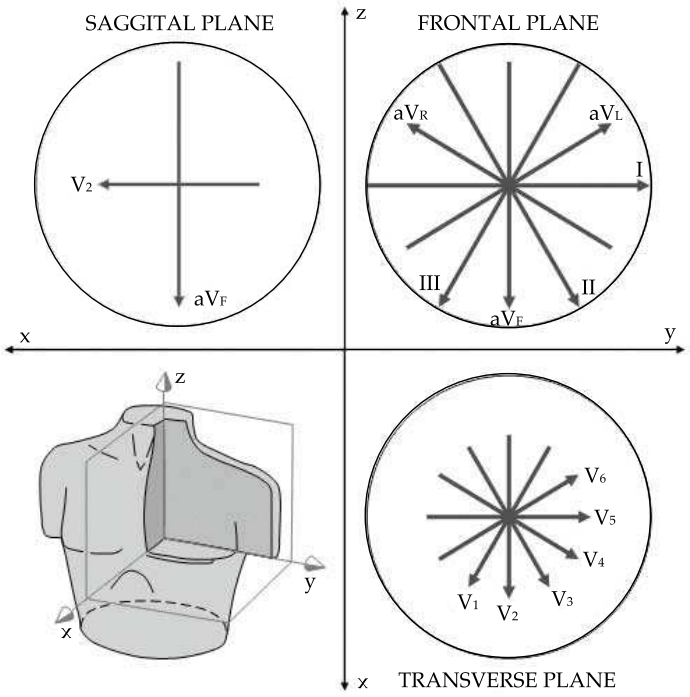

Figure 2.8. Projection of the 12-lead ECG system in three orthogonal planes [36].

Goldberger augmented limb leads (unipolar)

In 1942 E. Goldberger observed that the recorded ECG signals with the limbs leads could be be replaced with a new set of leads that are called augmented leads because of the augmentation of the signal [36]. These are termed unipolar leads because they are obtained by measuring the potential between a single limb electrode and a virtual negative electrode, which is the midpotential of the

two remaining electrodes. The positive electrodes for these augmented leads are located on the left arm (aV_L), the right arm (aV_R), and the left leg (aV_F) (see Figure 2.9). Notice that the Goldberger augmented leads are fully redundant with respect to the Einthoven leads I, II and III, with the following relationship [40]:

$$\begin{aligned} aV_R &= \Phi_R - \frac{\Phi_L + \Phi_F}{2} = -\frac{V_I + V_{II}}{2} \\ aV_L &= \Phi_L - \frac{\Phi_R + \Phi_F}{2} = V_I - \frac{V_{II}}{2} \\ aV_F &= \Phi_F - \frac{\Phi_R + \Phi_L}{2} = V_{II} - \frac{V_I}{2} \end{aligned} \tag{2.2}$$

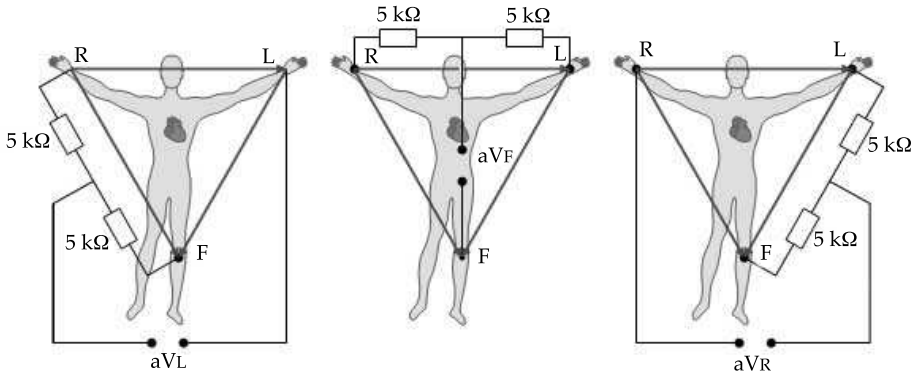

Figure 2.9. The circuit of the Goldberger augmented leads [36].

The three augmented leads are depicted using the axial reference system as Fig. 2.8 shows. The aV_L lead is at $-30°$ relative to the Lead I axis; aV_R and aV_F are at $-150°$ and $+90°$, respectively. The three augmented unipolar leads, coupled with the Einthoven limb leads, constitute the six limb leads of the ECG. These six leads system records the electrical activity along a single plane, termed the frontal plane relative to the heart. Using the axial reference system and these six leads, it is rather simple to define the direction of an electrical vector at any given instant in time. If a wave of depolarization is spreading from right to left along the $-0°$ axis, then Lead I will show the greatest positive amplitude. Likewise, if the direction of the electrical vector for depolarization is directed downwards ($+90°$), then aV_F will show the greatest positive deflection. If a wave of depolarization is moving from left to right at $+150°$, then aV_R will show the greatest negative deflection [36, 40].

Precordial leads (unipolar)

The six limb leads examine the electrical forces in the frontal plane of the body. However, since electrical activity travels in three dimensions, recordings from a perpendicular plane are also essential (see Figure 2.8). For this purpose, Wilson introduced the precordial leads in 1944. These leads consist of six positive electrodes placed on the surface of the chest over the heart and they are termed $V_1, V_2, \ldots, V_6$ by convention. As Figure shows 2.10, V_1 and V_2 are located at the fourth intercostal space on the right and left side of the sternum; V_4 is located in the fifth intercostal space at the midclavicular line; V_3 is located between the points V_2 and V_4; V_5 is at the same horizontal level as V_4 but on the anterior axillary line; V_6 is at the same horizontal level as V4 but at the midaxillary line [40].

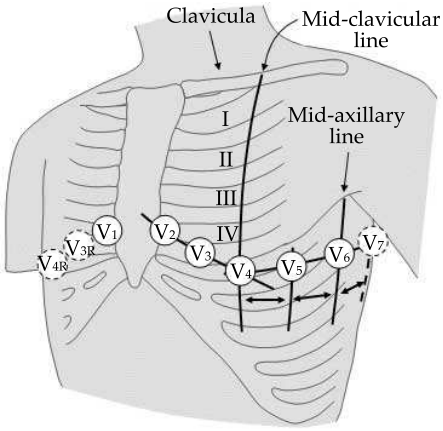

Figure 2.10. Precordial leads [36].

In his work, Wilson investigated how electrocardiographic unipolar potentials could be defined. Ideally, those are measured with respect to a remote reference (infinity). Wilson suggested the use of the Wilson Central Terminal (WCT) as this reference. It can be identified as the center of Einthoven's triangle and can be computed as average of the voltages measured on the right and left arms and the left leg. The WCT was formed by connecting a 5 $k\Omega$ resistor from each terminal of the limb leads to a common point. The potential of the WCT is calculated as [39, 40]:

$$\Phi_{WCT} = \frac{\Phi_R + \Phi_L + \Phi_F}{3} \tag{2.3}$$

Since the central terminal potential is the average of the Einthoven's triangle vertexes potentials, and the addition of these potentials is approximately zero, the WCT can be therefore considered as a satisfactory reference. Wilson advocated 5 $k\Omega$ resistances; these are still widely used, though at present the high-input impedance of the ECG amplifiers would allow much higher resistances. A

higher resistance increases the CMRR (common-mode rejection ratio) and diminishes the size of the artifact introduced by the electrode/skin resistance [40]. In Figure 2.11 it is shown how the WCT potential is obtained.

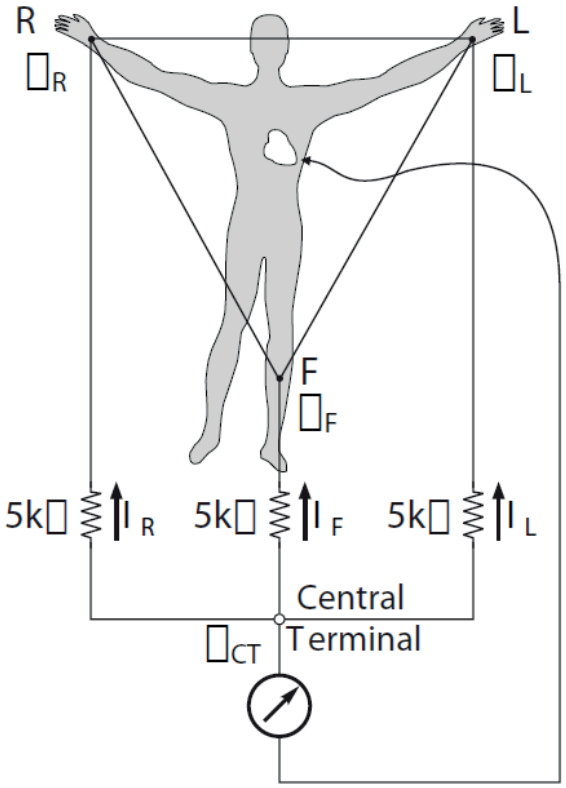

Figure 2.11. Formation of the Wilson Central Terminal [36].

The interpretation rules of the precordial leads are the same as for the limb leads. For example, a wave of depolarization travelling towards a particular electrode on the chest surface will elicit a positive deflection [40].

Standard ECG content

In principle, two of the limb leads (V_I, V_{II}, V_{III}) could reflect the frontal plane components, whereas one precordial lead could be chosen for the anterior-posterior component. The combination should be sufficient to describe completely the electric heart activity. The lead V_2 would be a very good precordial lead choice since it is directed closest to the x axis. It is roughly orthogonal to the standard limb plane, which is close to the frontal plane, see Figure 2.8. To the extent that the cardiac source can be described as a dipole, the 12-lead ECG could be thought to

have three independent leads and nine redundant leads [40]. However, in fact, the precordial leads detect also nondipolar components, which have diagnostic significance because they are located close to the frontal part of the heart. Therefore, the 12-lead ECG system has eight truly independent and four redundant leads [39, 40].

The main reason for recording all 12 leads is that it enhances pattern recognition. This combination of leads gives the clinician an opportunity to compare the projections of the resultant activity in two orthogonal planes and at different angles, see Figure 2.8. This is further facilitated when the polarity of the lead aV_R can be changed; the lead -aV_R is included in many ECG recorders [40].

In summary, for the approximation of cardiac electric activity by a single fixed-location dipole, nine leads are redundant in the 12-lead system, as noted above. If we take into account the distributed character of cardiac sources and the effect of the thoracic surface and internal inhomogeneities, we can consider only the four (of six) limb leads as truly redundant [40].

In conclusion, the twelve ECG leads provide different views of the same electrical activity within the heart. Therefore, the waveform recorded will be different for each lead [35].

2.3.2 Characterization of the ECG

Figure 2.12 represents the lead V_I from a normal ECG. The figure also includes definitions for various segments and intervals in the ECG. The tracing recorded from the electrical activity of the heart forms a series of waves and complexes that have been arbitrarily labelled (in alphabetical order) the P wave, the QRS complex, the T wave and the U wave [35, 39].

From electrocardiographic theory it is possible to examine the generation of the ECG by taking into account the progression of activation within a cardiac cycle. P wave corresponds to the atria depolarization and indicates the start of atrial contraction that pumps blood to the ventricles. The QRS complex reflects the depolarization of ventricular myocardium, and indicates the start of ventricular contraction that pumps blood to the lungs and the rest of the body. Notice that the QRS complex amplitude is higher than the P wave because more myocardial mass is involved in ventricular depolarization than in atrial depolarization. The T wave corresponds to the repolarization of the ventricular myocardium. The end of the T wave coincides with the end of ventricular contraction. Atrial depolarization is usually not visible as it normally coincides with the QRS complex. The significance of the U wave is uncertain, but it may be due to repolarization of the Purkinje system. U waves may be seen in a normal ECG, but are $< 10\%$ of the height of the QRS complex. They become prominent under abnormal conditions such as electrolyte imbalance and drug toxicity [33].

Different intervals can be defined in the ECG according to the names of the

waves already defined, see Figure 2.12. The PR segment is the time between the beginning of the P wave and the onset of the QRS complex and is an indirect measurement of the atrioventricular delay. In this period, the only electrical activity is the conduction of the impulses through the His bundle to the Purkinje fibers, participating a small number of cells. In consequence, the potentials recorded in the skin are almost 0. The QT interval comprises the time between the onset of the QRS complex and the offset of the T wave and represents a measurement of the time at which ventricular cells are depolarized (approximate measurement of the action potential duration). The ST interval is defined as the time between the offset of the QRS complex and the offset of the T wave and represents the repolarization time of the ventricles. The TP segment comprises the time between the offset of the T wave and the onset of the P wave. This segment represents a resting time in the heart at which no electrical activity is taking place in a healthy heart. The time interval between the offset of the T wave and the onset of the QRS complex is called TQ segment and represents the resting period of the ventricles. The time between two adjacent QRS complexes is called RR interval.

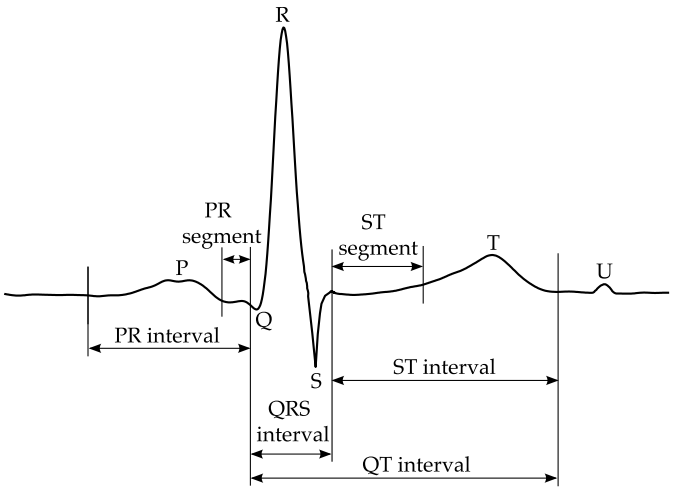

Figure 2.12. The normal ECG.

The normal ECG is characterized by:

- P wave:
  - Positive in V_I, V_{II}, aV_F, V_{3-6}
  - Negative in aV_R
  - Positive, negative or biphasic in V_{III}, aV_L, V_{1-2}
  - Maximum duration of 110 milliseconds (ms)
- Heart rate: 60 to 100 beats per minute in rest conditions

- PR segment: isoelectric and maximum duration between 120 and 200 ms
- QRS duration: between 60 and 120 ms
- T wave: same direction as QRS, asymmetric morphology, at least the tenth part of R high
- ST segment: must be isoelectric, although deviations between 0.05 and 0.2 millivolts may be normal in precordial leads
- U wave: occurs after the T wave and has the same direction, but frequently it is not registered

2.3.3 The ECG as a clinical tool for cardiac diagnosis

The electrocardiograph is the major diagnostic instrument of cardiac electrophysiology. It is estimated that approximately 100 million standard 12 lead ECGs are recorded annually in the United States. In addition the ECG is displayed or recorded during monitoring of critically ill patients, and patients in the operating room [41].

There are two aspects in the interpretation of the ECG. One is concerned with morphology of the waves and complexes, which make up a complete cardiac cycle. The other is concerned with timing of events and variations in patterns observed over many beats. Any change in cardiac electrical activity or in the volume conductor may be reflected in the ECG and provide diagnostic information. Cardiac electrical activity involves the shape of the action potential impulse and its propagation through the heart [41]. The ECG analysis is used in the diagnosis of a wide variety of abnormalities and diseases, such as [42]:

- Coronary artery disease. A disease in which blood flow to the heart and body is restricted due to hardening of the arteries (atherosclerosis).
- Heart attack, either previous or current. The ECG is an essential investigation for diagnosis of heart attack. Initial findings may determine which patient requires emergency cardiac catheterization and angioplasty or administration of thrombolysis.
- Arrhythmias. Abnormally fast (tachycardias) or abnormally slow (bradycardias) heart rhythms. For instance, the ECG may help to detect heart block abnormally slow heart rhythms due to either the partial or complete loss of electrical communication between the atria and ventricles. A pacemaker may be required as part of treatment. If the arrhythmia only occurs occasionally, the patient may be asked to wear a portable ECG called Holter monitor. This device allows to gather information about the heart's function over a prolonged period.
- Atrial fibrillation. See Section 2.4.

- Cardiac hypertrophy. An enlarged or thickened heart muscle. Several studies have shown benefit in ECGs to help distinguish between benign, physiological heart enlargement (e.g., from sustained, intense exercise) and pathological enlargement (from significant heart disease).
- Cardiomyopathy. A disease in which the heart muscle functions improperly due to a variety of conditions.
- Pericarditis. Inflammation of the pericardium.
- Long QT syndrome. A disorder of the heart electrical system, which could lead to fainting (syncope) or sudden cardiac death.
- Myocarditis. Inflammation of the heart muscle due to viral or bacterial infection.
- Certain congenital heart defects. Heart defects that someone is born with, such as Wolff-Parkinson-White syndrome.

Many people with coronary artery disease, heart valve disease or heart muscle disease will eventually show abnormal ECG readings. However, many ECGs are performed when the patient is at rest, which means certain abnormalities that occur during periods of stress may not show up. Because it is very common to see this false-negative result (e.g., the ECG does not find the damage or abnormality that is really present), a normal ECG is not enough to rule out suspected heart disease [42].

In some instances, patients may be asked to exercise lightly in conjunction with the ECG. This is called a stress test. It is used to evaluate the function of the heart under more strenuous conditions. If the patient is unable to exercise, they may be given drugs that stimulate the heart to beat more rapidly [42].

In conclusion, it can be stated that the ECG is a tool for cardiac diagnosis with great versatility, reliability, easy to use and with reduced cost. In consequence, despite of its age, it is still the diagnostic method most used, mainly, in the first stages of pathology detection.

2.4 Atrial Fibrillation

Atrial fibrillation (AF) is the most common sustained cardiac arrhythmia, increasing its prevalence with age [21]. Concretely, AF is present in approximately 1-2% of the general population [4, 2] and in more than 6% of those patients older than 65 years of age [1]. AF is responsible for significant patient morbidity and mortality produced by the hemodynamic compromise, tachycardia-induced cardiomyopathy, and thromboembolic events [43]. This arrhythmia is associated with a five-fold risk of stroke and a three-fold incidence of congestive heart failure [6, 8].

This arrhythmia is characterized by an abnormal atria excitation, where regular atrial activation coming from the SA node is replaced by several coexisting wavefronts called reentries, which continuously depolarize the atrial cells at a rate of 300-600 beats per minute [43]. As a result, atrial activity (AA) is disorganized and the atrial rate is increased. As consequence, the atria are unable to be contracted in a regular rhythm. The rapid atria rate and uncoordinated contraction leads to ineffective pumping of blood into the ventricles. Cardiac output falls by as much as 25%. Furthermore, the disorganized electrical activity in the atria leads to irregular conduction of impulses to the ventricles that generate the heartbeat. If each atrial impulse were conducted to the ventricles, such a rapid ventricular rate would result in a loss of the effective contraction of the ventricles and a rapid death. This is prevented by the filtering function of the AV node allowing only a part of the impulses to reach the ventricles. As a consequence of the irregular electrical activity of the atria and the effect of the AV node, the ventricular rate is also irregular. In AF, the ventricular contraction is commonly around 160 to 180 beats per minute when untreated (fast atrial fibrillation), and about 60 to 70 beats per minute when treated (slow atrial fibrillation) [33]. However, ventricular response to AF depends on electrophysiological properties of the AV node and other conducting tissues, the level of vagal and sympathetic tone, the presence or absence of accessory conduction pathways, and the action of drugs. Thus, regular cardiac cycles are possible in the presence of AV block or ventricular or AV junctional tachycardia. For instance, in patients with implanted pacemakers, diagnosis of AF may require temporary inhibition of the pacemaker to expose atrial fibrillatory activity [43].

The chaotic electrical activity associated to AF is reflected in the ECG by the substitution of consistent P wave by rapid oscillations of fibrillatory (f) waves that vary in size and shape and which rate typically ranges from 350 to 600 beats per minute [16]. A demonstration is illustrated in Figure 2.13. Additionally, the uncoordinated ventricular response causes an irregular RR interval [43], such as Figure 2.14 shows. Therefore, AF may be diagnosed analyzing and ECG. he diagnosis requires an ECG or rhythm strip demonstrating: (1) "absolutely" irregular RR intervals (in the absence of complete AV block), (2) no distinct P waves on the surface ECG, and (3) an atrial cycle length (when visible) that is usually variable and less than 200 milliseconds [14].

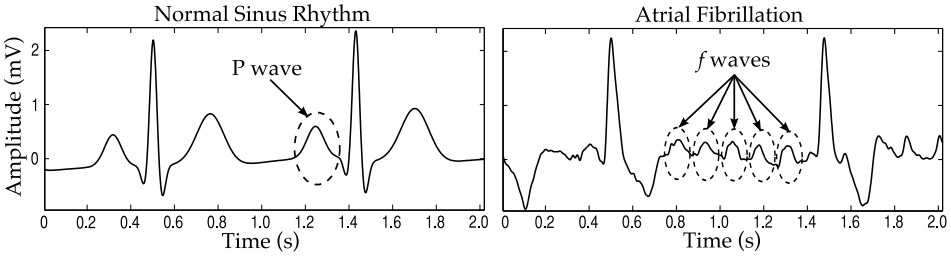

Figure 2.13. Example of surface ECG recordings corresponding to a patient in normal sinus rhythm (left) and other patient in atrial fibrillation (right).

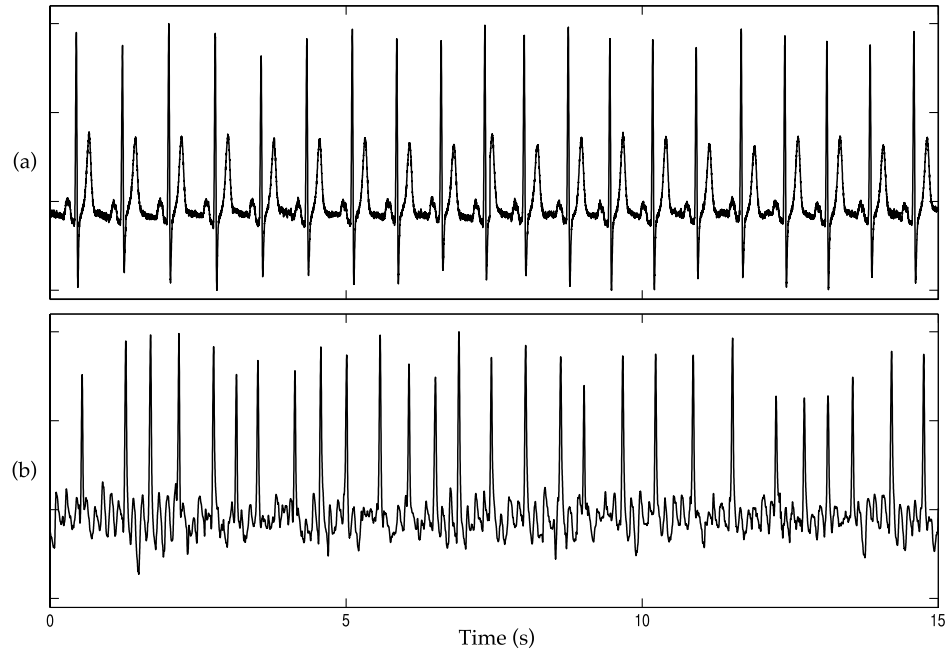

Figure 2.14. Example of surface ECG recordings with (a) normal sinus rhythm and (b) AF.

It is not uncommon to identify AF on a routine physical examination or ECG, as it may be asymptomatic in many cases [43]. In those cases the duration of the AF could be unknown. However, most of the patients have symptoms related to the rapid heart rate. Rapid and irregular heart rates may be perceived as palpitations, exercise intolerance, and occasionally produce angina (if the rate is fast and puts the heart under strain) and congestive symptoms of shortness of breath or edema. Sometimes the arrhythmia will be identified only with the onset of a stroke or a transient ischemic attack (TIA, stroke symptoms resolving within 24 hours) [43].

AF has a heterogeneous clinical presentation, occurring in the presence or absence of detectable heart disease. An episode of AF may be self-limited or require medical intervention for termination. Over time, the pattern of AF may be defined in terms of the number of episodes, duration, frequency, mode of onset, triggers, and response to therapy, but these features may be impossible to discern when AF is first encountered in an individual patient [43].

2.4.1 Epidemiology and Causes

Epidemiology

AF is the most common arrhythmia in clinical practice, accounting for approximately one-third of hospitalizations for cardiac rhythm disturbances [5]. It has been estimated that 2.2 million people in United States and 4.5 million in the European Union have paroxysmal or persistent AF [5]. The prevalence of AF is estimated at 0.4% of the general population, increasing with age. AF is uncommon in childhood except after cardiac surgery. The ATRIA study (the AnTicoagulation and Risk Factors In Atrial Fibrillation) [4] have shown that AF occurs in fewer than 1% of people under 60 years old but in more than 9% of those older than 80 years, see Figure 2.15. The age-adjusted prevalence of AF is higher in men, in whom the prevalence has more than doubled from the 1970s to the 1990s, while the prevalence in women has remained unchanged [5]. Based on limited data, blacks have less than half the age-adjusted risk of developing AF that is seen in whites [5, 4]. The frequency of lone atrial fibrillation was less than 12% of all cases of AF in some series but over 30% in others. The prevalence of atrial fibrillation increases with the severity of congestive heart failure or valvular heart disease [44].

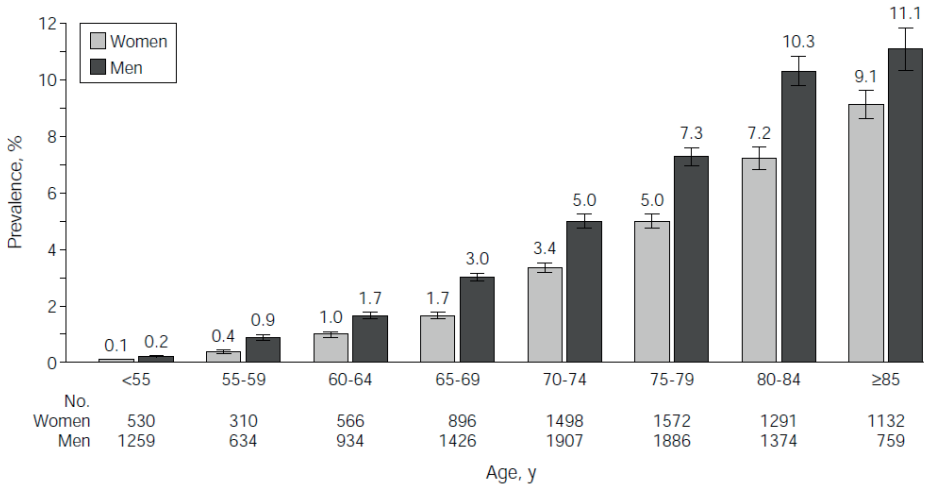

Figure 2.15. Prevalence of diagnosed AF stratified by age and sex. The mean age was 71.2 years. 9.9% of patients were younger than 55 years; 13.6%, 55 through 64 years; 31.9%, 65 throguh 74 years; 34.1% 75 trough 84 years and 10.5% 85 years or older [4].

The ATRIA study [4] also performed a projection to estimate the number of adults with AF in the year 2050. The results shown that in 2050 more than 5.6 millions people in United States would be affected by AF. This is an increase of 2.5 fold. The projection is shown in Figure 2.16.

The incidence of AF emerged from the Framingham Heart Study and the Car-

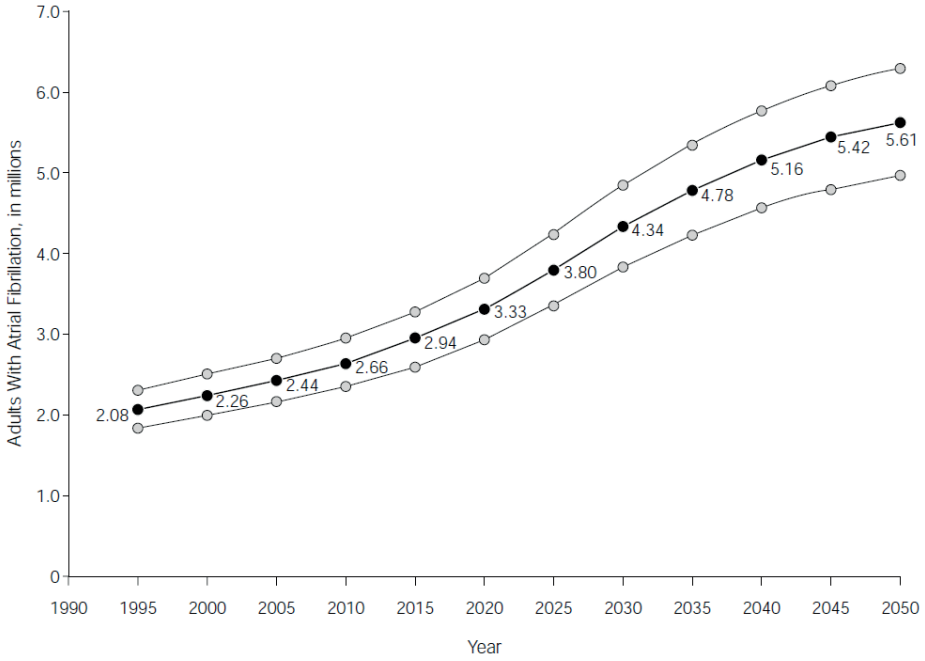

Figure 2.16. Projected number of adults with AF in the United States between 1995 and 2050. The upper and lower curves represent the upper and lower scenarios based on sensitivity analyses [4].

diovascular Heart Study (CHS) [45, 46] is show in Figure 2.17. The results shown that the incidence of AF increased from less than 0.1% per year in those under 40 years of age to more than 1.5% per year in women over 80 years of age and more than 2% per year in men over 80 years of age. The age-adjusted incidence increased over a 30-year period in the Framingham Study, and this may have implications for the future impact of AF on the population. During 38 years of follow-up in the Framingham Study, 20.6% of men who developed AF had congestive HF at inclusion vs. 3.2% of those without AF; the corresponding incidences in women were 26.0% and 2.9%. In patients referred for treatment of HF, the 2- to 3-year incidence of AF was 5% to 10% [47]. Additionally, a report of the American Heart Association shown hospitalizations, with AF as the first-listed diagnosis, increased by 34% from 1996 to 2001 [48] and by 13% in the past 2 decades in Europe [6]. Finally, the same study shown that in 2009, AF was mentioned on 100196 US death certificates and was the underlying cause in 15434 of those deaths [48].

AF is an extremely costly public health problem (16,17), with hospitalizations as the primary cost driver (52%), followed by drugs (23%), consultations (9%), further investigations (8%), loss of work (6%), and paramedical procedures (2%). Globally, the annual cost per patient is close to €3000 (approximately U.S. $3600) [5]. Considering the prevalence of AF, the total societal burden is huge, for example, about €13.5 billion (approximately U.S. $15.7 billion) in the European

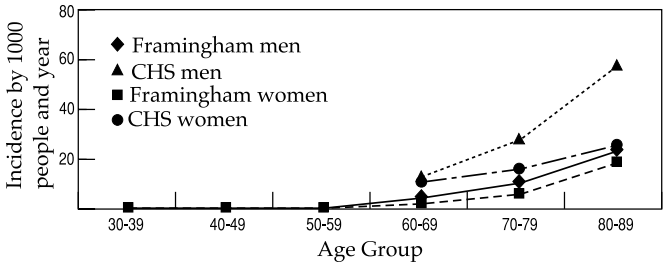

Figure 2.17. Incidence of AF in two American epidemiological studies. Framingham indicates the Framingham Heart Study [45], and CHS indicates Cardiovascular Health Study [46].

Union [5].

In sum, the prevalence and the incidence of the atrial fibrillation justify the importance of seeking for new techniques that improve the characterization of the arrythmia in order to choose its proper diagnosis and management.

Causes

The exact cause of AF is unknown, but it becomes more common with age and affects certain groups of people more than others. AF is common in people with [43]:

- Other heart condition such as:
  - Atrial fibrosis
  - Left atrial dilatation
  - High blood pressure
  - Atherosclerosis
  - Heart valve disease
  - Congenital heart disease
  - Cardiomyopathy
  - Sick sinus syndrome
  - Pericarditis
  - Heart attack
  - Dual-chamber pacemakers in the presence of normal atrioventricular conduction
  - Previous heart surgery
- Other medical conditions such as:

  - Hyperthyroidism
  - Metabolic imbalance
  - Viral infections
  - Sleep apnea
  - Asthma
  - Emphysema or other lung diseases
  - Diabetes
  - Carbon monoxide poisoning
  - Obesity
- Other conditions and situations that may trigger AF to develop include:
  - Excessive alcohol intake ("holiday heart syndrome")
  - Drinking lots of caffeine
  - Smoking
  - Taking illegal drugs, particularly amphetamines or cocaine
  - A family history of AF
- In some cases of AF there is no apparent cause

2.4.2 Classification

The American Heart Association, American College of Cardiology, and the European Society of Cardiology have proposed the following classification system based on simplicity and clinical relevance [43, 8]:

- First detected AF: any patient newly diagnosed with AF fits in this category, as the exact onset and chronicity of the disease is often uncertain.
- Recurrent AF: any patient with 2 or more identified episodes of AF is said to have recurrent AF. This is further classified into different groups based on when the episode terminates.
  - Paroxysmal: The arrhythmia initiates and terminates spontaneously, usually within 48 hours. Although AF paroxysms may continue for up to 7 days, the 48 hours time point is clinically important because after this the likelihood of spontaneous conversion is low and anticoagulation must be considered.
  - Persistent: The arrhythmia lasts more than 7 days or requires termination by cardioversion, either with drugs or by direct current cardioversion.
  - Long-standing persistent AF: The arrhythmia has lasted for more than 1 year when it is decided to adopt a rhythm control strategy.

- Permanent: The arrhythmia state is so advanced that either it can not be terminated, or after cardioversion a new AF episode is initiated again within a short period of time. Permanent AF is said to exist when the presence of the arrhythmia is accepted by the patient (and physician). Hence, rhythm control interventions are, by definition, not pursued in patients with permanent AF.

It is important to notice that persistent atrial fibrillation may be either the first presentation of the arrhythmia or the culmination of recurrent episodes of paroxysmal atrial fibrillation [43]. Therefore, first-detected AF may be either paroxysmal or persistent AF.

Finally, there is a special category known as "lone AF". It applies to young individuals (under 60 years of age) without clinical or echocardiographic evidence of cardiopulmonary disease, including hypertension [49]. In lone atrial fibrillation, the cause is often unclear, and serious complications are rare [43].

2.4.3 Mechanisms

The mechanisms underlaying development and maintenance of AF are still not well understood. Traditionally, two main theories to explain the AF mechanisms have been acceppted: enhanced automaticity in one or several rapidly depolarizing foci (see Figure 2.18(a)) and reentry involving one or more circuits (see Figure 2.18(b)). These mechanisms are not mutually exclusive and may at various times coexist in the same patient [43].

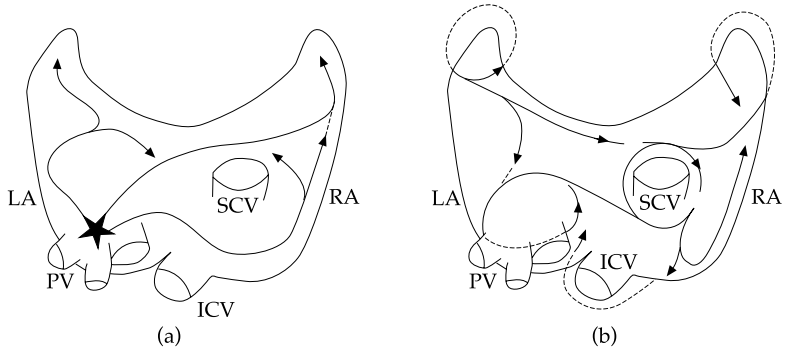

Figure 2.18. Principal electrophysiological mechanisms of AF. (a) Focal activation. The initiating focus (indicated by the asterisk) often lies within the region of the pulmonary veins. The resulting wavelets represent fibrillatory conduction, as in multiple-wavelet reentry. (b) Multiple-wavelet reentry. Wavelets (indicated by arrows) randomly reenter tissue previously activated by them or by another wavelet. The routes the wavelets travel vary. LA indicates left atrium; PV, pulmonary vein; ICV, inferior vena cava; SCV, superior vena cava; and RA, right atrium [43].

In the first mechanism, rapidly firing atrial foci can initiate atrial fibrillation in susceptible patients. The most frequent source of these rapidly atrial impulses

is the pulmonary veins. Nonetheless, foci also occur in the right atrium and infrequently in the superior vena cava or coronary sinus [50, 51]. The focal origin of AF is supported by experimental models and appears to be more important in patients with paroxysmal AF than in those with persistent AF [43]. This theory received minimal attention until the important observation that a focal source for AF could be identified in humans and ablation of this source could extinguish AF [51, 52].

The second theory, based on the reentry mechanism, is the most accepted. This theory considers the existence of multiple wave propagation fronts and was proposed by Moe in [53]. He postulated that AF perpetuation is based on the continuous propagation of multiple wavelets wandering throughout the atria. The fractionation of the wavefronts as they propagate results in self-perpetuating independent wavelets [54]. The number of simultaneous wavelets present at any time depends on the refractory period, excitable mass, and conduction velocity along the atria, because these parameters present severe inhomogeneities in AF [14]. Thus, during AF, several independent atrial propagation circuits are involved and the length of the path through which the depolarization wavefronts can travel is influenced by conduction velocity, anisotropies related to the orientation of atrial fibers and refractoriness, producing wave collision and reentry [43]. Perpetuation of AF requires the presence of a minimum number of co-existing wavelets and is favored by slowed conduction, shortened refractory periods, and increased atrial mass. Enhanced spatial dispersion of refractoriness promotes perpetuation by heterogeneous conduction delay and block [14]. Each wavelet requires a critical excitable mass of atrial tissue. Wether the wavelength is bigger than the propagating path, the wavefront disappears. On the other hand, an electric impulse may reenter in a blocked atrial area when the conduction velocity is slow enough to allow the atrial fibers to recover their excitability.

Despite these two theories have been widely used, new theories are appearing. One of the most accepted theories suggests that after AF is triggered, it is sustained by the electrical substrates of spiral waves (rotors) and focal sources [55]. According to this hypothesis, the activation wavefront rotates surrounding a pivot point, which remains unexcited, but not refractory, thus allowing the source to drift [56, 57].This pivot point is known as rotor or phase singularity. Rotors differ from leading circle reentry by exhibiting a central zone of extreme wave curvature that causes very slow conduction, allowing precession into excitable tissue, with emanating spiral waves that disorganize [58]. Another property of rotors is that they are the source of fibrillatory wavefronts, and thus "control" surrounding tissue that activates passively, and often via fibrillatory conduction [59]. Such wavefronts can collide/fuse, and exhibit rotational activation within a variable and often small spatial domain. If multiple rotors are present simultaneously, distal wavefronts collide at varying locations, also contributing to the appearance of global disorganization [59]. Recent studies in animals and humans support the presence of rotors in the atria during AF [60, 61]. Nevertheless, many questions essential to the understanding of the role of rotors in AF and of the mechanisms of AF in general remain unanswered [60]. Thus, the current evidences supporting

rotors as the main mechanism of AF maintenance in humans are still insufficient.

Finally, a different hypothesis based on the endocardial and epicardial dissociation has been proposed recently to explain AF maintenance [61]. In the normal healthy atrium, there are no significant differences between epicardial and en- docardial activations. However, in AF patients, the alteration of the atrial tissue properties produces a progressive dissociation between epicardial and endocar- dial activation patterns [62]. Thus, the atria would be transformed into an electrical double layer of dissociated waves that constantly 'feed' each other [61]. As a consequence, fibrillation waves propagate between epicardium and endocardium, and become visible as 'breakthrough waves' that add to the overall complexity of fibrillatory conduction and thus to AF stability [62]. This process greatly increases the effective surface area available to fibrillation waves and causes the atrial walls to behave as a 3-dimensional substrate [62]. Mapping studies performed in animals and humans have detected breakthrough waves in the epicardium whose appearance cannot be explained by propagation in the epicardium [63, 64]. Furthermore, epicardial breakthrough was enhanced in persistent AF patients, hypothesized to be due to more electrical dissociation between the epicardial layer and endocardial bundle network [61]. Finally, in a goat model, the simultaneous mapping of endocardial and epicardial activations revealed an increase in the dissociation between the activations in both layers as AF progressed [63]. However, although these observations are consistent with the double layer hypothesis, additional studies with simultaneous bi-atrial mapping and simultaneous endo-epicardial mapping are required to better characterize the role of endo-epicardial dissociation in the maintenance of AF.

Regardless of the mechanisms explaining AF, its self-perpetuating propensity is justified by the electrophysiological remodeling, a phenomenon consisting in the progressive shortening of effective refractory periods, thus increasing the number of simultaneous wavelets and, as a consequence, the episode duration [43]. Through the mapping of experimentally induced AF in canine hearts, the multiple wavelet hypothesis has been proved. Similar observations have been reported in humans [43, 54, 65].

2.4.4 Atrial fibrillation study from ECG

As it has been commented before, AF has some recognizable traces in the ECG, hence, the use of the ECG is a reliable tool to diagnose AF [26]. Thus, a standard 12-lead ECG is recorded in virtually every patient with AF. However, the ECG analysis has not been widely used to characterize the f waves. The overlapping of the ventricular activity with the AA hindered the application of analysis methods to the ECG. In fact, the only method used consisted on measuring with the aid of calipers the amplitude of the fibrillatory waves in those segments free of ventricular activity. This method was manual and dependent of user errors.

Recently, with the raise of signal processing techniques and electronic record-

ings, the information carried by the f waves has been explored in some detail [66]. In this sense, the development of algorithms to extract or cancel the ventricular activity has had a major importance to spur the characterization of the f waves [67]. These analyses have lead to identify different characteristics of the f waves that may be associated with the likelihood of AF termination [66]. Nevertheless, the current guidelines still do not consider ECG analysis as a potential tool to characterize AF [43, 6]. However, the proper application of spectral analysis, how to quantify different AF patterns in terms of organization, the correct measure of the f waves amplitude or how to deal with ventricular contamination before AF analysis are some aspects that could provide an improved scenario to the physician in the search of useful clinical information [68].

2.4.5 Treatment

One of the primary clinical problems associated with AF is thromboembolism. The loss of atrial contraction that leads to stasis of blood in the atria is the responsible to clot formation and the occurrence of thromboembolism which tends to propagate to other organs including the brain, kidneys or the heart itself. Thromboembolic risk is reduced by the administration of anticoagulants, but they increase the risk of bleeding complications.

In contrast to other cardiac arrhythmias for which safe and effective therapies have been developed, AF continues to be a challenge for both pharmacologic and non-pharmacologic approaches to treatment. Pharmacologic approaches include 2 types of medications that are used to treat atrial fibrillation. One type of medication is intended to prevent atrial fibrillation from occurring. This type includes medications such as propafenone, flecainide, sotalol, dofetilide, and amiodarone [5]. These same medications may restore the normal heart beat if taken during an episode of atrial fibrillation. The other type of medicine does nothing to restore the normal heart beat, but is intended simply to control the heart rate during atrial fibrillation. Prevention of a rapid heart beat during atrial fibrillation often makes the symptoms less severe. This type of medication includes digoxin, beta-blockers such as atenolol, propranolol, and metoprolol, and calcium channel blockers such as verapamil, and diltiazem [5]. However, it is important to keep in mind that medications do not cure atrial fibrillation. If a patient who is responding well to a medication stops taking it, the atrial fibrillation will return.

On the other hand, the aim of most of the non-pharmacological approaches is the termination of the arrhythmia. There are different techniques for this purpose. One, known as ECV, involves delivering controlled electrical impulses to the chest wall, in order to restore a normal heart rhythm in a patient with atrial fibrillation. It is an effective and useful way to restore a normal rhythm, but only if the atrial fibrillation has not been present for a long time [5]. If the atrial fibrillation has been present for more than a few months, there is a high probability that it will return shortly after cardioversion.

Another technique consists on AV node ablation and pacemaker implantation. This technique aims to eliminate the rapid and irregular heart beat that may accompany AF. This procedure is performed only in patients who do not respond to medications or cannot take them because of side effects, or who are not good candidates for a curative procedure. A catheter is inserted to the AV node radiofrequency energy is passed through the catheter to destroy the AV node. This eliminates the rapid and irregular heart beats caused by atrial fibrillation. The pulse rate usually drops to 30 beats per minute, and a pacemaker must be implanted to maintain a normal heart rate. The pacemaker will increase the heart rate during exertion or exercise, simulating a normal heart rhythm.

The next techniques involves ablation. One way is by means of the catheter ablation. In this procedure, thin and flexible tubes are introduced through a blood vessel and directed to the heart muscle. Then a burst of radiofrequency energy is delivered to destroy tissue that triggers abnormal electrical signals or to block abnormal electrical pathways. This type of procedure may be effective for either paroxysmal or chronic atrial fibrillation. However, it is unlikely to be effective if the left atrium is very enlarged.

Finally, there is an open-heart operation that can eliminate atrial fibrillation, whether paroxysmal or chronic. The operation is often referred to as a Cox-Maze surgery. The incision used for the operation usually is in the center of the chest and goes through the top to the bottom of sternum. The surgeon uses a combination of incisions, freezing (with a cryoprobe), and cauterization (with a radiofrequency energy probe) to destroy the short circuits that generate atrial fibrillation. When performed by an experienced surgeon, the operation eliminates atrial fibrillation in more than 90% of patients [9, 69]. Therefore, it is the most effective procedure and is detailed next.

2.5 Cox-Maze surgery

The Cox-Maze procedure is a surgical treatment for AF that was introduced in 1987 by Dr James Cox [11]. It is an open-heart intervention based on the theory that AF results from multiple macro-reentry circuits in the atria [10]. Thus, the procedure consists of forming scar tissue in the atria, by means of surgical incisions, which not only blocks atrial conduction and interrupts the conduction routes of the most common reentrant circuits, but also directs the sinus node impulse to the atrioventricular node along a specified route [17, 7].

Initially, Cox-Maze procedure (Cox-Maze I) excised both atrial appendages and isolated the pulmonary veins. Cox-Maze I included several incisions around the sinoatrial node, one of which was located directly anterior to the right atrium and superior vena cava junction (see Figure 2.19) [70]. Follow up evaluation raised the suspicion that this incision was the cause of patients inability to generate an appropriate sinus tachycardia in response to exercise [71]. In addition,

some patients presented left atrial dysfunction and the rate of pacemaker implantations was high [71]. In consequence, the incision was eliminated and a first modification was evaluated (Cox-Maze II procedure). The main change in this modification was that the previous incision had been deleted and the transverse atriotomy across the dome of the left atrium had been moved posteriorly to allow better intra-atrial conduction. Since the position of the left atrial dome incision determines the position of the atrial septal incision, moving the first posteriorly involves moving the latter posteriorly [71]. Thus the atrial septomy directly below the superior vena cava rather than anterior to the superior vena cava. This made exposure for the left atrial incisions difficult and, in consequence, transection of the superior vena cava is necessary to gain exposure of the left atrium, which is technically difficult and time consuming (see Figure 2.20) [71]. In addition, Cox-Maze II procedure did not appear to correct the occasional left atrial dysfunction. Therefore, further modifications of the technique were required. Studies to understand the cause of left atrial dysfunction revealed that, since the right atrium functioned normally, the most likely explanation for the left atrial dysfunction was interatrial conduction delay [71]. To solve the problem of interatrial prolonged time, the left atrial dome incision was moved more posteriorly and, in consequence, the atrial septal incision was moved posteriorly too (Cox-Maze III procedure) [71]. This change also allows a great exposure for the left atrial incisions. In conclusion, Cox-Maze III procedure addresses both the sinus node chronotropic incompetence and the left atrium occasional dysfunction while making the procedure much easier to perform technically(see Figure 2.21) [71].

The Cox-Maze III procedure is recognized as the most effective surgical procedure to treat AF [9] and has remained as the gold standard for AF treatment for more than a decade [19]. The introduction of ablation devices led to the replacement of traditional cut-and-sew lesions by lines of ablation using various energy sources such as radiofrequency, cryoablation or microwave. Elimination of cut and sew incisions allowed the doctors to simplify the procedure and decrease the time of surgery [72]. The new possibilities offered by the ablation devices led to a new version termed Cox-Maze IV procedure, which was performed in 2002 [69]. This new procedure differs from the Cox-Maze III procedure because it performs a separate isolation of the right and left pulmonary veins [72]. In addition, it preserves the right atrial appendage and leaves most of the posterior left atrium in electrical continuity by applying a connection lesion rather that the traditional box lesion set [19]. This procedure has the advantage of its technical simplicity, and although it is not as effective as the Cox-Maze III procedure, studies have reported around 90% freedom from AF at one year [69, 13].

Initially, Cox-Maze procedure was performed as lone procedure, but not all doctors adopted the procedure because it has been viewed as invasive and entailing significant morbidity because of the prolonged period of cardiopulmonary bypass required to perform the operation [11]. Different studies demonstrated that it had similar efficacy in patients with lone AF and in patients with AF associated to coronary, valve or congenital heart disease [74, 10]. Thus, Cox-Maze

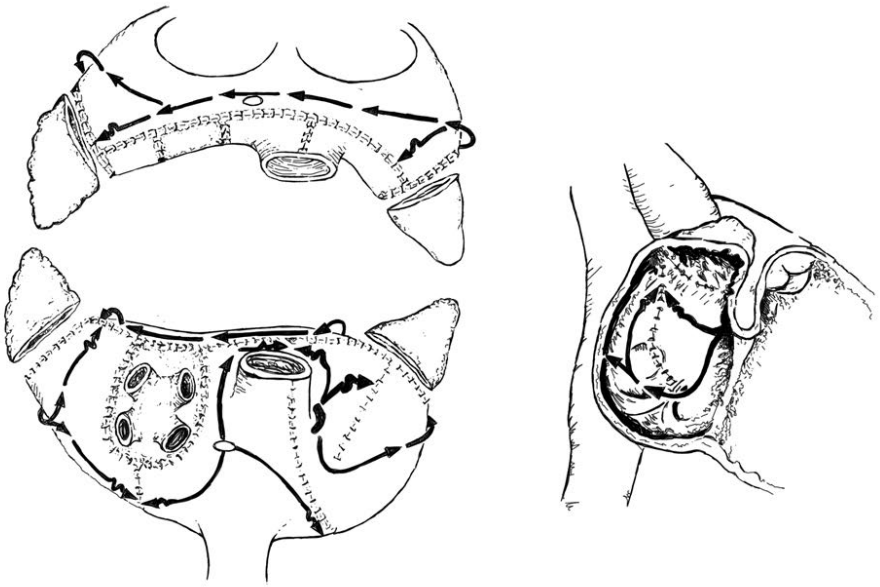

Figure 2.19. Two-dimensional representation of the original Cox-Maze I procedure for atrial fibrillation. In the left panels, the atria are depicted as if viewed from the posterior direction with the back of both atria in the lower panel. The atria are then divided in a sagittal plane and the anterior half of the atria are "flipped" up in the upper panel. The right panel shows the surface of the right atrial septum. Both atrial appendages are excised and the pulmonary veins are isolated [71].

procedure had similar operative risk and long term efficacy when it was applied as a lone procedure or as a concomitant procedure. In addition, in patients with AF and other heart disease, even after successful operation of the underlying disease, AF persists [74]. Therefore, since patients undergoing this operation are exposed to the risks and discomfort of open-heart surgery, the Cox-Maze procedure evolved to being performed concomitantly with other cardiac procedures and eventually this concomitant procedure has been incorporated to the guidelines for the prevention of postoperative AF [5, 6].

This procedure is a a complex surgery which requires multiple atrial incisions and has the potential risk of postoperative morbidities [11]. Additionally, the duration of hospitalization is usually about 1 week, and most patients can return to work within 1-2 months. Therefore, in order to avoid unnecessary risks and discomfort, it is important to maximize the success rate. Some studies suggest that treatment success may depend on adequate patient selection [21]. Therefore, an appropriate preoperative analysis and characterization would help to optimize the Cox-Maze efficacy. For this purpose, doctors use clinical information about the patient, to assess to likelihood of reverting the AF. However, this information can be inaccurate in some cases and there is not a complete consensus of the variables providing most information. In this sense, ECG analysis has not been considered potentially relevant for rendering more precise the clinical definition

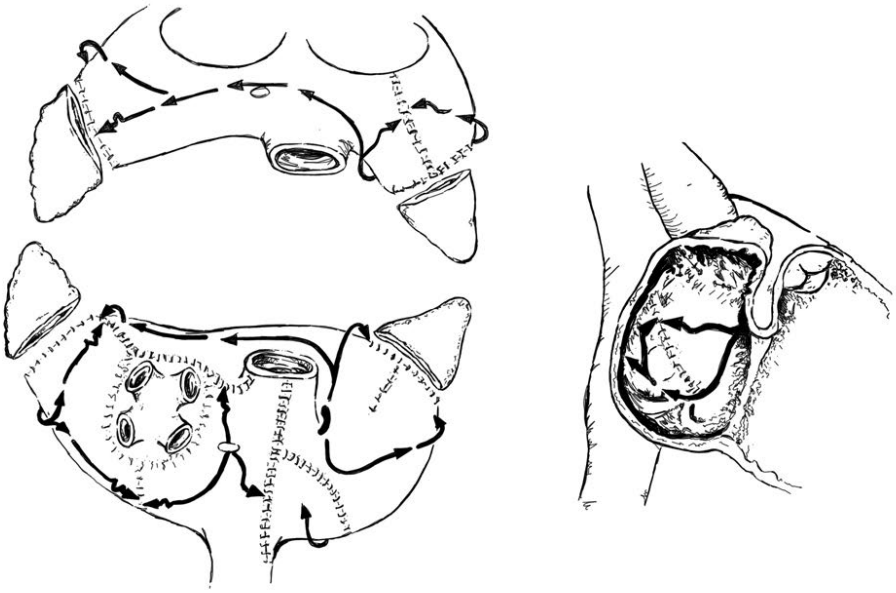

Figure 2.20. Cox-Maze II procedure: Same views as in Figure 2.19. Note that the previous incision through the sinus tachycardia area has been deleted and the transverse atriotomy across the dome of the left atrium has been moved posteriorly to allow better intra-atrial conduction [71].

of AF in current international guidelines [21]. However, it is highly likely that fibrillation of different origins or at different stages of progression, i.e. in different substrates, might manifest with different fingerprints in the ECG tracing [21]. In consequence, the analysis of preoperative ECG could provide useful information to perform a proper selection of patients that should undergo the Cox-Maze surgery. Furthermore, improving and refining the diagnosis of AF by linking it to the underlying causes and mechanisms may be a promising approach for developing a more specific therapy.

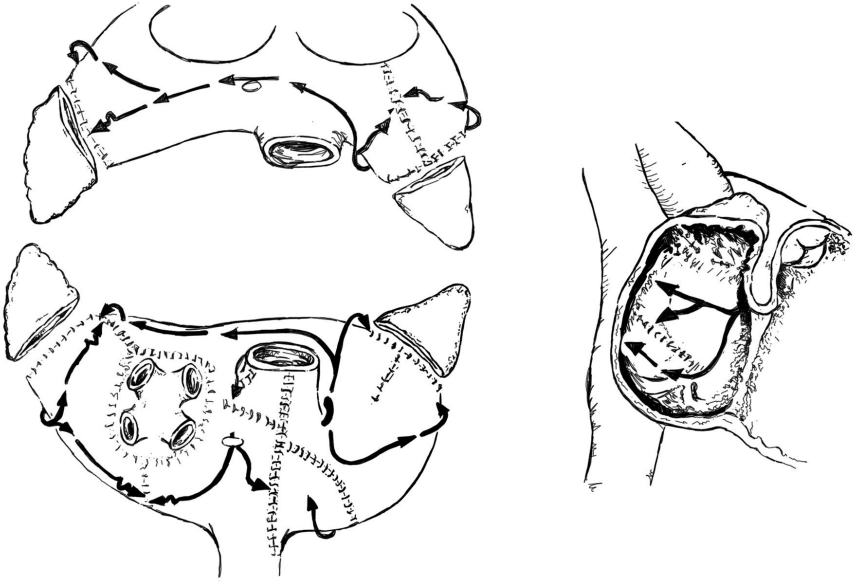

Figure 2.21. Cox-Maze III procedure: Same view as in Figure 2.19. Placement of the septal incision posterior to the orifice of the superior vena cava ,provides excellent exposure of the left atrium [71].

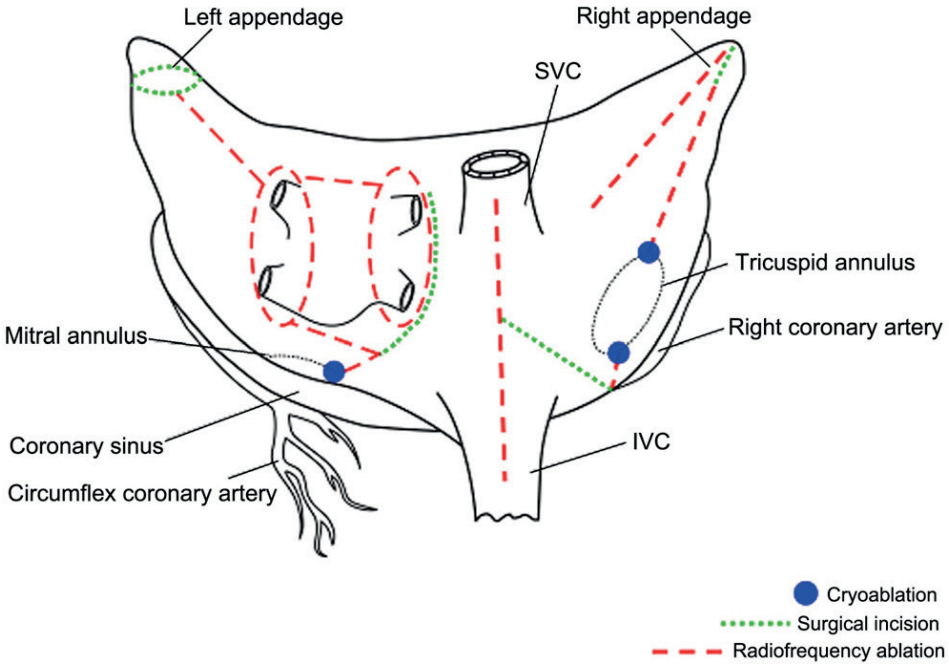

Figure 2.22. Lesions, which have to be set for a complete ablation of atrial fibrillation in the Cox-Maze IV procedure [73].

Chapter 3

Materials and methods

In this chapter, database, materials and methods employed to perform this work are detailed. This includes a description of the patients database gathered to perform the analysis, detailing clinical information and Cox-Maze outcome. Then, the procedure followed to extract the atrial activity from the ECG is explained, describing the signal processing performed. Finally, the indices studied in this work are defined and contextualized.

3.1 Database

The database was composed by 27 patients in persistent or permanent AF for, at least, 3 months, who underwent open heart surgery concomitantly with the Cox-Maze IV procedure. Their clinical characteristics and surgical procedures are shown in Table 3.1.

Patients were treated preoperatively with drugs according to their cardiologist prescription. This treatment included antiarrhythmic drugs, usually Digoxine, Amiodarone or beta blockers. Furthermore, the patients were also under anticoagulant treatment with Sintrom. However, for safety reasons, this treatment was suspended a week before the surgery. After the surgery, antiarrhythmic treatment was performed with Amiodarone (200 mg/day). In case of contraindications, Amiodarone was replaced by beta blockers, mainly Sotalol. Furthermore, the anticoagulant treatment was restarted. It consisted of a dose of Sintrom to maintain an INR between 2 and 3. This drugs prescription was maintained at discharge, regardless of the patient rhythm, and reevaluated after the blanking period (i.e. 3 months). At this period, antiarrhythmic drugs were withdrawn if a stable NSR was recorded. In contrast, if AF persisted after the blanking period, the application of ECV was studied to restore NSR [12]. Nonetheless, in order to avoid additional procedures that may alter the atrial substrate,the database is composed by patients who not underwent ECV. Finally, patients maintaining NSR after 6 months stopped the anticoagulant treatment.

Table 3.1. Description of the clinical characteristics and clinical procedures applied to the patients composing the database. Data are given as mean $\pm$ SD or number of patients. MVR = mitral valve replacement; AVR = aortic valve replacement; CABG= coronary artery bypass graft; TVP = tricuspid valvuloplasty

Clinical parameters		**Surgical cardiac procedures**	
Age (years)	67.1 ± 9.8	MVR	6
Male/female (n)	11/16	AVR	3
AF duration(years)	3.5 ± 3.4	CABG	2
<3 years (n)	12	MVR + TVP	8
3-6 years (n)	12	MVR + AVR	7
>6 years (n)	3	MVR + CABG	1
LA size (mm)	47.6 ± 7		

Regarding Cox-Maze results, at discharge, 15 patients (55.55%) had recovered the NSR while 12 (44.45%) patients remained in AF. Between discharge and the first follow up, which was after the blanking period, 4 patients restored the NSR while no patient relapsed to AF. Previous studies have shown that early arrhyth-

mias may be transient due to the atria inflammation [5]. In consequence, a blanking period of 3 months after the surgery has been defined before taking clinical decisions and reporting results [14]. Thus, the possibility of some patients restoring the NSR between discharge until the first three months was expected. Between 3 and 6 months, all patients maintained the previous rhythm. Hence, at 3 and 6 months follow up, 19 patients were in NSR (70%) and 8 patients were in AF (30%). Finally, between 6 and 12 months, a patient that was in AF at discharge and restored NSR before the blanking period relapsed to AF. In previous studies, early arrhythmias have been identified as a risk factor of late failure of AF surgical ablation [13, 75]. Therefore, this relapse was a possibility. In consequence, after 12 months follow up, 18 (66.67%) patients regained NSR while 9 (33.33%) patients remained in AF.

3.2 Methodology

In this work, a preoperative prediction of the Cox-Maze surgery outcome has been performed. In this way, the procedure efficiency could be improved and furthermore, useful information to understand the AF mechanisms could be obtained. For this purpose, traditional clinical information and information obtained from the ECG analysis was studied and a statistical analysis was made with these data. The prediction was carried out at discharge and then at 3, 6 and 12 months after the surgery. Between the surgery and the discharge, patients were hospitalized and, in consequence, their rhythm was evaluated routinely several times at day. However, after the discharge, patients were doing normal life and, hence, the rhythm was evaluated only in the moment of the follow up.

Regarding the clinical information, it was obtained from the medical history of each patient. Specifically, the information analyzed was the patient's age, the preoperative time in AF and the size of the left atria (LA size) since these indices have proven to be useful predicting AF reversion [11].

To perform the ECG analysis, segments of 20 seconds from standard 12 leads ECGs were recorded less than 24 hours before the surgery. These recordings were obtained using the EKG master USB® system (TEPA, Inc., Ankara, Turkey). This is a device for recording digitalized ECGs from a computer using the software WinEKG Pro® (TEPA, Inc., Ankara, Turkey). Data were recorded with a sampling frequency of 1kHz and with amplitude resolution of 0.4 μV.

The ECG files were analyzed with the software MATLAB® (MathWorks®, MA, USA). Using this software, a digital filtering was applied to the signals. The aim of the filtering was to cancel out noise and interferences such as baseline wander, powerline interference and high frequency and muscle noise. After the preprocessing, the lead V1 was selected to work because is the lead which best represents the AA [16]. On the lead V1, an adaptive cancelation method was applied to extract the AA present in the recording.

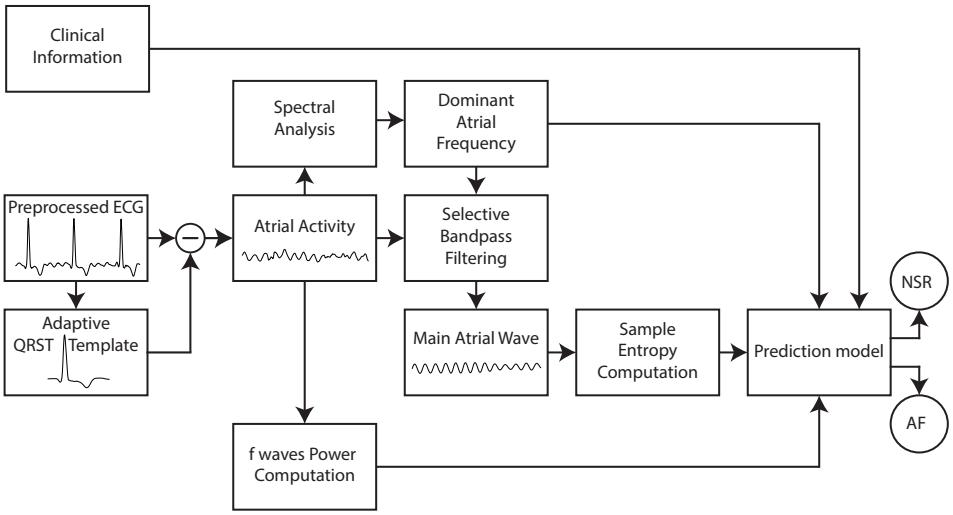

Figure 3.1. Block diagram describing the strategy proposed to predict preoperatively the Cox-Maze outcome.

After obtaining the AA, several algorithms were developed with MATLAB® to characterize the f waves. On one hand, the f waves organization was studied by means of the dominant atrial frequency (DAF) and by computing a non linear index such as the sample entropy (SampEn). On the other hand, the f waves amplitude was analyzed by obtaining the mean power of the AA (fWP).

Given that a non linear method was used in this work, data non linearity had to be studied first to confirm the suitability of the method. To perform the study, the surrogate data test was used. This test consists of generating a set of surrogate data from the original data and then computing a number that quantifies some aspect of the series. When the number computed is significantly different duration between the original data and the surrogate data, the non linearity can be assumed. To study the differences, the Wilcoxon T test was applied.

When all the indices were available, a statistical analysis was performed. First, using the software SPSS® (IBM® Statistics, IBM®, NY, USA) the normality and homoscedasticity of the data was assessed. Then, an analysis was performed to study if the results are statistically significant. After that, the ROC curve was computed over all the indices obtained and a threshold was selected following the criteria of maximizing the accuracy on the predictions. With the threshold selected, the sensitivity (Se), specificity (Sp) and accuracy (Acc) of each index was obtained. Finally, in order to optimize the prediction capability and to detect which indices were complementary, two prediction models were performed: a binary classification tree and a logistic regression. In Figure 3.1 a block diagram summarizing the procedure is shown.

3.3 Signal processing

3.3.1 Preprocessing

In the ECG signal, as in most biomedical signals, the presence of noise is a common problem hardly avoidable since the cardiovascular system cannot be isolated from other adjacent electrical sources [76]. The accurate recording and precise analysis of the ECG signals are crucial due to their extensive applicability and have always relied heavily on state-of-the-art signal processing [77]. Therefore, a set of algorithms which condition the signal with respect to different types of noise have been performed in order to achieve the most accurate analysis possible. The ECG signal is mainly affected by three different sources: the powerline interference, the high frequency and muscle noise and finally, the baseline wander. There are several ways of reducing the influence of these interferences, however, in this work the most widely technique accepted for each source has been performed.

The powerline interference is caused by the electromagnetic fields generated by the powerline. Depending on the region, such noise is characterized by 50 or 60 Hz sinusoidal interference, possibly accompanied by a number of harmonics [76]. Such narrowband noise renders the analysis and interpretation of the ECG more difficult, since the delineation of low-amplitude waveforms becomes unreliable and spurious waveforms may be introduced [78]. Although various precautions can be taken to reduce the effect of powerline interference, for example, by selecting a recording location with few surrounding electrical devices or by appropriately shielding and grounding the location, it may still be necessary to perform signal processing to remove such interference [76]. In this work, an adaptive notch filter at 50 Hz was used to remove the powerline interference because it preserves the ECG spectral information [77, 79].

Regarding the high frequency and muscle noise, it is produced by the recording of the muscle activity or by the movement of patients and electrode. In contrast with the powerline interference, it can not be removed by narrow band filtering, but presents a much more difficult filtering problem since the spectral content of muscle activity considerably overlaps that of the cardiac activity [76]. However, the muscle noise reaches higher frequencies than the ECG, therefore, a lowpass filtering is a usual way of reducing the muscle and high frequency noise. In this work, this noise was reduced by an eight-order forward/backward IIR Chebyshev lowpass filtering, whose cut-off frequency was 70 Hz [76]. In addition, a wavelet denoising was applied because previous studies shown that it is useful to improve signal to noise ratio by canceling out muscular noise [80, 81]. The mother wavelet selected to denoise the ECG was a level 8 Daubechies function [82].

Finally, the baseline wander is characterized as a low frequency noise, usually in the range below 0.5 Hz [76]. It is caused by varying electrode-skin impedance,

patient's movements and breath [83]. Removal of baseline wander is required in order to minimize changes in beat morphology which do not have cardiac origin. A bidirectional high-pass filtering with 0.5 Hz cut-off frequency was used to remove the baseline wander [84].

3.3.2 Ventricular activity cancelation

The analysis of AA in the ECG is complicated by the simultaneous presence of ventricular activity which overlap in time and frequency with the AA and is of larger amplitude [85]. Therefore, obtaining the AA from the ECG under the best conditions is crucial in the study of the electrophysiological processes that underlie AF, such as refractory periods, autonomic response, drugs effects, etc [86]. The extraction of an atrial signal during AF requires nonlinear signal processing since atrial and ventricular activities overlap spectrally and therefore cannot be separated by linear filtering [66]. There are to approaches to analyze the AA: isolate segments free of QRST segments where only f waves are present or cancel the ventricular activity and obtain a residual ECG that consists only of AA. However, although the analysis of ECG segments free of QRST segments offers a simple solution, it is not suitable when a continuous analysis is required or in patients with high ventricular rates, in which case the atrial signal can be completely obscured [87].

To date, several cancelation methods have been proposed to extract AA from the surface ECG. The most powerful techniques are those that exploit the spatial diversity of the multilead ECG [87] such as the method that solves the blind source separation problem [88] or the spatiotemporal QRST cancelation strategy [89]. However, the performance of these techniques is notably reduced when only a few leads are available [86].

For single-lead applications, average beat subtraction (ABS) is the most accepted technique for atrial signal extraction and relies on the fact that AF is uncoupled to the ventricular activity [66]. This method was presented first by Slocum et al [90] and is based on the assumption that the average beat can represent approximately each individual beat. In this method, fiducial points from ventricular complexes are detected and aligned. Next, an average beat is generated where the window length is determined by the minimum or mean RR interval [68]. The window was aligned such that 30% of it preceded the fiducial point and 70% followed it [91]. A template of average beats was constructed and subtracted from the original signal, resulting in the atrial activity with subtracted ventricular activity [68]. ABS relies on the assumption that an average beat represents each individual beat accurately [85]. However, QRST morphology is often subject to minor changes caused by respiration, patient movement, etc, and, therefore, QRST residua and noise are often present in the estimated AA or remainder ECG [85]. Additionally, in clinical practice the ECG consists of recordings that are 10 s long and, therefore, a high-quality QRST cancelation template may be difficult to obtain [86]. In consequence, in this work, a modification of the ABS method, which

is based on adaptive singular value cancellation (ASVC) of each single beat [86], was used.

The ECG signal presents a high degree of temporal redundancy which is exploited by the ASVC method for perform ventricular activity cancellation. First, this method detects all the R waves using the Pan and Tompkins technique [92]. Next, the starting point of each QRST complex is defined as $s_i = r_i - 0.3 \cdot RR_{min}$, being r_i the R peak wave event and RR_{min} the minimum RR interval found in the ECG. On the other hand, the ending point of each QRST segment is defined as $e_i = r_i + 0.7 \cdot RR_{min}$ [86]. Figure 3.2 depicts the fiducial points and relevant time instants described herein.

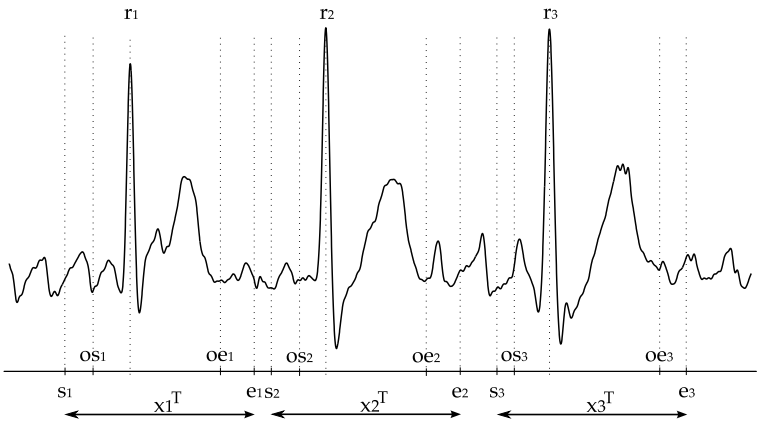

Figure 3.2. Relevant temporal instant used by the ASVC. The points s_i and e_i are the start and end points of the i-th QRST complex which is represented by x_i, respectively. The points os_i and oe_i define the zones, at the beginning and the end of the i-th QRST complex, that will be processed to avoid sudden transitions after ventricular cancellation [86]

For a compact notation, each QRST segment was assumed to be represented by a column vector of the matrix $\mathbf{X} \in \Re^{L \times N}$:

$$\mathbf{X} = [\mathbf{x}_1, \mathbf{x}_2, \ldots, \mathbf{x}_N] \tag{3.1}$$

where $\mathbf{x}_i$ contains L samples of i-th complex, and N is the complexes number in the analyzed ECG.

Once the QRST segments are defined, all the beats are temporally aligned using its R peak timing and their eigenvector sequence is obtained by singular value decomposition (SVD). SVD of the $\mathbf{X}$ matrix can be expressed as:

$$\mathbf{X} = \mathbf{U}\mathbf{S}\mathbf{V}^T \tag{3.2}$$

where $\mathbf{U} \in \Re^{L \times N}$ is an unitary matrix so that $\mathbf{U}\mathbf{U}^T = \mathbf{I}$, $\mathbf{S} \in \Re^{N \times N}$ is an diagonal matrix, and $\mathbf{V} \in \Re^{N \times N}$ fulfills $\mathbf{V}\mathbf{V}^T = \mathbf{I}$, $\mathbf{I}$ being the identity ma-

trix. The matrix $\mathbf{U}$ contains the N normalized principal components of $\mathbf{X}$, so that the columns of $\mathbf{U} = [\mathbf{u}_1 \ldots, \mathbf{u}_N]$ are the eigenvectors of $\mathbf{X}$, and their cross-correlation coefficients are nulls. The matrix $\mathbf{S}$ contains the amplitude coefficients corresponding to the N principal components of $\mathbf{X}$. These coefficients are called eigenvalues or singular values and are sorted in descending order. Thus, the N non-normalized principal components can be obtained as the columns of the matrix $\mathbf{P} = \mathbf{US}$, and can be interpreted as follows [86]:

- The most significant component is related to the main QRST waveform.
- Subsequently, there are several components related to AA.
- The remaining components correspond to noise.

As the ABS, this method relies on the assumption that the AA can be viewed as being uncoupled to ventricular activity and noise. Thus, each observed beat can be modelled as a sum of AA ($\mathbf{x}_{AA}$), ventricular activity ($\mathbf{x}_{VA}$) and noise ($\mathbf{x}_n$) [93, 88]:

$$\mathbf{x} = \mathbf{x}_{AA} + \mathbf{x}_{VA} + \mathbf{x}_n \tag{3.3}$$

Hence, the first principal component of $\mathbf{X}$, which is called $\mathbf{t}$ and is the one with the highest variance is considered as the representative ventricular activity. Thereby, it can be used as QRST template to cancel out ventricular activity. However, since there are considerable differences in the R peak amplitude between each individual QRST complex and template, the $\mathbf{t}$ amplitude is individually adapted to each beat:

$$\mathbf{t}_i = \frac{QR_i}{QR_{\mathbf{t}}} \cdot \mathbf{t} \tag{3.4}$$

where QR_i and $QR_{\mathbf{t}}$ are the distances between the Q and R points of the i-th complex and template, respectively. Then, in other to obtain the AA estimation, the adapted template is temporally aligned with its corresponding R peak, and the AA estimation ($\widehat{\mathbf{X}}_{AA}$) contained in every QRST interval is obtained as:

$$\widehat{\mathbf{X}}_{AA} = \mathbf{X} - \mathbf{T} \tag{3.5}$$

being $\mathbf{T}$ the matrix constituted by the column vectors $\mathbf{t}_i$:

$$\mathbf{T} = [\mathbf{t}_1, \mathbf{t}_2, \ldots, \mathbf{t}_N] \tag{3.6}$$

In most of the ABS works, the ventricular template has been performed using all the available beats. However, the ASVC selects the most suitable complexes

to obtain the most accurate QRST template for each beat [86]. A correlation-similarity-based strategy is applied and the N most similar QRST complexes to those under cancelation are used to generate the template. The similarity between QRST complexes is evaluated using the cross-correlation. In this work, since the initial recordings are 4 minutes long, following previous studies, the 24 beats most similar to the one to be canceled have been used to generate the template [86].

In the AA reconstructed from $\widehat{\mathbf{X}}_{AA}$, sudden transitions may occur at the beginning or the end of each QRST segment, see Figure 3.3(b). They are provoked by the subtraction between each individual complex and the ventricular cancellation template. In order to avoid these transitions and obtain a more accurate AA, two steps are developed before $\widehat{\mathbf{X}}_{AA}$ is obtained. Firstly, within two P samples intervals after the start point and before the end point of each QRST complex respectively, the points os_i and oe_i are selected, see Figure 3.2. In these temporal instants, the absolute minimum difference between the i-th complex and $\mathbf{t}_i$ is obtained:

$$os_i = \min_{k=1,\ldots,P}(|x_i(k) - t_i(k)|) \tag{3.7}$$

$$oe_i = \min_{k=L-P,\ldots,L}(|x_i(i) - t_i(k)|) \tag{3.8}$$

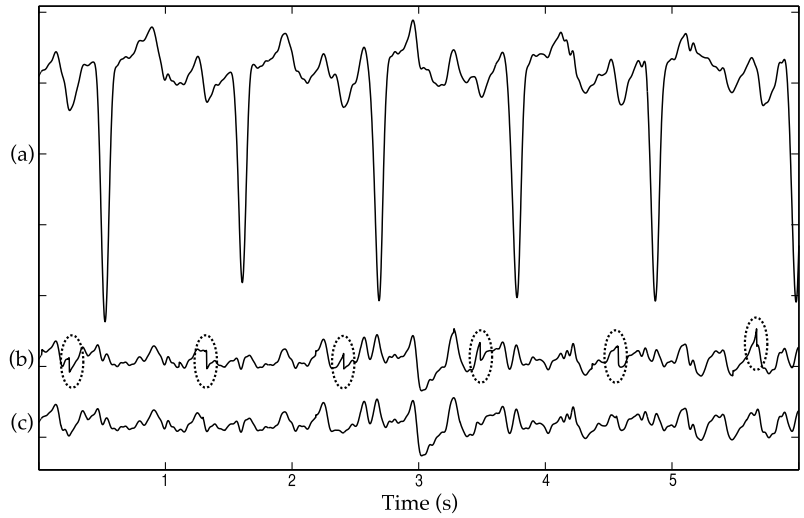

Figure 3.3. (a) Synthetic ECG. (b) AA obtained with sudden transitions ($\widehat{\mathbf{X}}_{AA} = \mathbf{X} - \mathbf{T}$). (c) AA obtained without transitions.

Considering these instants, the ventricular template adapted to each beat is modified as follows:

$$\tilde{\mathbf{t}}_i = [\underbrace{0,\ldots,0}_{os_i-1}, t_i(os_i), t_i(os_i+1), \ldots, t_i(L-oe_i-1), t_i(L-oe_i), \underbrace{0,\ldots,0}_{oe_i-1}]^T \quad (3.9)$$

The new AA is obtained as $\widehat{\mathbf{X}}_{\mathbf{AA}} = \mathbf{X} - \widetilde{\mathbf{T}}$ and, thus, the sudden transitions are minimized. Secondly, in order to removed completely these transitions, a processed $2{\cdot}M$ samples-length gaussian window is added to AA over each transition. The Gaussian window with a maximum amplitude of 1 is generated and divided into two parts. The first M samples form the signal w_1 whereas the last M samples are w_2. These signals are weighted by the constants k_s and k_e, which are calculated as the midpoints between the i-th complex and $\tilde{\mathbf{t}}_i$ values at the instants os_i and oe_i, respectively:

$$k_s = \frac{\widehat{x}_{AA}(s_i + os_i - 1) - \widehat{x}_{AA}(s_i + os_i)}{2} \quad (3.10)$$

$$k_e = \frac{\widehat{x}_{AA}(e_i - oe_i) - \widehat{x}_{AA}(e_i - oe_i + 1)}{2} \quad (3.11)$$

Note that $\widehat{x}_{AA}$ is the representation of the AA signal obtained from $\widehat{\mathbf{X}}_{\mathbf{AA}}$ after the ventricular activity cancelation. Finally, the two transitions relative to the i-th complex are removed by adding or subtracting to AA the signals w_1 and w_2 weighted by the constants k_s and k_e as follows:

$$\begin{aligned}[\widehat{x}_{AA}(s_i + os_i - M), \ldots, \widehat{x}_{AA}(s_i + os_i)]^T = \quad (3.12)\\ = [\widehat{x}_{AA}(s_i + os_i - M), \ldots, \widehat{x}_{AA}(s_i + os_i)]^T - k_s \cdot w_1^T\end{aligned}$$

$$\begin{aligned}[\widehat{x}_{AA}(s_i + os_i + 1), \ldots, \widehat{x}_{AA}(s_i + os_i + M)]^T = \quad (3.13)\\ = [\widehat{x}_{AA}(s_i + os_i + 1), \ldots, \widehat{x}_{AA}(s_i + os_i + M)]^T + k_s \cdot w_2^T\end{aligned}$$

$$\begin{aligned}[\widehat{x}_{AA}(e_i - oe_i - M), \ldots, \widehat{x}_{AA}(e_i - oe_i)]^T = \quad (3.14)\\ = [\widehat{x}_{AA}(e_i - oe_i - M), \ldots, \widehat{x}_{AA}(e_i - oe_i)]^T - k_e \cdot w_1^T\end{aligned}$$

$$\begin{aligned}[\widehat{x}_{AA}(e_i - oe_i + 1), \ldots, \widehat{x}_{AA}(e_i - os_i + M)]^T = \quad (3.15)\\ = [\widehat{x}_{AA}(e_i - oe_i + 1), \ldots, \widehat{x}_{AA}(e_i - oe_i + M)]^T + k_e \cdot w_2^T\end{aligned}$$

Therefore, with the described process an AA signal without sudden transitions can be obtained, such as Figure 3.3(c) shows. Following previous studies optimizing P and M, the values selected were 40 and 20 samples respectively.

Finally, note that the AA obtained contains the noise present during the recording process (x_n). Anyway, this interfering signal is of notably lower amplitude than the AA during a normal recording. Moreover, a relevant part of it can be removed through the preprocessing methods described in section 3.3.

As an illustration on how the ABS-based methods can behave, Figure 3.4 plots the comparison between the simple ABS method and the ASVC method. As can be appreciated, the AA obtained with ASVC presents lower ventricular residue and higher similarity of atrial segments than those obtained with ABS.

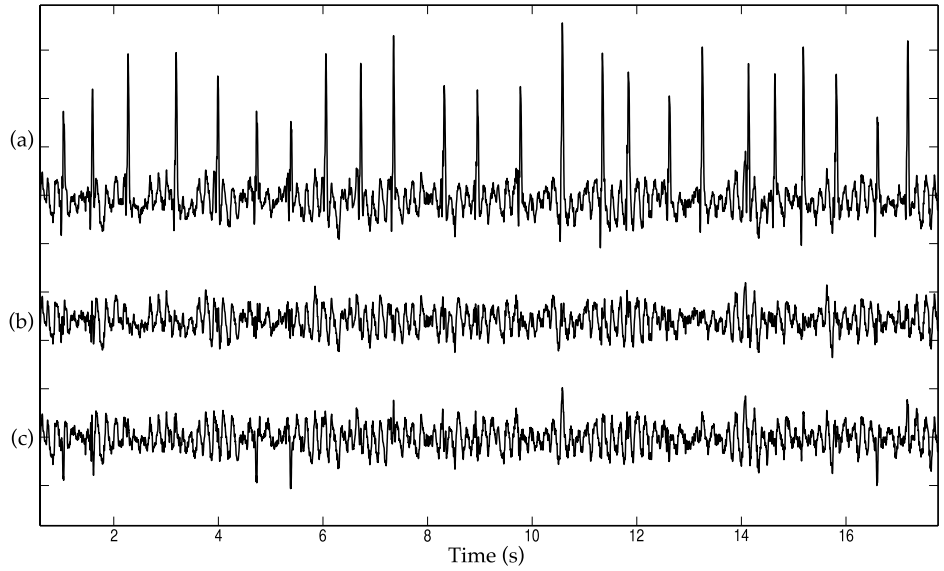

Figure 3.4. (a) Real ECG of a patient. The corresponding AA signals obtained with (b) ASVC and (c) ABS methods.

There are also, some techniques that exploit the spatial diversity of the multilead ECG [87], such source separation [88] or the spatiotemporal QRST cancelation strategy [93]. In the spatiotemporal QRST cancellation, the average beats of adjacent leads are mathematically combined with the average beat of the analyzed lead in order to suppress the electrical axis alterations and produce optimal cancelation [93]. On the other hand, source separation techniques exploit the property that atrial and ventricular activities arise from different bioelectrical sources [66]. These two sources, exhibiting different statistical properties, can be separated when multi-lead ECG recordings are available [85]. Source separation techniques are able to use the multi-lead information provided by the ECG to obtain a unified atrial activity dominated by the lead with the largest atrial ac-

tivity [66]. This techniques are powerful, however, these methods are addressed to multilead ventricular activity cancelation. In this work, since the metrics computed are used in one lead (V1), the study is focused in just one lead, thus a single lead cancellation method was selected. In addition, multilead methods are complicated to implement while the ASVC is simpler to understand and perform. Finally, the ASVC provides an accurate enough cancellation, as Figure 3.4 shows.

3.4 Clinical indices

Clinical and electrophysiological studies have lead to a better understanding of AF. From these studies several causes that promote AF maintenance and recurrence have been detected. The most important clinical causes observed are AF duration, atrial dilatation and patient's age [14, 21]. This information has also be found as the most relevant risk factors of AF recurrence after Cox-Maze procedure [11]. Therefore, these three causes were studied.

3.4.1 Preoperative atrial fibrillation duration

An important clinical observation is that AF itself modifies the atrial properties and, therefore, the higher the time in AF the higher the probability of AF maintenance and AF recurrence [94, 95]. In fact, AF duration has proven to be a risk factor to AF recurrence in many different scenarios [11, 96].

In the classic experiments of Wijffels and co-workers in goats [15], AF induced by rapid atrial pacing became sustained over time. In these studies, marked changes were observed in the atrial refractory period which, during the first 24 hours of fibrillation. This progressive shortening of the wavelength by atrial fibrillation provides a good explanation for the observed stabilization of AF with time [96]. In addition, AF duration also decreases the rate adaptation of the atrial refractory period [95, 15]. This anomalous rate adaptation can cause atrial fibrillation to become sustained and play an important role in the recurrences of AF [15]. These changes in the atrial refractory period are produced in the first stages of AF, however, a long standing AF results in the development of progressive structural changes [95, 97, 98]. Therefore, preoperative AF duration may be also related to a more significant atrial tissue remodeling, resulting in extensive fibrosis, electrical remodeling and loss of atrial muscle mass [19]. Regarding its relation with the Cox-Maze procedure, several studies have found this information as a risk factor to long term AF recurrence [11, 19, 99].

The problem with the AF duration is that usually it is difficult to know the first episode of AF in a patient, therefore, this value may be inaccurate sometimes. In this study, the preoperative AF duration has been measured from the first recorded AF episode until the surgery day.

3.4.2 Left atrial size

Atrial dilatation can be the cause as well as the consequence of AF [96]. The high incidence of AF in the presence of mitral stenosis and/or mitral insufficiency strongly suggests atrial dilatation to be a cause of AF[96]. Other evidence that atrial stretch may cause an increased propensity for AF was provided by animal studies in which AF was produced by mitral insufficiency or acute volume expansion [100, 101]. However, other studies found that with the maintenance of AF, the atrial size increased [98, 65]. In addition, some studies shown that after successful cardioversion, the dimensions of the atria decreased [102, 103]. In consequence, several studies were performed relating the atrial dilatation with the Cox-Maze long term outcome [11, 99, 13]. Therefore, atrial dilatation is considered a well-established risk factor for the development and maintenance of AF [95, 104].

Atrial dimensions are a particularly important determinant of the occurrence of multiple-circuit reentry [105]. Larger atrial size increases the amount of atrial tissue that can accommodate reentry circuits and, therefore, long-wavelength circuits that are too large for a normal atrium can be supported [105] (Figure). As a consequence, in larger hearts atrial fibrillation is more stable and of longer duration [15]. This can be easily understood by realizing that the number of circuits in the atria increases with the square of the atrial diameter and that in larger mammals the wavelength of the atrial impulse does not increase proportionally to the size of the atria [15]. In conclusion, the ability of the atria to fibrillate is determined by the relation between the effective refractory period of the atrial myocardium and the atrial area available for the macroreentrant circuit, thus an enlarged atrial size is more likely to have AF recurrence [106].

Traditionally, atrial dilatation has been studied through the left atrial size [11, 107, 20]. Therefore, in this work the left atrial size has been obtained through echocardiography.

3.4.3 Patient's age

The AF is an arrhythmia that increases its prevalence with age [5]. This increasing prevalence is likely due to accumulating predisposing factors and increasing myocardial fibrosis, which also involves the atria [21]. Therefore, AF development and recurrence may be promoted by natural aging changes in the atria. In consequence, several works have studied and found increased age as a risk factor of AF recurrence after the Cox-Maze procedure [11, 20, 108]. However, it has not been reported as a predictor for late failure in all studies [11, 19, 13]. In any case, increased age is considered as one of the most significant risk factors for the development and maintenance of AF [6, 95]. In addition, AF risk prediction based on risk factors is supposedly less accurate in older persons than in middle-aged adults [21].

In the studies of Spach and Dolber [109], they found that the anisotropic electrical properties of human atrial muscle change with advancing age to produce increasingly complex pathways of propagation at a microscopic level. The progressive change from uniform to nonuniform anisotropic electrical properties with increasing age causes that reentries are able occur in progressively smaller regions [109]. It has also been found a generalized conduction slowing with increasing age, frequently associated with intersticial fibrosis [110]. Additionally, in older people, there is a larger interregional dispersion in the action potential duration [111]. Spatial differences in refractoriness may cause transient conduction block in localized areas, and slow conduction in such a setting may be dependent on encroachment into the relative refractory period [111]. The described changes are consistent with the development of AF [95].

On the other hand, atrial refractory period has been found to increase with age [5, 110]. Additionally, the study of Anyukhvosky in dogs [111] found that persistent and permanent AF decreased the action potential duration heterogeneity in older dogs while in young dogs the effect of AF increased it. Although these characteristics might potentially be protective, it is probable that this effect is overshadowed by the conduction changes and structural abnormalities [110].

These studies suggest that the mechanism triggering AF may be different between younger and older patients with AF, because younger patients did not have a marked substrate for AF and might need many trigger beats to induce AF. These studies also point that the structural changes associated with age may promote AF, creating an substrate for atrial propensity to AF [110].

3.4.4 Patient's weight

The presence of overweight and obesity has demonstrated to be an independent risk factor for development of AF in the general population [112, 113]. Additionally, a recent longitudinal cohort study over 21 years suggested that obesity was an independent predictor of progression from paroxysmal to permanent AF [114]. Although the precise mechanism for this association is not well understood, changes in atrial and ventricular structure, diastolic function, autonomic function, and increased total blood volume might play a role [115].

Regarding the relation between weight and AF recurrence after reversion therapies, the results are inconclusive. Studies relating ECV and obesity have obtained that the ability to perform it successfully was similar regardless of the body mass index (BMI) [116]. However, studies related to internal cardioversion found that larger BMIs are associated with increased defibrillation thresholds [117]. With respect to the catheter ablation technique, there are studies that found obesity significantly associated with a higher incidence of recurrence of AF [118, 119, 120] while other studies did not found any relation [121]. Finally, other studies found an decrease in ablation success but without obtaining statistical significant differences [122, 123].

To the best of our knowledge, there are no studies relating obesity and Cox-Maze outcome. However, since patient's weight is related to AF onset and may be related to AF recurrence, the patient's weight and BMI have been studied as potential predictors of Cox-Maze outcome.

3.5 Electrocardiographic indices

From a clinical point of view, the characterization of the AF from the standard surface ECG is very interesting, because it can be easily and cheaply obtained [16]. In addition, previous AF studies have shown to be capable of predicting AF termination in different scenarios such as spontaneous termination [28] or ECV [29]. These studies obtain the AA from the ECG and then characterize it. However, ECG analysis has not been widely used to predict the outcome after an aggressive intervention, such as the Cox-Maze surgery. Therefore, the ECG analysis was used to predict preoperatively the Cox-Maze outcome. The AA characteristics used were the f waves organization and amplitude.

AF organization has been defined as how repetitive the AA signal pattern is [31]. It has been related to the number of coexisting wavelets, which is determined by the product of conduction velocity and refractory period (wavelength) [27, 30]. The smaller the wavelength, either by conduction slowing, refractory period shortening, or both, the greater the number of possible reentrant circuits and, subsequently, the more easily AF is induced and maintained [30]. Two metrics have been used to assess the AF organization. The first one is a widely used index, the dominant atrial frequency (DAF) [27]. On the other hand, the second way to get a non-invasive estimate of AF organization has been based on a nonlinear regularity index, such as sample entropy [124].

Regarding the f waves amplitude, it has been used to predict long term Cox-Maze surgery outcome with accurate results [24]. In fact, low amplitude fibrillatory wave is accepted as a risk factor of late recurrence of AF after surgical treatment[106, 125]. The f waves amplitude represents the sum of local depolarization phenomena involving cardiac cells, which is related to the magnitude of remaining viable atrial muscle[25]. Therefore, f wave amplitude is mainly affected by the state of the atrium, such as atrial fibrosis and degeneration as well as the atrial size [24]. In consequence, a lower f amplitude is associated with greater atrial fibrosis and degeneration resulting in a lower likelihood of NSR restoration.

3.5.1 Dominant atrial frequency

Previous studies have demonstrated that the atrial component during AF is typically an oscillation with a main frequency in the 3-9 Hz range [27, 30], therefore, spectral analysis applied to the AA signal is an appropriate approach to its characterization. The dominant atrial frequency (DAF) is defined as the frequency

with the highest amplitude in the 3-9 Hz band of the AA power spectrum [93]. This metric has been related to the atrial refractoriness and, therefore, to the main atrial cycle length, which reflects the atrial organization [126]. Moreover, it has been suggested that patients with low DAF have longer atrial wavelengths and, therefore, a smaller number of activation wavefronts [127]. On the contrary, patients with a high fibrillatory frequency present shorter wavelengths and higher number of simultaneous wavelets [127].

Spectral techniques have been widely used to measure organization during AF through detecting the main average fibrillatory rate [128]. Initially, the spectral analysis was performed over endocardial electrograms [129, 130]. However, the rise of the AA extraction methods from ECGs allowed to perform spectral analysis over surface recordings. To this respect, validations were performed to ensure the reliability of estimating the DAF over the ECG. These studies compared the results with atrial electrograms and showed that the DAF obtained from the standard lead V1 is highly correlated with the fibrillatory rate of the right atrium [27, 131, 132]. In consequence, several studies have been performed over surface ECG [30, 28, 133].

To compute the DAF, the Power Spectral Density (PSD) was obtained by using the Welch periodogram. As computational parameters, a Hamming window of 4096 points in length, a 50% overlapping between adjacent windowed sections and a 8192-point fast Fourier transform (FFT) were used [134]. These parameters have proved their effectiveness in finding the DAF in a number of previous studies [133, 135]. On Figure 3.5, the DAF obtained from a patient recording is illustrated.

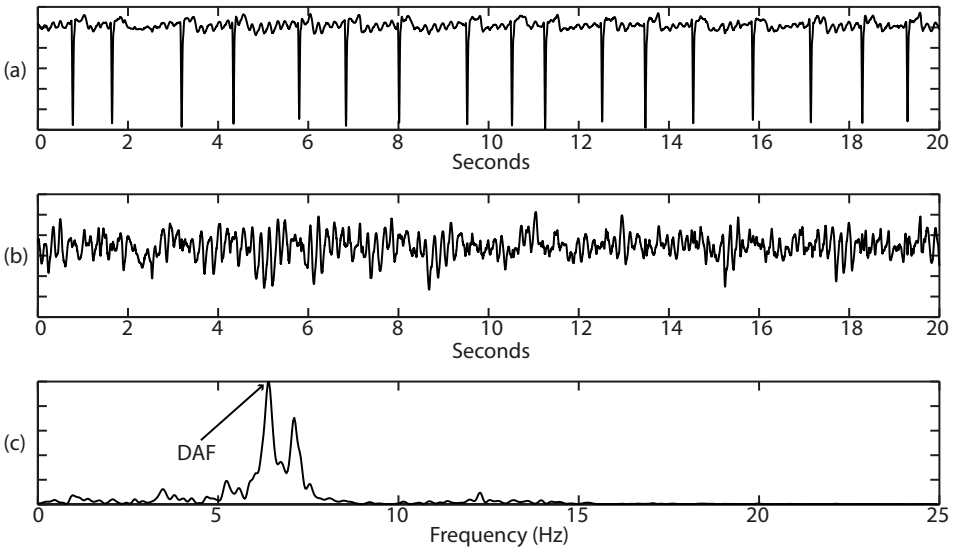

Figure 3.5. (a) Real ECG of a patient. (b) AA extracted from the ECG. (c) Computed PSD from the AA and DAF obtained

3.5.2 Sample Entropy

SampEn is a non-linear index used as a measure of time series regularity [124], thus, this metric is applied to assess f waves regularity and thereby, to measure AA organization. SampEn application to AF is justified because non-linearity is a necessary condition for a chaotic behaviour, and therefore, is present in a diseased heart with AF at cellular level and because the electrical remodeling in AF is not a linear process [136]. According to these conditions, several studies have demonstrated that SampEn is an accurate index of AF termination [29, 137].

SampEn examines time series for similar epochs and assigns a non-negative number to the sequence, with larger values corresponding to more complexity or irregularity in the data [124]. Two input parameters must be specified to compute SampEn, the length of the sequences to be compared, m, and the pattern similarity tolerance, r. In principle, the accuracy and confidence of the entropy estimate improve as the number of length m matches increases. The number of matches can be increased by choosing small m (short templates) and large r (wide tolerance). However, penalties appear when too relaxed criteria are used [138]. For smaller r values, poor conditional probability estimates are achieved, while for larger r values, too much detailed system information is lost and SampEn tends to 0 for all processes. To avoid a significant noise contribution on SampEn calculation, one must choose r larger than most of the noise [138]. As suggested in previous studies, in the context of AF, the optimal values are $m = 2$ and $r = 0.35$ times the data standard deviation [139]. Therefore, these values were selected.

$SampEn(m, r, N)$, being N the length of the time series, is the negative natural logarithm of the conditional probability that two sequences similar for m points remain similar at the next point, where self-matches are not included in calculating the probability. Thus, a lower value of SampEn also indicates more self-similarity in the time series. Unlike other nonlinear regularity indices, SampEn is largely independent on record length [124].

Formally, given N data points from a time series $\{x(n)\} = x(1), x(2), \ldots, x(N)$, SampEn can be defined as follows:

1. Form m vectors $X_m(1), \ldots, X_m(N-m+1)$ defined by $X_m(i) = [x(i), x(i+1), \ldots, x(i+m-1)]$, for $1 \leq i \leq N-m+1$. These vectors represent m consecutive x values, starting with the ith point.

2. Define the distance between vectors $X_m(i)$ and $X_m(j)$, $d[X_m(i), X_m(j)]$, as the absolute maximum difference between their scalar components:

$$d[X_m(i), X_m(j)] = \max_{k=0,\ldots,m-1} \Big(|x(i+k) - x(j+k)| \Big) \tag{3.16}$$

3. For a given $X_m(i)$, count the number of j ($1 \leq j \leq N-m$, $j \neq i$), denoted as B_i, such that the distance between $X_m(i)$ and $X_m(j)$ is less than or equal

to r. Then, for $1 \leq i \leq N-m$,

$$B_i^m(r) = \frac{1}{N-m-1} B_i \tag{3.17}$$

4. Define $B^m(r)$ as

$$B^m(r) = \frac{1}{N-m} \sum_{i=1}^{N-m} B_i^m(r) \tag{3.18}$$

5. Increase the dimension to $m+1$ and calculate A_i as the number of $X_{m+1}(i)$ within r of $X_{m+1}(j)$, where j ranges from 1 to $N-m$ ($j \neq i$). We then define $A_i^m(r)$ as

$$A_i^m(r) = \frac{1}{N-m-1} A_i \tag{3.19}$$

6. Set $A^m(r)$ as

$$A^m(r) = \frac{1}{N-m} \sum_{i=1}^{N-m} A_i^m(r) \tag{3.20}$$

Thus, $B^m(r)$ is the probability that two sequences will match for m points, whereas $A^m(r)$ is the probability that two sequences will match for $m+1$ points. Finally, sample entropy can be defined as:

$$SampEn(m,r) = \lim_{N\to\infty} \Big\{ -\ln \Big[\frac{A^m(r)}{B^m(r)} \Big] \Big\} \tag{3.21}$$

which is estimated by the statistic

$$SampEn(m,r,N) = -\ln \Big[\frac{A^m(r)}{B^m(r)} \Big] \tag{3.22}$$

Main atrial wave

A SampEn shortcoming is that is sensitive to noise and ventricular residues [140, 141]. Therefore, previous works have proved that in order to obtain a more reliable result, by reducing the influence of these nuisance signals as well as to enhance the fundamental features of the AA, the SampEn has to be computed over the Main Atrial Wave (MAW) [141]. MAW can be considered as the fundamental waveform associated to the AA, its wavelength being the inverse of the AA dominant frequency [27]. The MAW was extracted by applying a selective filtering to the AA signal centered on the DAF.

To prevent distortion, a FIR filter was used [76]. Chebyshev approximation was preferred because all the filter parameters can be suitably fitted and minimum ripple in the pass and stop bands was needed. Therefore, a high order filter should be used, such as the Kaiser approximation marks [142]:

$$L = \frac{-20\log_{10}(\sqrt{\delta_1\delta_2}) - 13}{14.6\Delta f} + 1 \tag{3.23}$$

where L is the filter order, δ_1 and δ_2 are the pass and stop bands ripple, respectively, and Δf is the transition bandwidth between bands. A selective filter must have δ_1 and δ_2 lower than 0.5% of the gain and Δf lower than 0.01 Hz, thereby its order must be greater than 250.

The selected filter bandwidth should be lower than 6 Hz because the typical AA frequency range is around 3-9 Hz [93, 66]. and the first armonic has to be excluded. Following previous works, the filter had a 3 Hz bandwidth and 768 filter coefficients with a sidelobe attenuation of 40 dB [141].

Surrogate data test

Given that SampEn is a non-linear metric, data non-linearity was analyzed by means of the surrogate data test. The technique involves specifying a null hypothesis H_0 describing a linear process and then generating a set of surrogate data from the original signals [143]. Then, a number that quantifies some aspect of the series, called discriminating statistic, is computed over the dataset. When the discriminating statistic of the original series is significantly different than the surrogate data values, non-linearity can be assumed [144]. In the present work 40 surrogate data were generated for each AA signal by means of the iterative amplitude adjusted Fourier transform algorithm[145]. The analyzed statistic was SampEn and the Wilcoxon T test was performed to compare the distributions of the SampEn from the original data and surrogate data.

3.5.3 Fibrillatory waves mean power

Initially, the f waves amplitude was estimated measuring the greatest f wave, with the aid of calipers, from the upper edge of the trough to the upper edge of the peak, and expressing it in millimeters [23, 24]. Later Xi *et al* [146] proposed an algorithm in which the f wave amplitude was computed as the mean value of the four waves with the highest amplitude. However, these methods are manual and , therefore, user dependent. In this work, an automatic and reliable method as been used, the f waves mean power (fWP) [133].

The fWP index can be considered as a robust estimation of the energy carried by the AA signal within the interval under analysis. As a consequence, it can also be considered as a reliable indicator of the AA signal amplitude [133]. Thereby, the fWP was obtained by computing the root mean square value of the AA [133]. Before extracting the AA signal, each analyzed ECG segment was normalized to its maximum R peak amplitude. This operation avoided all the effects that can modify the ECG amplitude as a function of the different gain factors during

recording, electrodes impedance, skin conductivity, etc [133]. In any case, this intra-patient normalization did not affect the computation of DAF and SampEn. In the first case, because the spectral distribution of a signal is independent of its amplitude. In the second, because the tolerance r was normalized to the standard deviation of the data.

3.6 Prediction model development

This work analyzes the performance of many different predictors individually. However, these predictors may contain complementary information and, therefore, the accuracy could be optimized by combining the predictors. Hence, with the aim of optimizing the prediction capability and investigating the relationship between predictors, predictive modelling was used.

Predictive modelling is a name given to a collection of mathematical techniques having in common the goal of finding a mathematical relationship between a target, response, or "dependent" variable and various predictor or "independent" variables. This relations are suppose to allow to predict future values of the target variable by measuring values of those predictors and inserting them into the mathematical relationship. The use of a predictor model allows the complex combination of many potential predictor variables allowing a better use of all the information available.

In this work, the result is a binary variable (NSR or AF), therefore, the models that must be used are classification models. In this way, two of the most widely used classification models were used: a classification tree and a logistic regression [147].

3.6.1 Classification tree

A classification tree is a popular tool in applied statistics because it is easy to understand and the interpretation of the output is straightforward. In addition, a classification tree is non parametric and therefore, this method does not require specification of any functional form. This prediction model works by specifying a set of rules and the resulting prediction [147]. For this purpose, a tree is built with the input features starting from a root node, which includes all patients [148]. Beginning with this node, an input parameter is used to perform a classification rule in order to split the node into two child nodes [148]. When a node can not split, it becomes a leaf node. Leaf nodes give a classification that applies to all instances that reach the leaf [147]. Therefore, when generating a classification tree, the main steps at each node is to determine which input is to be tested together with which of the many possible tests of the parameters values should be performed and checking if the node meets the stopping criteria [149].

The input parameter selected to split the node is the one that minimizes the weighted sum of the class impurities of each branch, or, equivalently, the partition that maximizes the impurity improvement or "gain" [149]. There are a variety of impurity measures. The two most often used are the Gini's diversity index, used in CART algorithm [150], and entropy, used in ID3, C4.5 and C5 tree-generation algorithms [151]. The Gini's index is defined as [150]

$$G = 1 - \sum_i \frac{n_i^2}{N^2} \tag{3.24}$$

where n_i is the number of cases belonging to the class i and N is the total number of cases. A node with just one class is known as pure node and has Gini index 0. In any other case the Gini index is positive. On the other hand, with n_i and N defined as for the Gini's index, the entropy index is defined as [151]

$$H = -\sum_i \frac{n_i}{N} * log \frac{n_i}{N} \tag{3.25}$$

A classification tree searches for the independent variable in order to find the split point that produces the highest reduction in the impurity of a node [150]. The reduction is calculated by comparing the purity of the root node with the sum of the impurities of the child nodes [150]. The independent variable that produces the highest reduction in the impurity is selected for the first splitting of the sample [150]. Subsequently each resulting node is split by means of the same procedure and, in the continuation of the partition process, the dependent variable is progressively classified into smaller groups [150]. The process continues until the stop criteria is reached [150].

Despite of applying two splitting rules, the stop criteria remained the same in both cases. In this work, the classification tree stopped splitting when met one of these points: (1) there is only one observation in each of the child nodes; (2) all observations within each child node have the identical distribution of predictor variables, making splitting impossible; or (3) there are fewer than 15% observations in a node. When a node stops splitting, it becomes a leaf node, which classifies between AF or NSR.

3.6.2 Logistic Regression

Logistic regression is a member of the family of methods called generalized linear models [152]. This model presents the advantage that it does not need that the included predictors have a normal distribution[152]. It is intended for the prediction of dichotomous categorical outcomes using one or more predictor variables [153]. Therefore, despite of the name, this is a model for classification rather than regression [153]. In consequence, a continuous criterion as a transformed

version of the dependent variable must be defined [154]. This transformation is essential because in binary logistic regression, the outcome ranges between 0 and 1, however, the continuous input variables may range between $-\infty$ and $+\infty$. For this purpose, a logistic regression takes the natural logarithm of the probability of the dependent variable belonging a class (referred to as the logit or log-odds) to create the continuous criterion [154]. Thus, the logit transformation is known as the link function in logistic regression and is the criterion upon which linear regression is conducted, replacing the binomial dependent variable [154].

To apply the logit transformation, first define $\pi(x)$ the probability of belonging to one class of the dependent variable. Then, the logistic function can be written as [154]:

$$\pi(x) = \frac{e^{\beta_0+\beta_1 x_1+...+\beta_n x_n}}{1+e^{\beta_0+\beta_1 x_1+...+\beta_n x_n}} = \frac{1}{1+e^{-(\beta_0+\beta_1 x_1+...+\beta_n x_n)}} \tag{3.26}$$

where β_0 is the constant of the equation, β_i are the coefficients of the predictors variables and x_i are the predictor variables. On the other hand, in terms of $\pi(x)$, the logit transformation is defined as follows [154]:

$$logit(x) = ln[\frac{\pi(x)}{1-\pi(x)}] = \beta_0 + \beta_1 x_1 + ... + \beta_n x_n \tag{3.27}$$

After this transformation, the principles that guide an analysis using linear regression will also guide the logistic regression [154]. Hence, to fit the logistic regression model, the values of $\beta_0...\beta_n$ must be estimated. In this work, the regression coefficients were estimated through an iterative maximum likelihood method [154]. This method is an indispensable tool in non-linear modeling with non-normal data [155]. A way to express the contribution to the likelihood function for the pair formed by the set of independent variables and the observed class (x_i, y_i) is [154]

$$\pi(x_i)^{y_i}[1-\pi(x_i)]^{1-y_i} \tag{3.28}$$

Since the observations are assumed to be independent, and considering a set of m independent variables, the likelihood function is obtained as the product of the terms given in equation 3.28 as [154]

$$L(\beta) = \Pi_{i=1}^{m}\pi(x_i)^{y_i}[1-\pi(x_i)]^{1-y_i} \tag{3.29}$$

The estimate value of β would be the value which maximizes the expression in equation 3.29. However, it is easier to work with the logarithm of the likelihood function [155]. This expression is defined as [154]

$$l(\beta) = ln[L(\beta)] = \Sigma_{i=1}^{m}\{y_i ln[\pi(x_i)] + (1 - y_i) ln[1 - \pi(x_i)]\} \tag{3.30}$$

To find the values of β that maximizes $l(\beta)$, the expressions are differentiated respect to the coefficients (β), then set to zero. These expressions, known as the *likelihood equations* are [154]:

$$\sum_{i=1}^{m} [y_i - \pi(x_i)] = 0 \tag{3.31}$$

for the constant coefficient β_0, and

$$\sum_{i=1}^{m} x_{ij}[y_i - \pi(x_i)] = 0 \tag{3.32}$$

for the rest of the coefficients, being $j = 1, 2...n$.

For logistic regressions, the expressions in equations 3.31 and 3.32 are non linear in β and therefore it can not be solved exactly. In consequence, they must be sought numerically using nonlinear optimization algorithms [155]. The idea of this nonlinear optimization is to find optimal parameters that maximize the log likelihood [155]. This is done by searching smaller sub-sets of the multi-dimensional parameter space rather than searching the whole parameter space, which becomes intractable as the number of parameters increases [155]. The search proceeds by trial and error over the course of a series of iterative steps [155]. Specifically, on each iteration, a new set of parameter values is obtained by adding small changes to the previous iteration parameters in such a way that the new parameters are likely to lead to improved performance [155]. There are different optimization algorithms, which differ in how this updating routine is conducted. The iterative process continues until the parameters are considered to have converged to the optimal set of parameters and accomplish a predefined stopping criteria [155]. Examples of the stopping criterion include the maximum number of iterations allowed or the minimum amount of change in parameter values between two successive iterations [155]. The value of β given by the solutions to equations 3.31 and 3.32 is called the maximum likelihood estimate. In this work, the optimization algorithm was the Newton-Raphson type which is one of the most ancient and important methods for solving systems of nonlinear equations [156]. In consequence, this is the method that most statistical packages use [157]. The algorithm stopped when the amount of change in parameter values between two successive iterations was fewer than 10^-8 or when 20 iterations were reached.

Regarding the model variable selection, several methods are available. The first one is the forced entry method, which involves entering in the model any variable included in the variable list. The problem with this method, is that the

more variables included, the greater the estimated standard errors become, and the more dependent the model becomes on the observed data [154]. Therefore, minimizing the number of variables the resultant model is more likely to be numerically stable and more easily generalized. In consequence, stepwise methods were performed [154]. There are two different stepwise methods: forward and backward. The forward method starts from a model using only a constant and keeps adding variables to the model while these variables show a significance lower than a threshold selected. In each iteration, if the significance of one variable included becomes higher than another threshold selected it is removed. The iterations continue until the outside variables significance is higher than the include criteria threshold or when removing a variable, the resultant model is the same as a previous model [154].

On the other hand, the backward model starts from a model using all the available variables. Then the significance of each variable is computed. The variable with the largest variable is higher than the threshold removing criteria, the variable is excluded. This procedure continues until no more variables can be excluded. At this point, the significance of the excluded variables is computed. If the significance of the variable with the smallest significance is less than the including criteria, the variable is included. When no more variables can be included or when including a variable the model resultant is a previous model, the algorithm stops [154].

The problem with the forward stepwise method is that it could use few variables because the rest show little statistical significance. However, it is possible for individual variables not to exhibit strong confounding, but when taken collectively, considerable confounding can be present in the data [154]. With the backward method, the first model uses all the variables and less significant variable is removed in each step. In this way, the corresponding model in each step can be analyzed, and the model with the highest prediction can be selected. To confirm if the model selected fits properly the data, the Hosmer-Lemeshow statistic was used [154]. This statistic indicates a poor fit if the values is less than 0.05.

The logistic regressions were performed using the statistical software SPSS®. This software computes the score statistic to determine whether the variable should enter the model in the stepwise method. On the other hand, three options are given to use as criteria to determine wether a variable should be removed: wald statistic, likelihood ratio and conditional statistic. Nevertheless, the accuracy and model obtained were in any case the same, regardless of the removing statistic used.

3.7 Statistical analysis

The first step in the statistical analysis was to study the significant differences between NSR and AF groups. However, before applying a test, it is necessary to

discern which one is more appropriate for the data. For this purpose, a Shapiro-Wilk test was applied to analyze data distributions and a Levene test was applied to check homoscedasticity of the data. Once the data normality and homoscedasticity were studied, the *t*-Student test was applied to parameters with normal and homoscedastic distribution and the U Mann-Whitney test was applied in the remaining cases. In both tests, a statistical significance $p < 0.05$ was considered as significant.

On the other hand, a classification threshold was defined for each studied predictor to discern between NSR and AF. The threshold was obtained by computing the corresponding receiver operating characteristic (ROC) curve. This curve is a graphical representation of the tradeoffs between sensitivity and specificity. In this work, sensitivity was the proportion of patients in AF correctly identified, whereas specificity was considered as the proportion of patients in NSR correctly classified. The value providing the highest rate of patients properly discerned (i.e., the diagnostic accuracy) was selected as the optimum threshold. Once the threshold was obtained, the sensitivity, specificity and accuracy of the indices was computed to assess the predictions performed. Furthermore, in order to perform a more precise analysis of the indices prediction capability, the area under the ROC curve (AUC) was also computed.

Finally, in order to analyze the results robustness, a cross validation test was performed on the individual indices and on the classification tree generated. Given that the number of patients is relatively low, the test selected was the leave one out.

Chapter 4

Results

This chapter presents the statistical results and the prediction capabilities computed with the indices described. First, non linear behavior of the signals requiring is assessed. Then, in order to present the follow up results, three different sections have been defined, one for each follow up period, since no change in patients' rhythm was observed between three and six months follow up.

4.1 Nonlinearity and nonstationarity

The Wilcoxon T test applied to the surrogate data proved that the signals presented a non-linear behavior. To this respect, Figure 4.1 shows the boxplot of the SampEn values distribution associated to the 40 surrogate data generated from each patient. By contrast, the original signal SampEn value is presented as a circle outside the boxplot whiskers. As can be observed, the non-linear behavior of the AA pattern can be considered, thus making it feasible the application of SampEn from a formal perspective.

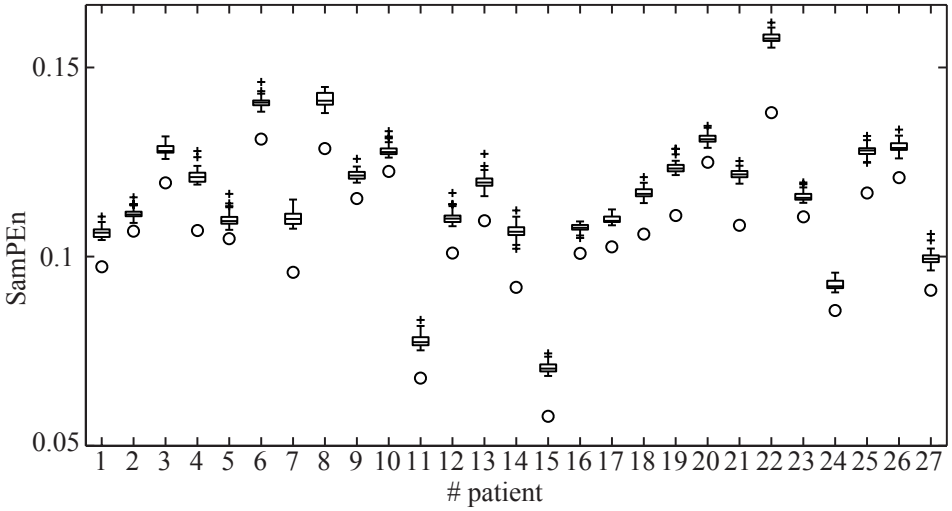

Figure 4.1. SampEn results for the surrogate data test (presented as a box and whiskers plot) and the original AA (circles) for each patient. As the AA value is outside the surrogate data distribution, non-linearity can be assumed.

Patient's rhythm was assessed in four different follow up periods. In consequence, in order to show the results in a simple and organized way, each follow up is presented separately. Nevertheless, since the patient's rhythm between 3 and 6 months did not change, these two periods are commented together.

4.2 MAZE outcome prediction at discharge

As commented in Section 3.1, at discharge 15 patients were in NSR whereas 12 patients were in AF. Table 4.2 shows mean values and standard deviation of the analyzed indices for the 15 patients in NSR and the 12 patients in AF. Additionally, the statistical significance differences between NSR and AF groups and the threshold that separates these groups are also represented. As can be appreciated, the prediction results for those patients in NSR at discharge presented higher organization, i.e., lower DAF and SampEn together with higher fWP. On the other

hand, regarding the clinical information, predictions for the NSR group showed lower preoperative AF duration and younger patients than the AF group. On the other hand, it is remarkable that weight and BMI results associated a higher value to the NSR group. Nonetheless, the most noteworthy result is related to the LA size, where a bigger value is related to the NSR group. In contrast, previous studies relate larger atrial sizes with higher likelihood of AF relapse [11]. It is also remarkable that the threshold selected with the ROC curves for the LA size is lower than the mean in both groups.

Regarding the analysis performed looking for statistical significant differences between groups, fWP and SampEn were statistically significant while DAF was not. On the other hand, from the clinical indices studied, only the preoperative AF duration showed statistically significant differences at discharge.

Table 4.1. Mean and standard deviation values obtained for the indices associated to patients with preoperative prognostic of NSR and AF at discharge. The last two columns present the optimal threshold to separate between groups and the statistical significance.

	NSR	AF	Threshold	p
DAF (Hz)	6.17 ± 0.88	6.79 ± 0.76	6.2	0.065
SampEn	0.086 ± 0.018	0.1 ± 0.013	0.0903	0.029
fWP	0.042 ± 0.017	0.029 ± 0.012	0.0353	0.006
AF duration (years)	2.2 ± 1.98	5.15 ± 4.11	2.5	0.044
LA size (mm)	47.9 ± 7	47.3 ± 7.3	46	0.806
Age (years)	66.2 ± 10.69	68.25 ± 8.9	71.5	0.599
Weight (kg)	77.33 ± 18.98	69.38 ± 13.98	75	0.237
BMI	29.5 ± 6	27.57 ± 4.09	27.97	0.341

Furthermore, with the aim to provide a graphical summary of the results, including data dispersion, obtained thresholds as well as classification ability, the isolated indices distribution for NSR and AF patients have been graphically represented. In these graphics, the threshold between groups provided by the ROC curves have been also represented. Figure 4.2 shows the DAF distribution. Values over the threshold are supposed to be in AF while values below the threshold are related to NSR. As it is showed, values lower than the threshold, have little probability of relapsing to AF at discharge. However, above the threshold there are several patients of both groups. Furthermore, DAF values are grouped close to the threshold, with only a few values away from it. Thus, DAF have little variance.

Figure 4.3 represents the SampEn distribution. SampEn distribution is quite similar to DAF distribution. As in the DAF, values below the threshold are mostly from NSR groupd while over the threshold both groups are mixed.

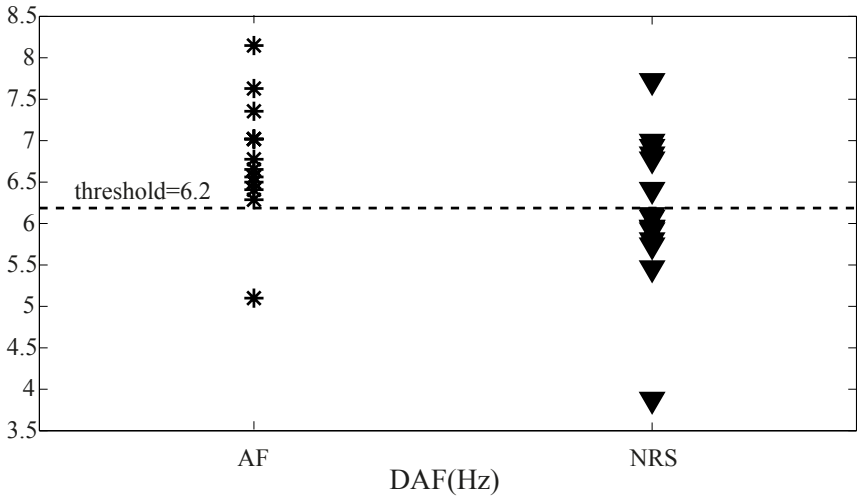

Figure 4.2. DAF values associated to AF and NSR groups at discharge. Threshold between groups is also displayed.

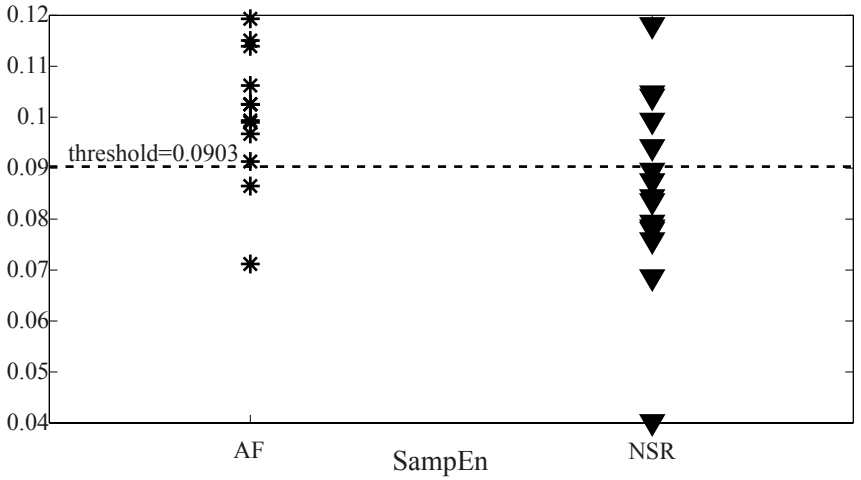

Figure 4.3. SampEn values associated to AF and NSR groups at discharge. Threshold between groups is also displayed.

Addtionally, most values are gathered around the threshold, with only a few being far from it.

On Figure 4.4 fWP values are showed. In this case, values over the threshold are associated with NSR and values below the threshold to AF. Patients with fWP values over the threshold have great likelihood to be in NSR at discharge. On the other hand, below the threshold patients are mostly in AF but 3 of them are also in NSR.

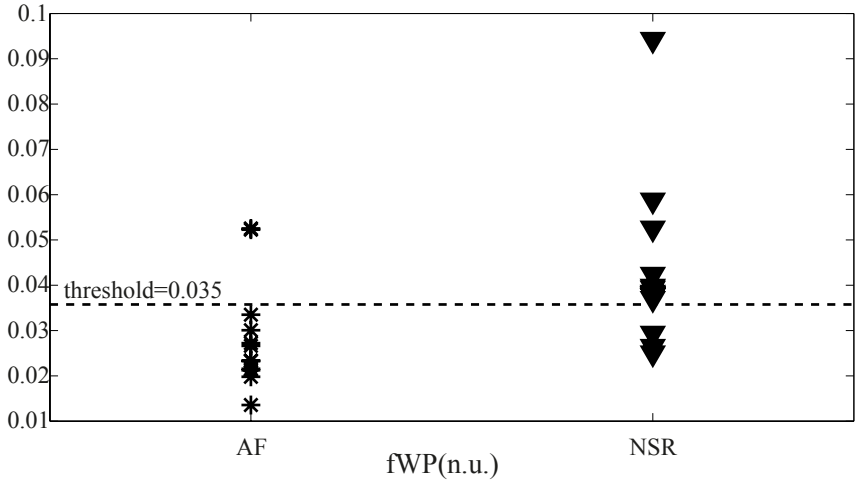

Figure 4.4. fWP values associated to AF and NSR groups at discharge. Threshold between groups is also displayed.

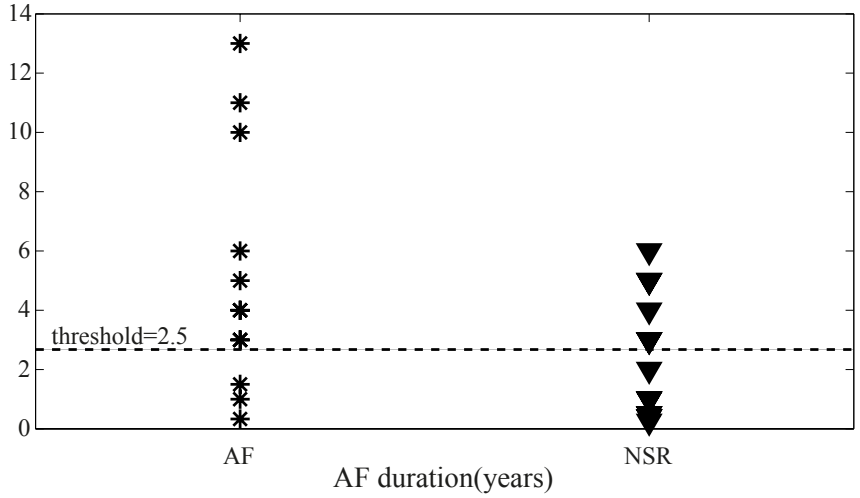

Figure 4.5. AF time values associated to AF and NSR groups at discharge. Threshold between groups is also displayed.

AF duration results are represented on Figure 4.5. This index have a wide values range, going from 0.25 to 14 years. Although the threshold computed from the ROC is 2.5, there are patients from both groups below an above the threshold. However, maximum values for NSR patients is 6 while AF group yields 14 years. This causes the big difference in mean value between groups despite the overlapping of both groups and also that statistically significant differences have been found.

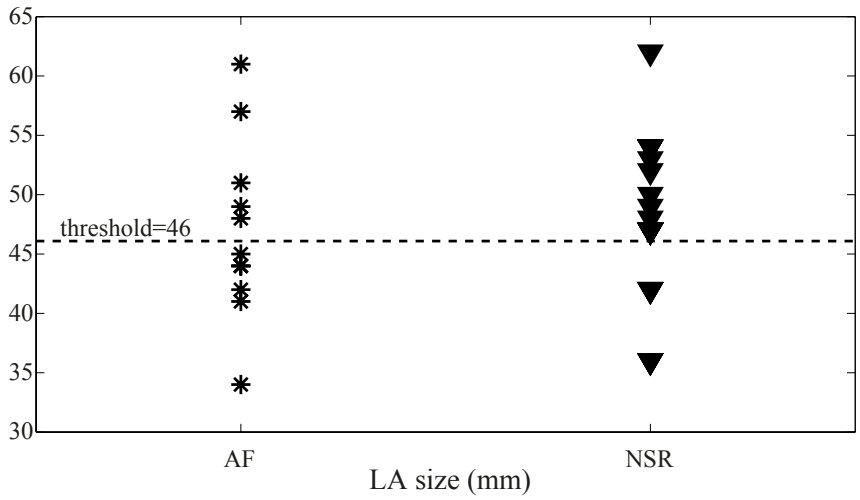

Figure 4.6. LA size values associated to AF and NSR groups at discharge. Threshold between groups is also displayed.

Regarding the LA size, its values are graphically represented on Figure 4.6. The threshold computed is 46 mm, however, the values distribution is overlaped in both groups. In consequence, the LA size prediction capability is limited and the results are not statistically significant. Furthermore, the mean value for each group is almost the same.

With respect to the age, it is represented on Figure 4.7. The values range from 40 to 80 years, with a threshold of 71.5 years. As in the LA size, values of both groups are overlapped. In consequence, its results are not statistically significant, and its prediction capability is limited.

On the other hand, weight is represented on Figure 4.8. The values go from 40 kg to 110 kg, and, despite overweight is considered a cardiac risk, there are more patients in AF with weight values lower than the threshold, which is 75 kg. However, the greatest and smallest weight values are in the NSR group. Thus, the information provided by the weight seems limited.

Finally, Figure 4.9 contain the BMI values. The distribution is similar to the weight distribution with little differences. These differences affects its prediction capability, since more NSR patients have BMI values below the threshold, and therefore, the overlapping between groups is greater.

With respect to the ROC curves analysis to obtain the indices accuracy, Table 4.2 shows the values of sensitivity, specificity and accuracy, together with the AUC of the ROC curves. Table 4.2 also shows the accuracy obtained when applying the leave one out test.

As it can be observed, the fWP obtained the highest accuracy and also the

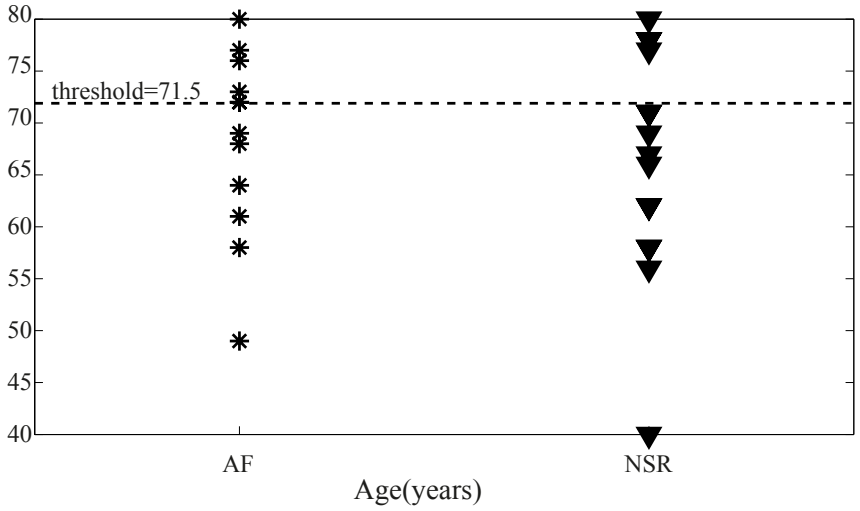

Figure 4.7. Age values associated to AF and NSR groups at discharge. Threshold between groups is also displayed.

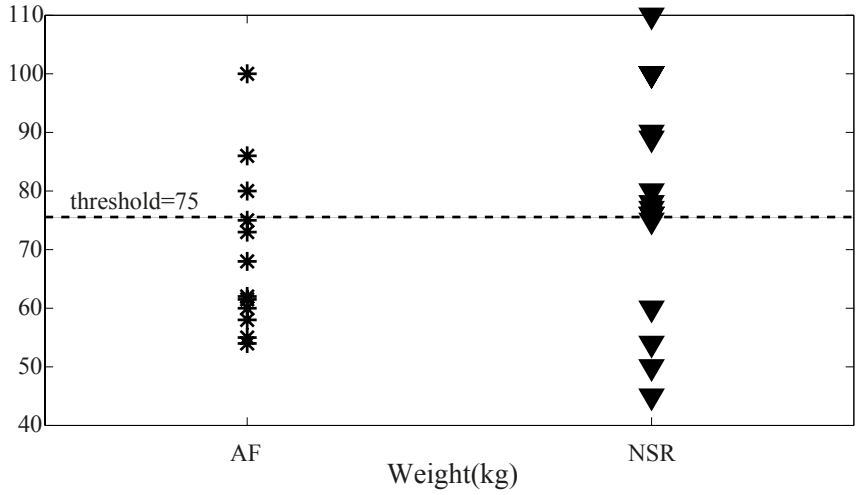

Figure 4.8. Weight values associated to AF and NSR groups at discharge. Threshold between groups is also displayed.

highest AUC. Furthermore, in general the ECG parameters obtained higher accuracy than the clinical parameters. To this respect, patient's weight is the only clinical parameter surpassing 70% of accuracy. It is also worthy to note that, despite showing statistically significant differences, the preoperative AF duration obtained a low accuracy (i.e. 66.67%). On the other hand, DAF and SampEn obtained the same accuracy that weight. However, the SampEn showed the highest AUC between these three indices, followed by the DAF with weight yielding the lowest AUC.

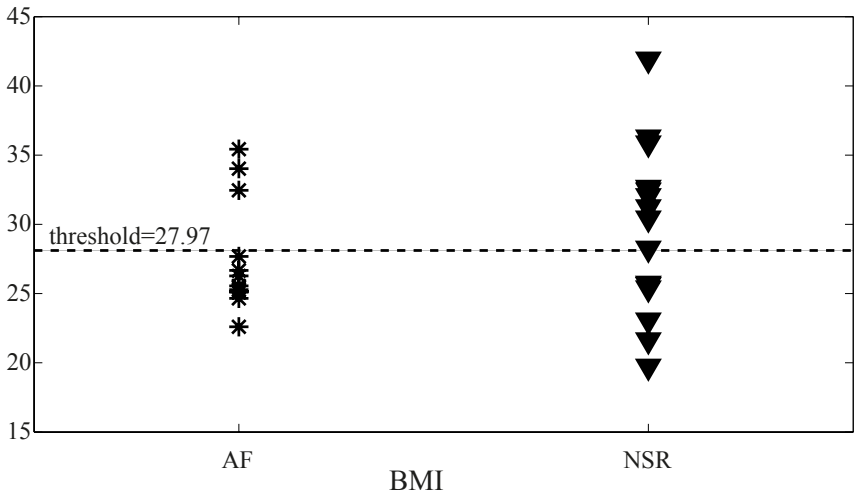

Figure 4.9. BMI values associated to AF and NSR groups at discharge. Threshold between groups is also displayed.

Table 4.2. Results of sensitivity, specificity and accuracy of the indices when classifying preoperatively into AF and NSR at discharge, together with their AUC. Furthermore, the leave one out test results are included.

	Sensitivity	Specificity	Accuracy	AUC	Leave one out
DAF	91.67%	60%	74.08%	0.7222	66.67%
SampEn	75%	73.33%	74.08%	0.7444	70.37%
fWP	83.33%	80%	81.48%	0.8111	81.48%
AF duration	75%	60%	66.67%	0.6944	55.56%
LA size	50%	73.33%	62.96%	0.5611	62.96%
Age	50%	73.33%	62.96%	0.5444	51.85%
Weight	75%	73.33%	74.08%	0.6556	66.67%
BMI	75%	60%	66.67%	0.6111	59.26%

Finally, the leave one out test show accuracy loss in most of the indices. SampEn and especially fWP, which had no accuracy loss, were the only exceptions.

Once the prediction capability of the individual indices was assessed, they were combined through prediction models. The first model used for indices combination was a classification tree. Three trees were created: one using ECG indices, another using clinical indices and finally, one combining both types. Furthermore, two split criterion were used, the Gini's diversity index and the entropy index. Figure 4.10, Figure 4.11 and Figure 4.12 represent these trees.

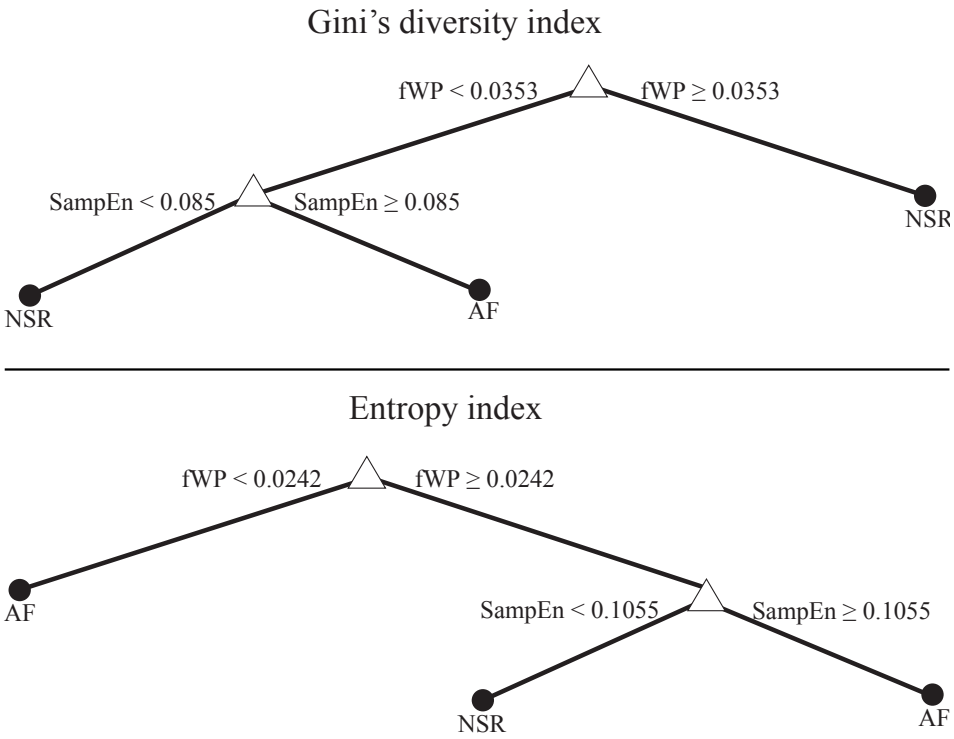

Figure 4.10. Classification tree predicting rhythm at discharge using ECG indices with Gini's diversity index as split criterion (top) and with entropy index as split criterion (bottom).

Regarding the accuracy results obtained with the classification trees, Table 4.3 shows the sensitivity, specificity and accuracy of each model. In addition, the leave one out results obtained for each model are also included in Table 4.3. As it can be noticed, the classification trees outperformed the individual indices. The ECG tree and the clinical tree yielded the same accuracy, whereas the combination tree outperformed both. However, the leave one out results were low, especially when using the clinical indices. Hence, the tree results may change if a wider database would be used.

Besides of classification trees, logistic regressions were also defined. The logit function associated to the regressions using ECG indices, clinical indices and the combination of both types are showed below:

$$logit_{ECG} = 69.48 SampEn - 96.64 fWP - 3.38 \tag{4.1}$$

$$\begin{aligned} logit_{clinical} &= 0.81 AFduration - 0.216 LAsize - \\ &- 0.043 Age - 0.141 weight + 0.341 BMI + 10.727 \end{aligned} \tag{4.2}$$

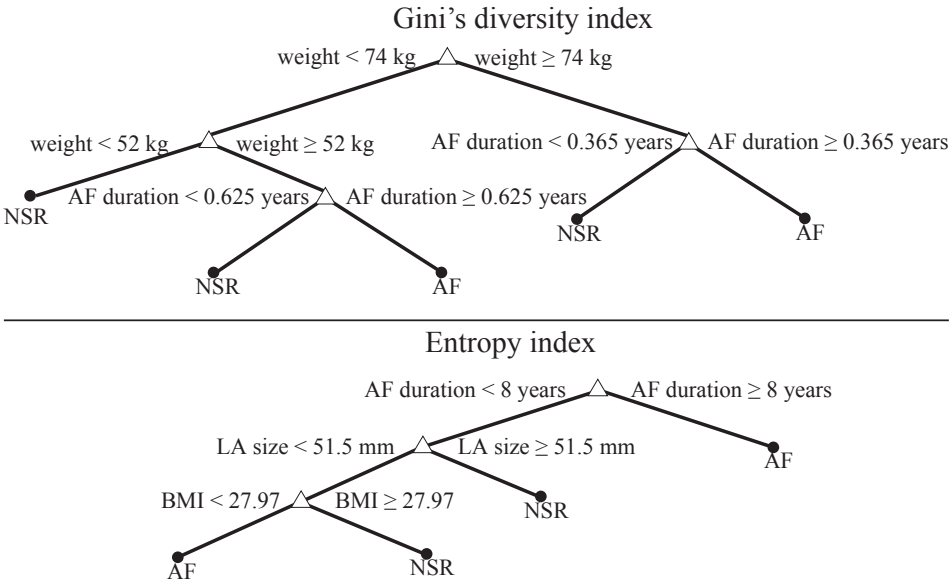

Figure 4.11. Classification tree predicting rhythm at discharge using clinical indices with Gini's diversity index as split criterion (top) and with entropy index as split criterion (bottom).

Table 4.3. Results of sensitivity, specificity and accuracy of the classification trees at discharge, together with the leave one out test results.

	Split criterion	Sensitivity	Specificity	Accuracy	Leave one out
ECG indices	Gini's index	75%	93.33%	85.19%	70.37%
	Entropy index	75%	93.33%	85.19%	70.37%
Clinical indices	Gini's index	75%	93.33%	85.19%	66.67%
	Entropy index	83.33%	80%	81.48%	66.67%
Combination	Gini's index	83.33%	100%	92.6%	59.26%
	Entropy index	100%	73.33%	85.18%	59.26%

$$\begin{aligned} logit_{combination} = -96.034fWP + 0.714AFduration - \\ -0.147LAsize - 0.134weight + 0.294BMI + 8.982 \end{aligned} \tag{4.3}$$

As can be seen, the logistic regression generated with the ECG indices used SampEn and fWP whereas it excluded DAF. Regarding the model with clinical indices, its logit function included all the available indices. On the other hand, the regression combining both types of indices included all of them but age, SampEn and DAF.

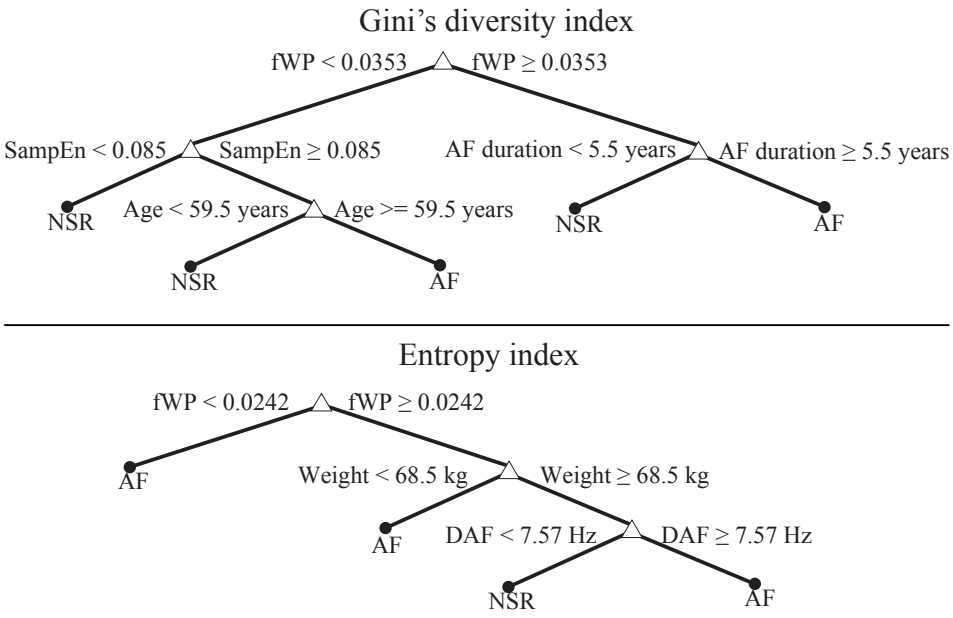

Figure 4.12. Classification tree predicting rhythm at discharge combining ECG and clinical with Gini's diversity index as split criterion (top) and with entropy index as split criterion (bottom).

Table 4.4. Sensitivity, specificity and accuracy of the logistic regression together with the Hosmer-Lemeshow test result and the logit function at discharge.

	Sensitivity	Specificity	Accuracy	Hosmer-Lemeshow
ECG indices	75%	80%	77.78%	0.191
Clinical indices	75%	86.67%	81.48%	0.667
Combination	91.67%	86.67%	88.9%	0.881

With the logit functions defined, the next step was to assess their prediction capability. Table 4.4 shows the sensitivity, specificity, accuracy and the Hosmer-Lemeshow test result of the three regression generated. The first remarkable observation is that the Hosmer-Lemeshow test obtained values over 0.05 in every regression. Hence, the three models fit properly the data. However, comparing with individual indices it is worth to note that the regression with ECG indices obtained lower accuracy than fWP alone and the regression with clinical indices obtained the same accuracy than this index. On the other hand, the regression combining both types of indices yielded an accuracy of 88.9%.

4.3 MAZE outcome prediction after a 6 months-length follow up

Between discharge and the 3 months follow up, four patients in AF recovered the NSR. In consequence, the parameters distribution and their prediction capability changed. Table 4.5 shows the new values distribution for NSR and AF groups as well as the statistical significance and the threshold set to perform the patients classification. As can be observed, the values distribution maintained the tendency showed at discharge. Regarding the significant differences, at this follow up, the three ECG parameters showed statistically significant differences. On the other hand, from the clinical parameters, AF duration and age were statistically significant.

Table 4.5. Mean and standard deviation values obtained for the indices associated to patients with preoperative prognostic of NSR and AF at 3 and 6 months after the procedure. The last two columns present the optimal threshold to separate between groups and the statistical significance.

	NSR	AF	Threshold	p
DAF (Hz)	6.17 ± 0.83	7.09 ± 0.6	7	0.009
SampEn	0.087 ± 0.017	0.11 ± 0.01	0.098	0.009
fWP	0.04 ± 0.017	0.028 ± 0.011	0.0353	0.022
AF duration (years)	2.37 ± 1.87	6.23 ± 4.67	4.5	0.043
LA size (mm)	48.1 ± 6.3	46.5 ± 8.8	46	0.595
Age (years)	65.16 ± 10.77	71.75 ± 4.92	67.50	0.039
Weight (kg)	74.5 ± 18.25	72.125 ± 15.08	75	0.749
BMI	28.82 ± 5.54	28.2 ± 4.93	25.56	0.785

Regarding the indices distribution, Figure 4.13 shows the DAF distribution at 3 and 6 months. With four patients recovering NSR, the threshold change from the discharge follow up to 7 Hz. With this change, only one patient with a value over the threshold is in NSR. Opposed to the distribution at discharge, below the threshold there are more patients in AF. Furthermore, the AF mean value has incremented compared to the discharge follow up, pointing that patients that recovered NSR were patients with lower DAF in the group. Finally, with the threshold change, NSR values are less gathered around it.

Analyzing the SampEn values, which are represented in Figure 4.14, the values distribution is still similar to the DAF. Additionally, the threshold has also changed, increasing to 0.098. Nevertheless, the groups distribution related to the threshold has not changed from the discharge analysis. In this way, below the threshold there is only one patient in AF. Finally, as in the DAF, the increase in the threshold caused that the NSR values were less gathered around it.

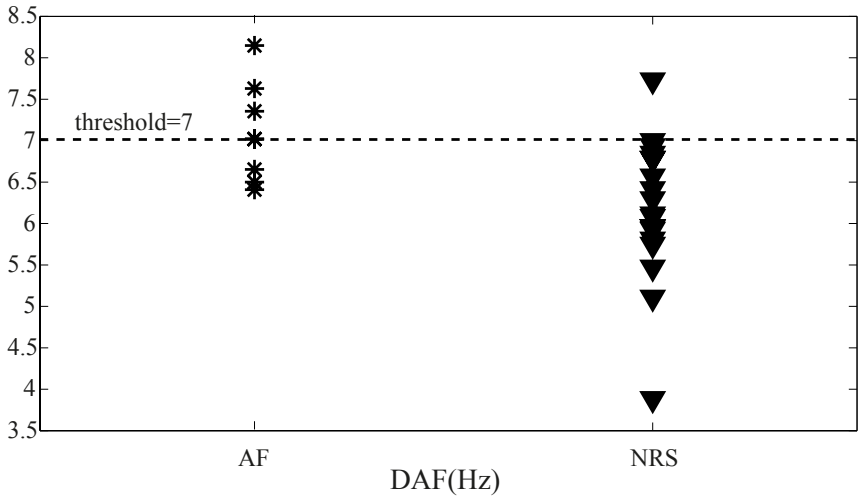

Figure 4.13. DAF values associated to AF and NSR groups 3 and 6 months after surgery. Threshold between groups is also displayed.

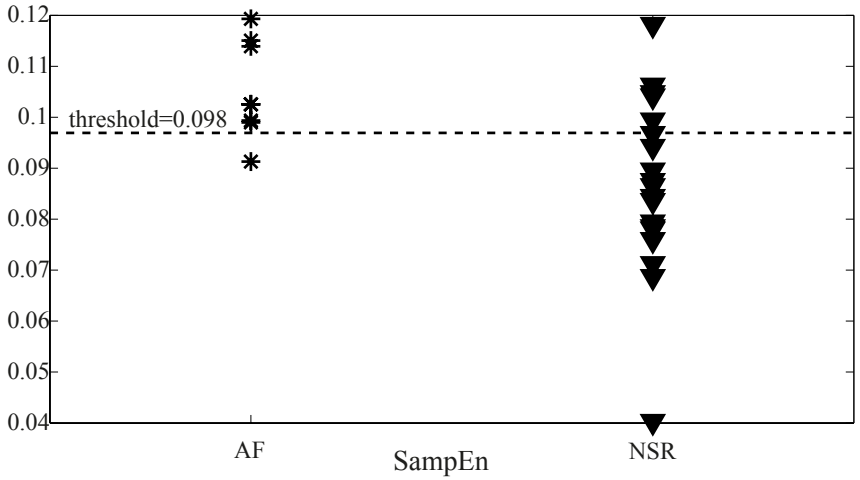

Figure 4.14. SampEn values associated to AF and NSR groups 3 and 6 months after surgery. Threshold between groups is also displayed.

Figure 4.15 contains the fWP graphical distribution. In this case, despite the rhythm change of 4 patients, the threshold remained the same. Therefore, the four patients recovering NSR have fWP values below the threshold. Thus, there is more overlap when the patien have fWP values below the threshold, worsening its prediction capability. This also ment that the fWP mean value for the NSR group decreased while the mean value for the AF group remained similar.

Looking to Figure 4.16, AF time distribution is represented. At this follow up, the threshold increased from 2.5 years to 4.5 years. In this way, the 4 patients

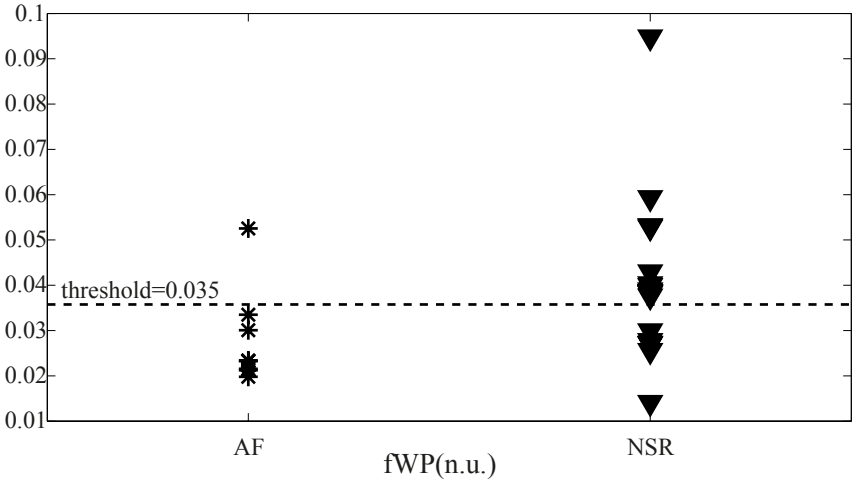

Figure 4.15. fWP values associated to AF and NSR groups 3 and 6 months after surgery. Threshold between groups is also displayed.

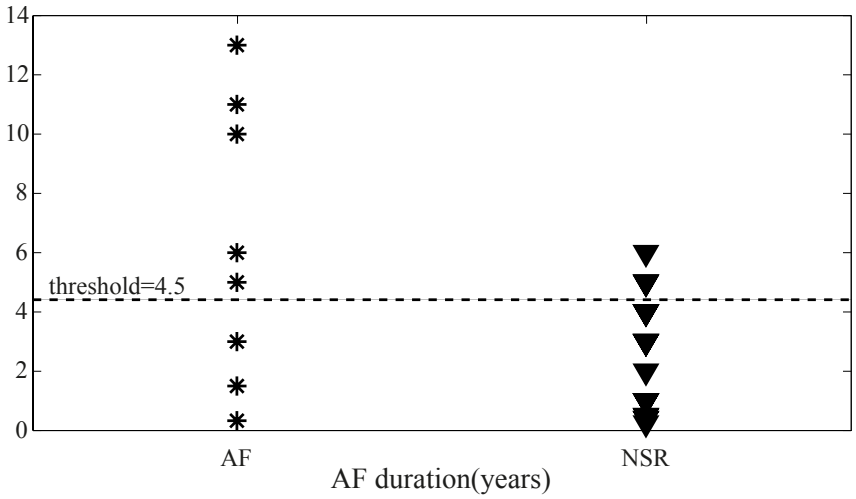

Figure 4.16. AF time values associated to AF and NSR groups 3 and 6 months after surgery. Threshold between groups is also displayed.

recovering NSR presented values below the threshold, and in consequence, the AF duration prediction capability increased significantly in this follow up analysis. Additionally, the AF group mean value increased in more than a year. Thus, patients regaining NSR were patients with AF time values smaller than the mean AF value for the AF group at discharge, which was 5.15 years.

With regard to the LA size, its distribution is in Figure 4.17. This index, maintained the same threshold value that at discharge follow up. Three of the patients

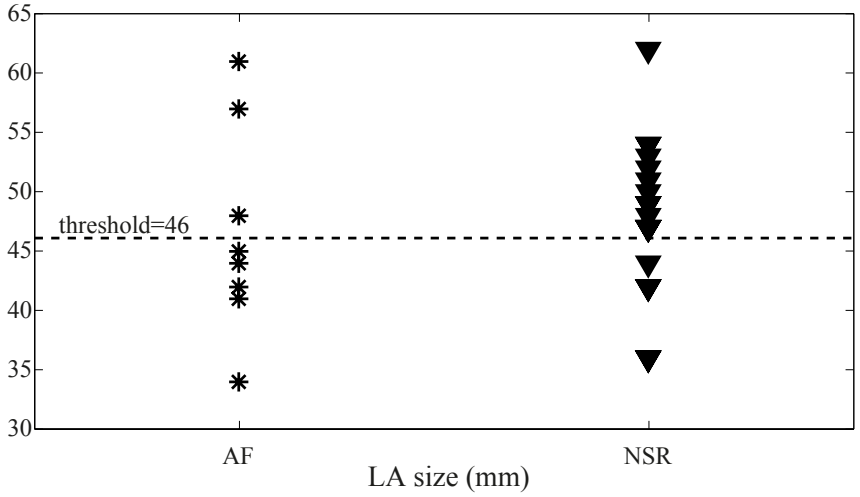

Figure 4.17. LA size values associated to AF and NSR groups 3 and 6 months after surgery. Threshold between groups is also displayed.

had a LA size over the threshold while one had a value lower than the threshold. However, due to the considerable overlapping between groups, the results are not statistically significant, and its prediction capability keeps being limited.

Regarding patients' age, it is graphically represented on Figure 4.18. Compared to the results at discharge, the threshold has decreased from 71.5 years to 67.5 years. The threshol change together with the patients' rhythm change caused that, below the threshold, only one patient maintained the AF. However, the patients in NSR are distributed randomly in both sides of the threshold. Therefore, the changes between discharge and 6 months follow up had no influende in the prediction capability. However, the age mean value from the AF group increased in 3.5 years and, additionally, its standard deviation decreased in 4 years.

Studying patients weight, which is represented in Figure 4.19, the threshold remained without changes. However, patients recovering NSR had weight values associated to AF. As a result, the mean value of AF group increased 3 kg, while the NSR mean value increased the same 3 kg. Also, another result is the loss of prediction capability at 6 months follow up. Furthermore, as in the previous follow up, there is a considerable overlapping between groups and, in consequence, no statistically significant differences were found.

Finally, analyzing the BMI values distribution from Figure 4.20, it is noticeable that the threshold decreased 2.5 units. Thus, although BMI is related with weight, their behaviour is different. Patients recovering NSR had values below the threshold, but with values very close to it. The threshold adaptation caused that these patients were correctly classified, however, since there is a considerable overlapping in the values distribution, other patients were missclasified. Consequently, there is only a slight increase in the predicton capability.

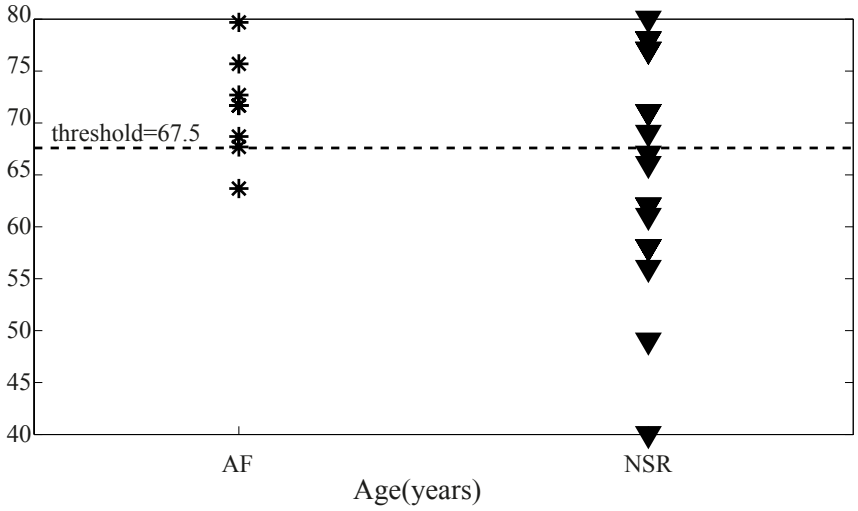

Figure 4.18. Age values associated to AF and NSR groups 3 and 6 months after surgery. Threshold between groups is also displayed.

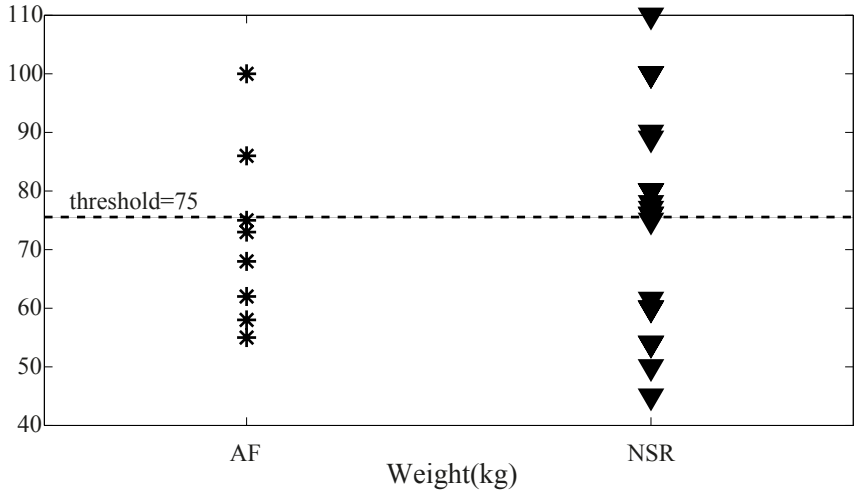

Figure 4.19. Weight values associated to AF and NSR groups 3 and 6 months after surgery. Threshold between groups is also displayed.

With respect to the prediction capability, results are showed in Table 4.6. As it can be noticed, DAF was the most accurate parameter. However, the leave one out test performed over this index showed a considerable decrease in its accuracy. After DAF, the next indices with the highest accuracy were SampEn and AF duration, both with the same accuracy. Furthermore, these two indices showed the best results for the leave one out test, yielding, both, 74.07%. Nevertheless, the SampEn AUC was highest that the AF duration AUC. The next index with the highest accuracy was fWP, however, its AUC was greater than the AF du-

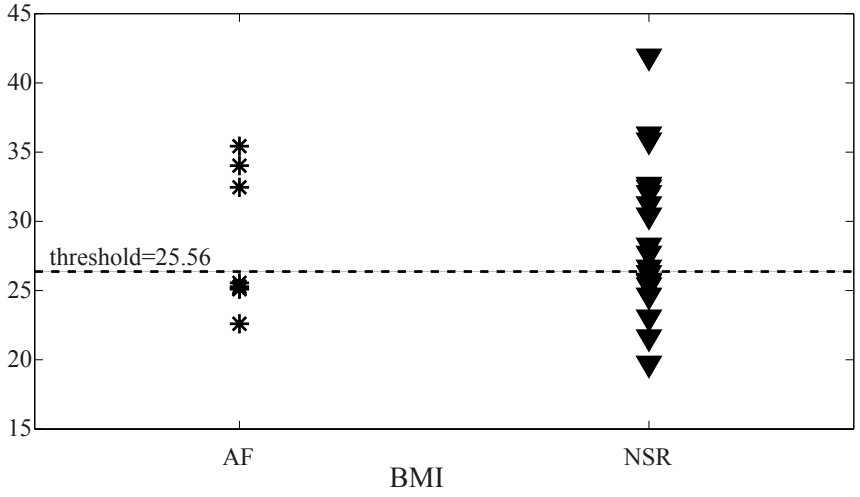

Figure 4.20. BMI values associated to AF and NSR groups 3 and 6 months after surgery. Threshold between groups is also displayed.

Table 4.6. Results of sensitivity, specificity and accuracy of the indices when classifying preoperatively into AF and NSR at 3 and 6 months after the procedure, together with their AUC. Furthermore, the leave one out test results are included

	Sensitivity	Specificity	Accuracy	AUC	Leave one out
DAF	62.5%	94.74%	85.19%	0.8355	62.96%
SampEn	87.5%	73.68%	77.78%	0.8224	74.07%
fWP	87.5%	68.42%	74.07%	0.7829	66.67%
AF duration	62.5%	84.21%	77.78%	0.7303	74.07%
LA size	62.5%	73.68%	70.37%	0.625	55.56%
Age	87.5%	57.89%	66.67%	0.6908	59.26%
Weight	75%	63.16%	66.67%	0.5658	59.26%
BMI	62.5%	73.68%	70.37%	0.5724	62.96%

ration AUC. It is also remarkable that despite of showing statistical significant differences, age showed the lowest accuracy with a 66.67%.

After reevaluating the indices prediction capability, new prediction models were generated. Regarding the classification trees, the new models generated using the two split criteria are represented in Figure 4.21 to Figure 4.23. Complementary, the accuracy yielded with these models is showed in Table 4.7. As it can be observed, trees with entropy index presented same or higher accuracy than the ones using Gini's index. In addition, they also obtained better leave one

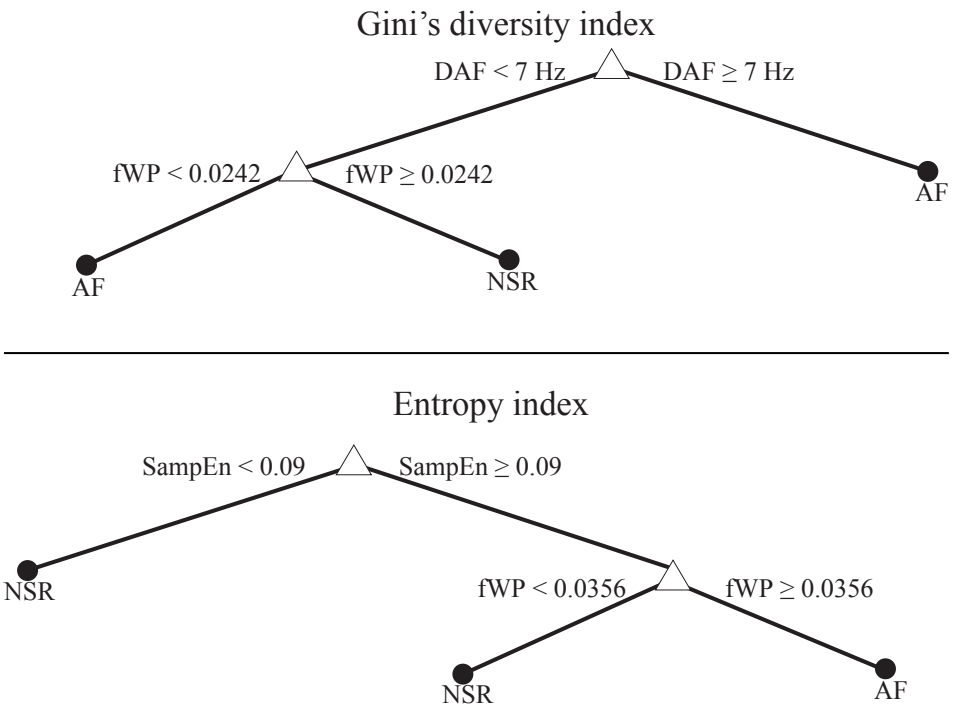

Figure 4.21. Classification tree predicting rhythm 3 and 6 months after the Cox-Maze procedure using ECG indices with Gini's diversity index as split criterion (top) and with entropy index as split criterion (bottom).

Table 4.7. Results of sensitivity, specificity and accuracy of the classification trees, together with the leave one out test results when predicting patient's rhythm 3 and 6 months after the Cox-Maze procedure

	Split criterion	Sensitivity	Specificity	Accuracy	Leave one out
ECG indices	Gini's index	87.5%	89.47%	88.9%	70.37%
	Entropy index	87.5%	89.47%	88.9%	74.07%
Clinical indices	Gini's index	37.5%	100%	81.48%	70.37%
	Entropy index	75%	100%	92.6%	77.78%
Combination	Gini's index	87.5%	89.47%	88.9%	70.37%
	Entropy index	87.5%	100%	96.3%	77.78%

out results. Regarding the comparison between clinical indices and ECG indices, when using the Gini's diversity index the model generated with ECG parameters outperformed the model with clinical information. The opposite occurred when the model were generated with the entropy index. Finally, the model combining indices and using the entropy index yielded the best results.

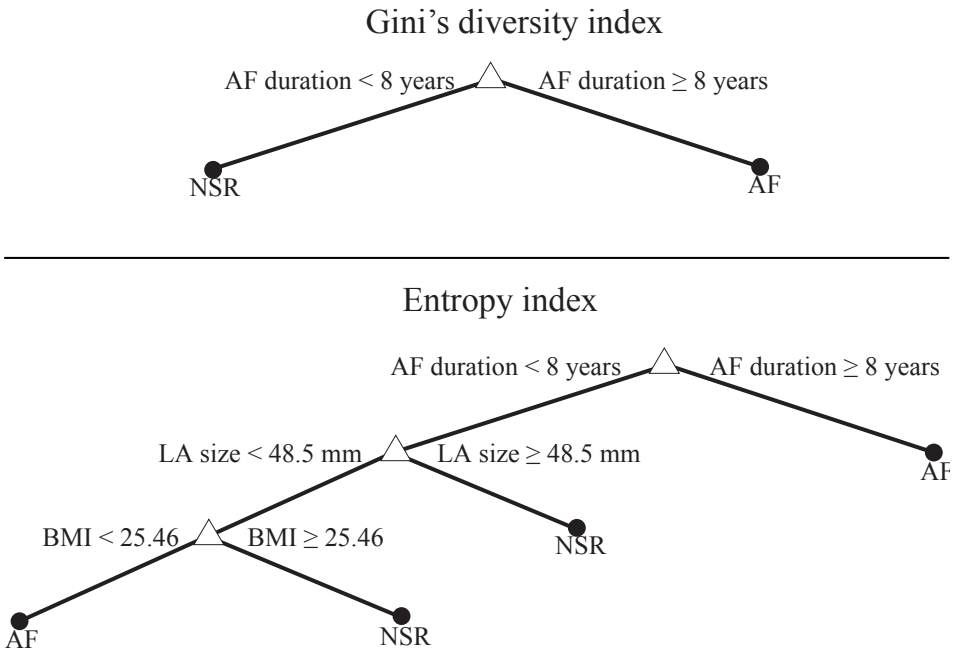

Figure 4.22. Classification tree predicting rhythm 3 and 6 months after the Cox-Maze procedure using clinical indices with Gini's diversity index as split criterion (top) and with entropy index as split criterion (bottom).

Regarding the logistic regression, the logit functions defined for the ECG indices, clinical indices and combination are showed below:

$$logit_{ECG} = 112.94SampEn - 80.36fWP - 9.2 \tag{4.4}$$

$$logit_{clinical} = 0.96AFduration - 0.346LAsize - 0.031weight + 13.4 \tag{4.5}$$

$$\begin{aligned} logit_{combination} = 3.46DAF - 132.51fWP + 1.42AFduration - \\ -0.587LAsize + 0.07age - 0.21weight + 0.67BMI - 6.1 \end{aligned} \tag{4.6}$$

The logit function of the ECG parameters regressions used SampEn and fWP to define the logistic regression. On the other hand, the regression using clinical indices defined the logit function using AF duration, LA size and weight. Finally, the logistic regression designed with the combination of both indices defined a logit function using all the parameters. Regarding their prediction capability, Table 4.8 shows the accuracy results. As it can be noticed, the Hosmer-Lemeshow

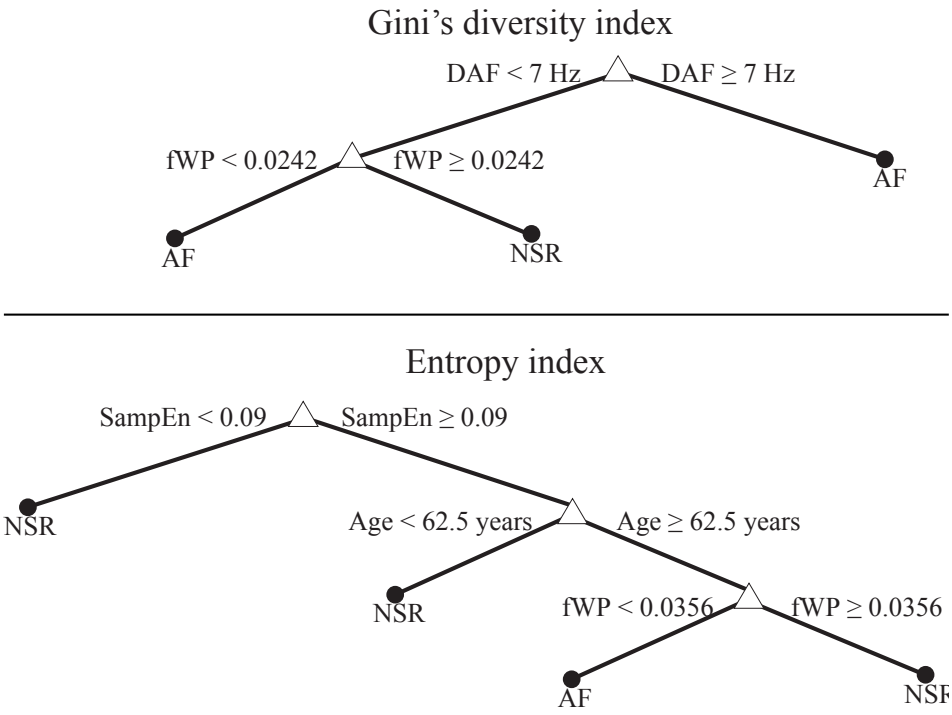

Figure 4.23. Classification tree predicting rhythm 3 and 6 months after the Cox-Maze procedure combining ECG and clinical with Gini's diversity index as split criterion (top) and with entropy index as split criterion (bottom).

Table 4.8. Sensitivity, specificity and accuracy of the logistic regression together with the Hosmer-Lemeshow test result awhen predicting patient's rhythm after 3 and 6 months.

	Sensitivity	Specificity	Accuracy	Hosmer-Lemeshow
ECG indices	75%	84.2%	81.5%	0.86
Clinical indices	75%	94.7%	88.89%	0.419
Combination	87.5%	94.7%	92.6%	0.982

results confirmed the model suitability to the data in every case. With respect to the accuracy, the logistic regression with ECG indices yielded lower accuracy than the DAF alone. On the other hand, the other two regressions were more accurate that the indices alone. From these two logistic regressions, the one combining both types of indices was the most accurate.

4.4 MAZE outcome prediction after a 12 months-length follow up

Finally, in the time passed between 6 months and 12 months, a patient who recovered the NSR between discharge and 3 months relapsed to AF. Hence, parameter distribution and prediction capability of indices and models changed. Therefore, they were recomputed. The new indices mean values are showed in Table 4.9 with their statistical significance and the threshold discriminating between groups. As can be noticed, the distributions followed the tendency showed in previous follow up controls. At this period, all the ECG indices were statistically significant whereas from the clinical indices, only the AF duration was statistically significant.

Table 4.9. Mean and standard deviation values obtained for the indices associated to patients with preoperative prognostic of NSR and AF 12 months after the procedure. The last two columns present the optimal threshold to separate between groups and the statistical significance.

	NSR	AF	Threshold	p
DAF (Hz)	6.15 ± 0.85	7.03 ± 0.59	6.45	0.01
SampEn	0.086 ± 0.018	0.1 ± 0.01	0.0955	0.008
fWP	0.041 ± 0.016	0.027 ± 0.011	0.0353	0.004
AF duration (years)	2.28 ± 1.88	5.98 ± 4.42	3.5	0.03
LA size (mm)	48.1 ± 6.5	46.8 ± 4.2	46	0.662
Age (years)	65.39 ± 11.03	70.56 ± 5.83	67.5	0.203
Weight (kg)	74.19 ± 18.73	73 ± 14.34	75	0.868
BMI	28.89 ± 5.69	28.14 ± 4.61	25.6	0.737

With regards to the graphical indices distribution, Figure 4.24 represents DAF values at 12 months follow up. In this follow up, threshold value has decreased to 6.45 Hz. With this change, DAF recovers the behaviour of the discharge analysis, having only one patient below the threshold in AF, and being this patient in the edge value. However, due to the overlapping with the values over the threshold, decreasing it causes in general a prediction loss when comparing with 3 and 6 months follow up.

On the other hand, SampEn distribution is represented on Figure 4.25. As with DAF, the threshold has changed from 3 and 6 months follow up, to 0.0955, and, in consequence, the SampEn distribution behaves as at discharge. Although there is overlapping with values over the threshold, the values are not as close to the threshold as they are in DAF. Hence, the SampEn prediction capability at 12 months follow up is greater than the DAF prediction capability.

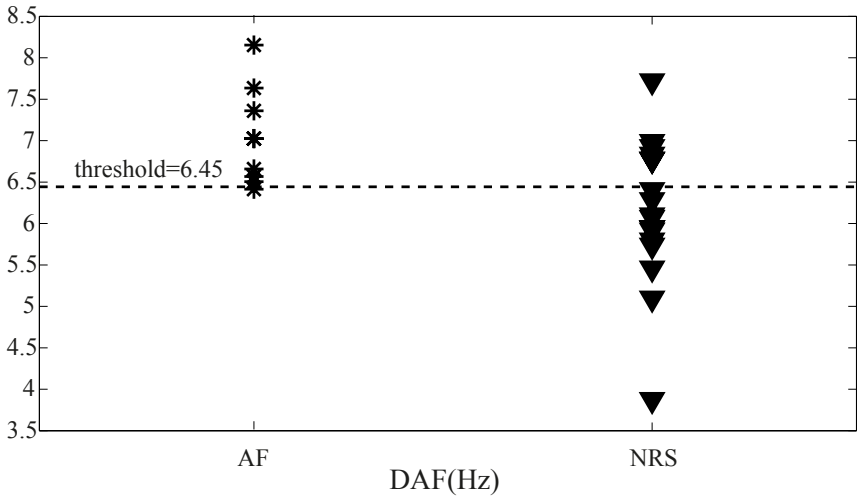

Figure 4.24. DAF values associated to AF and NSR groups 12 months after surgery. Threshold between groups is also displayed.

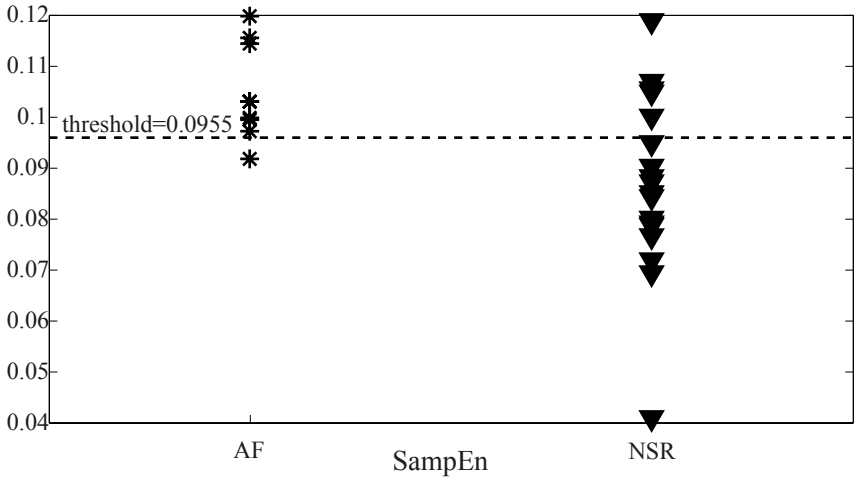

Figure 4.25. SampEn values associated to AF and NSR groups 12 months after surgery. Threshold between groups is also displayed.

Regarding *f* waves amplitude, the fWP distribution can be seen on Figure 4.26. As in previous follow ups, the threshold remains constant. Indeed, the patient relapsing to AF presented the lowest fWP value from all the patients. In consequence, at 12 months follow up, the behavior is the same and the prediction capability is increased comparing to 6 months follow up.

Next, the AF duration distribution can be observed on Figure 4.27. In this case, the threshold computed change to 3.5 years. In this way, there is a loss of prediction capability. However, the AUC, which is the way to compute the

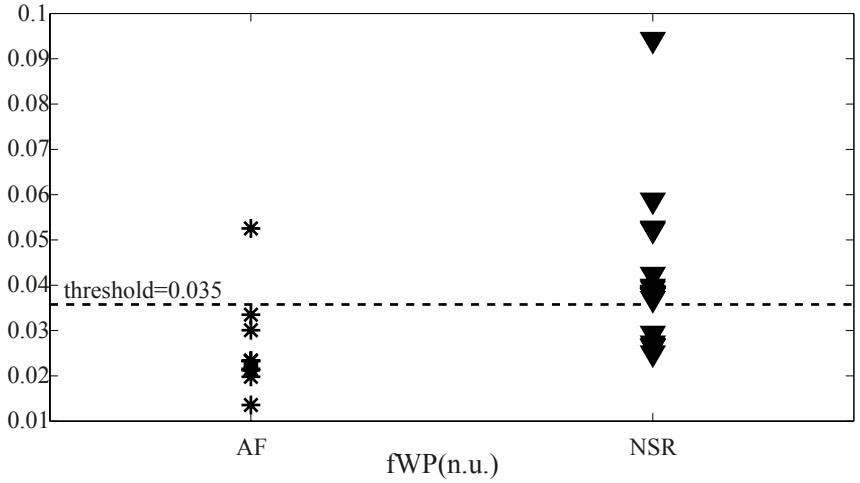

Figure 4.26. fWP values associated to AF and NSR groups 12 months after surgery. Threshold between groups is also displayed.

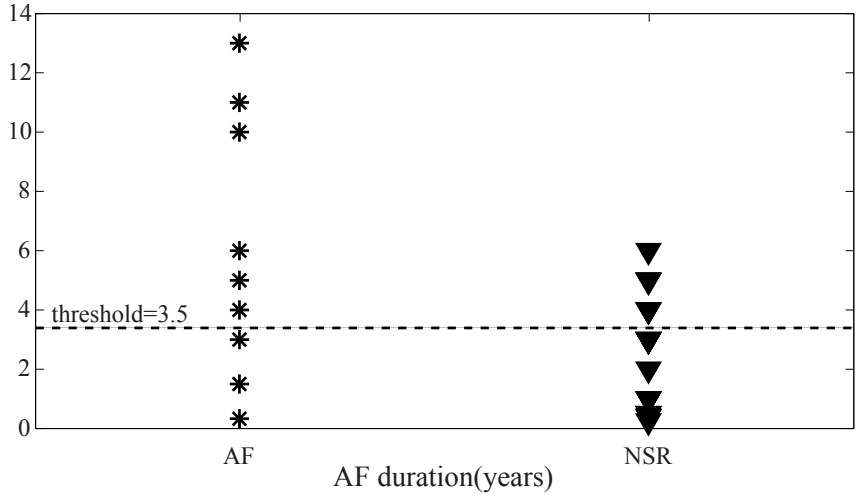

Figure 4.27. AF time values associated to AF and NSR groups 12 months after surgery. Threshold between groups is also displayed.

threshold is maximized. Additionally, the distribution shows that there are no patients in the NSR group with more than 6 years in AF. Consequently, a "virtual" threshold may be set at 6 years used to skip further analyses in those patients with an AF duration greater than 6 years.

With respect to LA size, Figure 4.28 shows its distribution. Its threshold is 46 mm, which is the same that in other follow up perdiods. However, the change causes a loss in the prediction capability since the patient relapsing to AF had

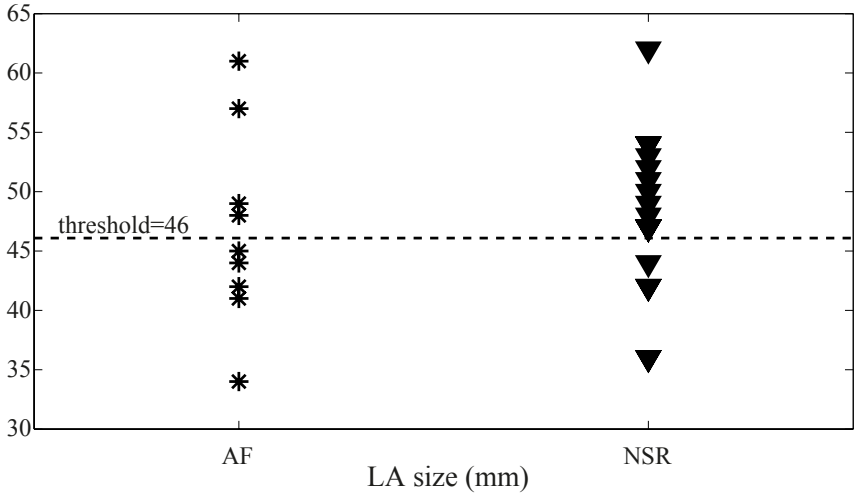

Figure 4.28. LA size values associated to AF and NSR groups 12 months after surgery. Threshold between groups is also displayed.

a LA size of 49 mm. Nevertheless, due to LA size distribution, no change in threshold would improve the accuracy.

Regarding age values, they are showed in Figure 4.29. In this follow up period, the threshold is the same value that at 3 and 6 months, 67.5 years. However, the patient relapsing to AF is 60 years old. Therefore, the age accuracy decreases in this period. This change algo decreases the mean value of the AF group in one year.

Finally, regarding weight and BMI, their distributions are showed in Figure 4.30 and Figure 4.31. In both cases, the consequences of the patient changing rhythm are the same that the ones for LA size and age. No threshold change, loss in the prediction capability, but still the prediction is maximized.

Next to recomputing the indices distribution, prediction capability for the 12 months follow up was assessed. In Table 4.10 these results are showed. The best predictors were fWP and SampEn, nevertheless, the fWP yielded a higher AUC. Following these indices in accuracy was the DAF, which, additionally, had greater AUC than the SampEn. Hence, ECG indices were best predictors than clinical indices. From these latter, only AF duration surpassed the 70% of accuracy.

As in previous follow up analysis, next step was to redesign the classification trees. Figure 4.32 to Figure 4.34 show the trees generated with ECG indices, clinical indices and combining both types of indices respectively. In each figure, two different trees are showed, one defined with the Gini's diversity index as split criterion and the other using the entropy index. It is worthy to note that trees generated combining the ECG and clinical indices are identical regardless of the split criterion used. Specifically, the tree uses first the fWP, which is the best in-

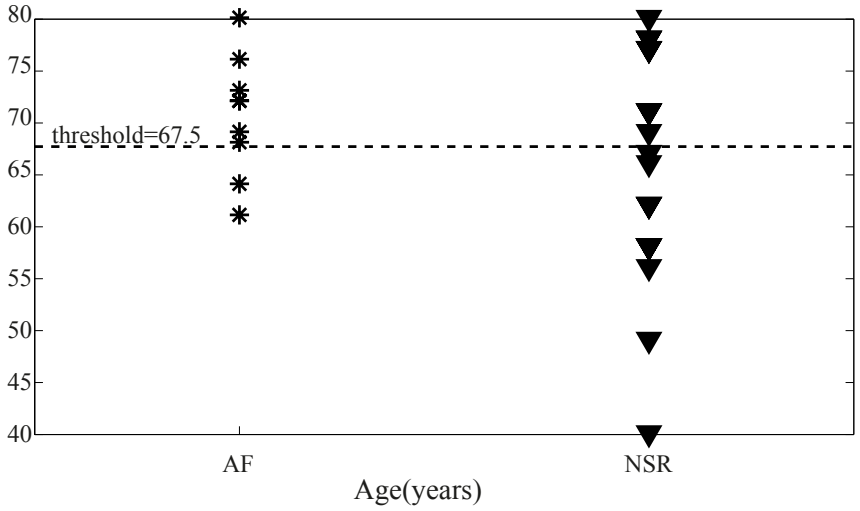

Figure 4.29. Age values associated to AF and NSR groups 12 months after surgery. Threshold between groups is also displayed.

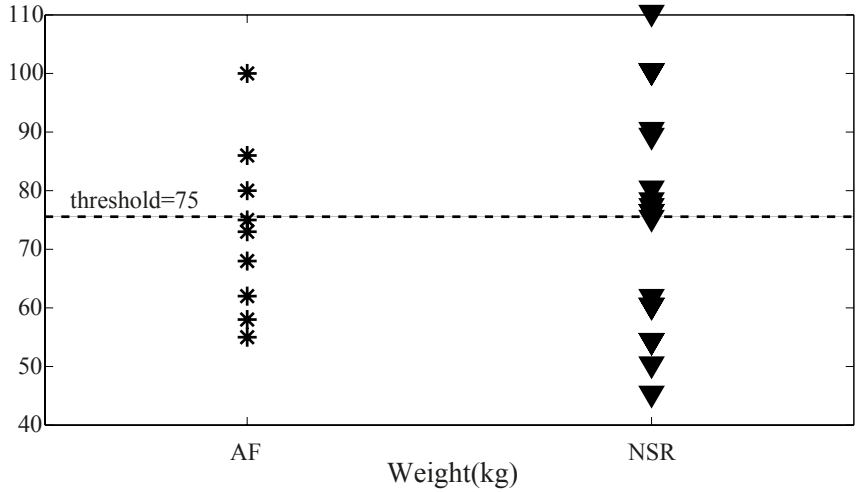

Figure 4.30. Weight values associated to AF and NSR groups 12 months after surgery. Threshold between groups is also displayed.

dividual predictor and then the AF duration, setting a threshold of 5.5 years to divide between AF and NSR. This threshold coincides with the ”virtual index” comented above.

Table 4.11 shows the accuracy obtained with the prediction models. All models designed surpassed the results obtained with individual indices. The highest accuracy is yielded by the tree combining ECG and clinical indices and by the tree using clinical indices and Gini's index as split criterion. However, the lat-

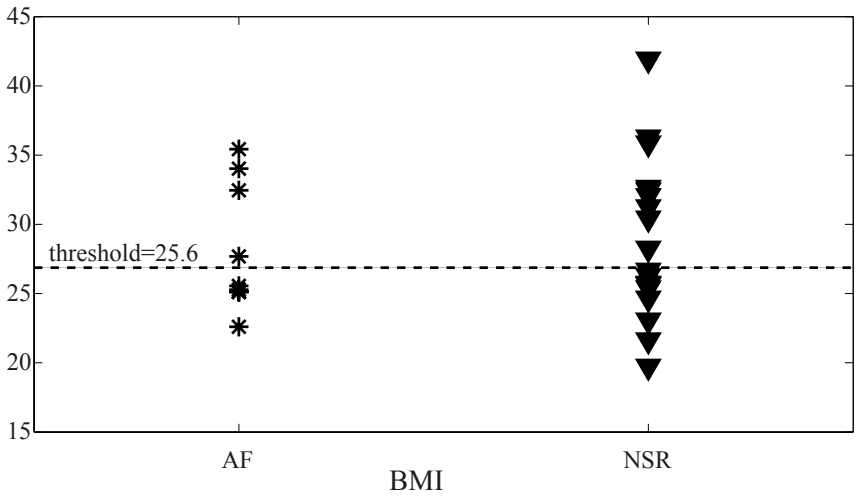

Figure 4.31. BMI values associated to AF and NSR groups 12 months after surgery. Threshold between groups is also displayed.

Table 4.10. Results of sensitivity, specificity and accuracy of the indices when classifying preoperatively into AF and NSR 12 months after the procedure, together with their AUC. Furthermore, the leave one out test results are included

	Sensitivity	Specificity	Accuracy	AUC	Leave one out
DAF	88.89%	66.67%	74.08%	0.821	70.37%
SampEn	88.89%	72.22%	77.78%	0.809	74.08%
fWP	88.89%	72.22%	77.78%	0.8457	70.37%
AF duration	66.67%	72.22%	70.37%	0.7346	66.67%
LA size	55.56%	72.22%	66.67%	0.6049	48.15%
Age	77.78%	55.56%	62.97%	0.6358	55.56%
Weight	66.67%	61.11%	62.97%	0.5309	55.56%
BMI	55.56%	72.22%	66.67%	0.5617	59.26%

ter has many branches with several combinations of the indices, suggesting that the tree results could not be robust with different databases. This hypothesis is reinforced by the leave one out test, where the clinical indices tree yielded only a 66.67%. On the other hand, tree using all the indices yielded a 92.6% of accuracy in the leave one out test. Furthermore, the models were very similar in each iteration, suggesting that data used is representative.

Regarding the split criterion, it is noticeable that besides the clinical indices, it has no effect in the Se, SP and accuracy of any tree. Furthermore, it does not

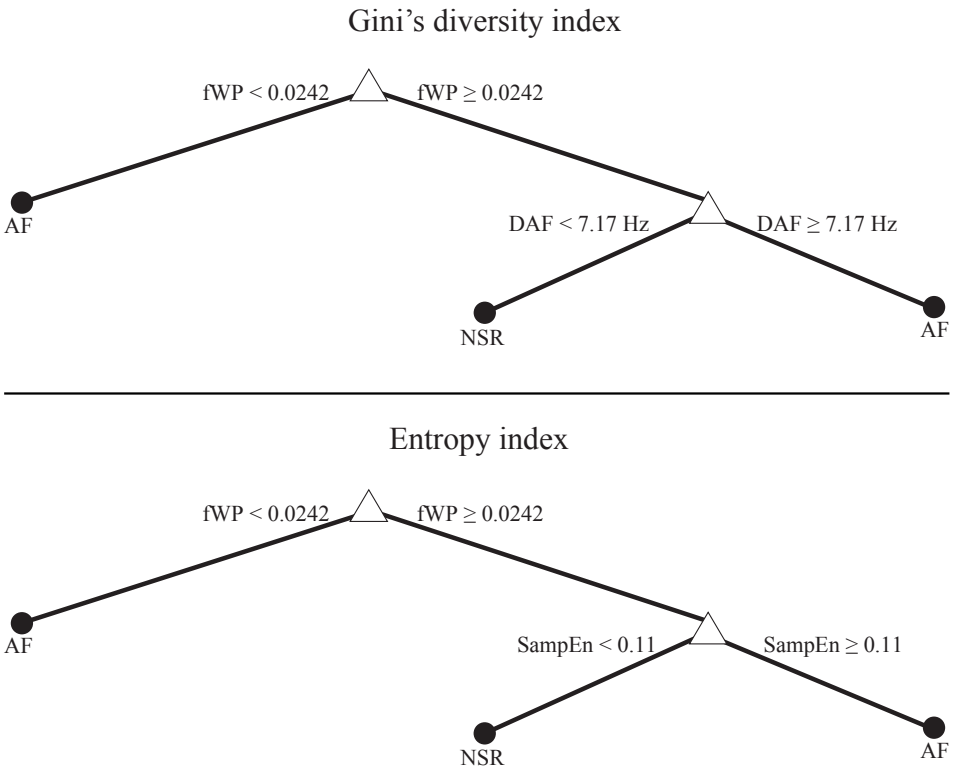

Figure 4.32. Classification tree predicting rhythm 12 months after the Cox-Maze procedure using ECG indices with Gini's diversity index as split criterion (top) and with entropy index as split criterion (bottom).

affect the leave one out test neither. However, despite obtaining the exact same results, the ECG trees generated are different. Both start with fWP but then next branch in the Gini tree uses DAF while in the entropy tree uses SampEn. Hence, the information contained in SampEn and DAF should be very similar.

Finally, the logistic regressions computed are showed below:

$$logit_{ECG} = 0.326DAF + 96.77SampEn - 126.87fWP - 8.05 \tag{4.7}$$

$$\begin{aligned} logit_{clinical} &= 0.792AFduration - 0.25LAsize + \\ &+0.02age + 0.005weight - 0.067BMI + 8.256 \end{aligned} \tag{4.8}$$

$$\begin{aligned} logit_{combination} &= 3.69DAF - 58.82SampEn - 207.17fWP + \\ &+1.36AFduration - 0.49LAsize + 0.12age - 3.3 \end{aligned} \tag{4.9}$$

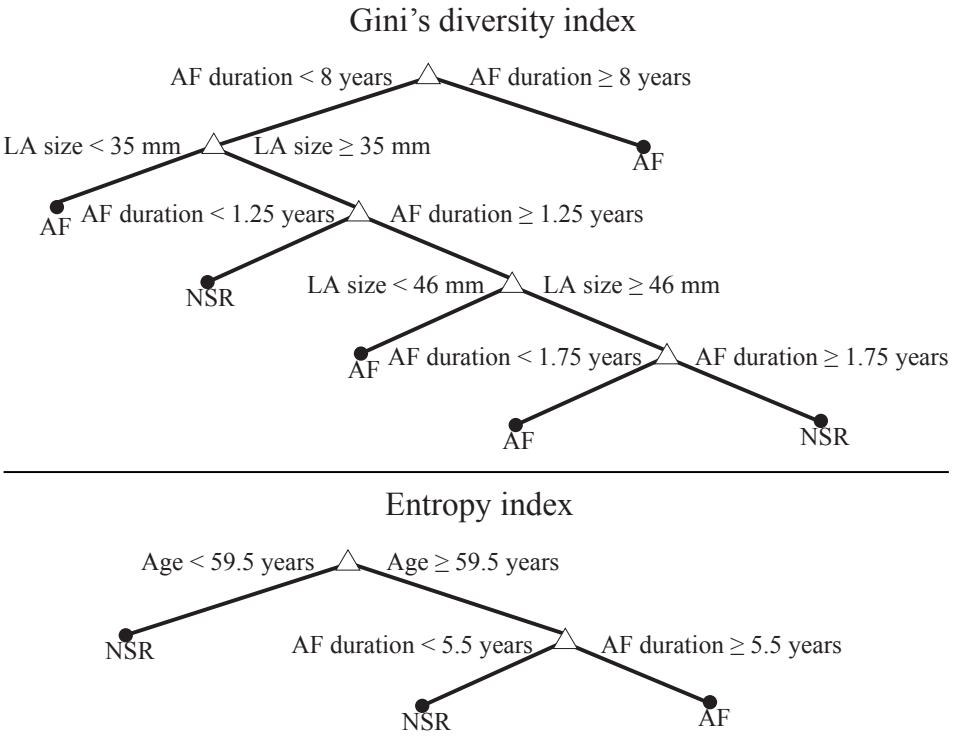

Figure 4.33. Classification tree predicting rhythm 12 months after the Cox-Maze procedure using clinical indices with Gini's diversity index as split criterion (top) and with entropy index as split criterion (bottom).

Table 4.11. Results of sensitivity, specificity and accuracy of the classification trees, together with the leave one out test results when predicting patient's rhythm 12 months after the Cox-Maze procedure

	Split criterion	Sensitivity	Specificity	Accuracy	Leave one out
ECG indices	Gini's index	88.9%	94.44%	92.6%	85.19%
	Entropy index	88.9%	94.44%	92.6%	85.19%
Clinical indices	Gini's index	88.9%	100%	96.3%	66.67%
	Entropy index	77.78%	83.33%	81.5%	66.67%
Combination	Gini's index	100%	94.44%	96.3%	92.6%
	Entropy index	100%	94.44%	96.3%	92.6%

As it can be observed, the functions with the ECG indices and clinical indices used all of them. On the other hand, in the combination function, the parameters related with weight were excluded. Regarding the prediction results, they are showed in Table 4.12. In this follow up, every regression obtained highest accuracy than the indices alone. Regressions with ECG indices and with the indices

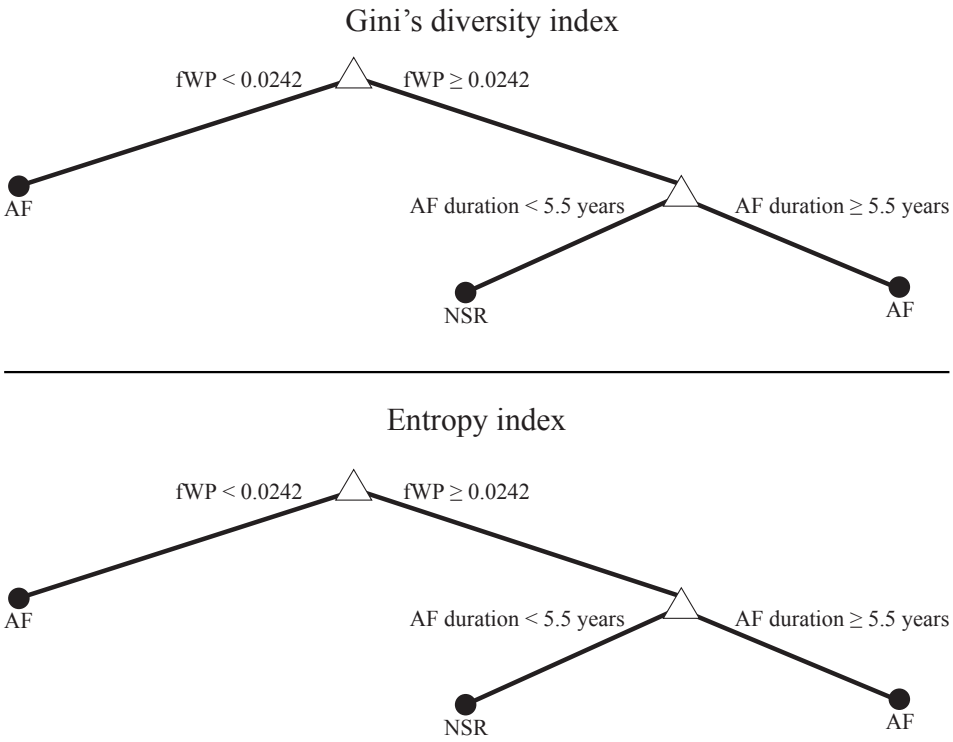

Figure 4.34. Classification tree predicting rhythm 12 months after the Cox-Maze procedure combining ECG and clinical with Gini's diversity index as split criterion (top) and with entropy index as split criterion (bottom).

Table 4.12. Sensitivity, specificity and accuracy of the logistic regression together with the Hosmer-Lemeshow test result when predicting patient's rhythm after 12 months.

	Sensitivity	Specificity	Accuracy	Hosmer-Lemeshow
ECG indices	88.9%	88.9%	88.9%	0.259
Clinical indices	66.7%	88.9%	81.5%	0.465
Combination	77.8%	94.4%	88.9%	0.811

combination yielded the same accuracy, which was higher than the accuracy of the regression with clinical indices. Finally, the Hosmer-Lemeshow test proved that the models fit properly the data.

Chapter 5

Discussion

In this section, the meaning and clinical implications of the results obtained are studied and explained by means of previous literature. Furthermore, new findings and hypothesis made are detailed. Since there are 8 different indices, each one of them is analyzed separately. Afther that, the implications of the prediction models developed are state and, finally, an overall analysis is performed.

To the best of our knowledge, this thesis has introduced for the first time a new set of ECG parameters able to predict preoperatively AF reversion after Cox-Maze surgery. The indices studied have been related to the f waves amplitude (fWP) and the organization of the arrhythmia (DAF and SampEn). Traditionally, only clinical data have been widely analyzed to predict preoperatively the patient's rhythm at long term, i.e., several months or even years after the procedure [11, 13]. However, no studies have paid attention to the analysis of the ECG within this context.

Nevertheless, based on its value for understanding the pathophysiology of AF, its contribution for reconstructing the history of AF in a single patient, and its expected strong contribution for treatment decisions at the individual patient level, it is foreseeable that advanced ECG analysis should become a key element in AF characterization and be included as such in future classifications of AF [21]. As a matter of fact, ECG has been analyzed successfully to predict AF reversion under several scenarios, such as electrical or pharmacological cardioversion [29, 66], this work is focused on assessing the capability of several ECG key features to predict the Cox-Maze outcome.

In this work, the predictions are performed during the first year follow up visits, which are at discharge and then after 3, 6 and 12 months. However, given that between 3 and 6 months there were no rhythm change in any patient, these two follow ups were studied together. Furthermore, clinical data widely used to predict Cox-Maze outcome such as AF duration, LA size and age [11] have been also studied, together with new clinical parameters that could be useful in the prediction, specifically weight and BMI. In this way, new ECG and clinical information has been analyzed and compared with the typical predictors and, complementary, a combination of clinical and ECG features has been performed to maximize the predictions accuracy.

The Cox-Maze long term outcome prediction could help avoiding the procedure in those patients with low probability of success [11, 13]. This is the aim of the prediction after 12 months. Hence, a preoperative prediction of patient's rhythm after 12 months could help to raise the Cox-Maze procedure efficiency by performing a proper patient selection. In this sense, patient's with low risk of maintaining NSR after 12 months would not undergo the surgery.

As commented above, the long term prediction is clinically relevant and in consequence, it has been widely analyzed in previous studies [11, 19]. In contrast, little attention has been paid yet to short term outcome predictions, especially at discharge. One possible reason to this lack of studies could be that after surgery the heart is recovering and transient arrhythmias may occur [75]. As a result of this rhythm instability in the early postoperative stages, a blanking period without taking any postoperative decision before reporting conclusive outcomes is usually defined [14]. In consequence, most hospitals dispense the same postoperative treatment to all the patients, regardless of their rhythm, consisting of oral anticoagulants and antiarrhythmic drugs [12].

However, surgery outcome prediction at discharge could also be clinically useful for an improved management of the patients. Hence, it would be more appropriate to be able to supply a personalized treatment to every patient as a function of the rhythm at discharge. Thus, patients with a high probability of maintaining NSR could avoid standard drug treatment and their stay in the hospital could be reduced. In contrast, for patients in high-risk of AF at discharge, appropriate drugs and a longer stay in the hospital could be planned. In this way, the effectiveness of any treatment could be maximized and the risk of adverse outcomes could be controlled [32]. Moreover, during the time between surgery and discharge a detailed follow-up protocol for the patients could be designed, including ECV-related decisions in those ones with higher likelihood of AF recurrence. Furthermore, some hospitals treat post-surgery AF with chemical or electrical cardioversion before discharge [13]. Hence, the possibility to predict the patient's rhythm at discharge could be used to avoid cardioversion in those patients in whom AF only appears transitorily. In this way, the patient's quality of life could be improved and clinical resources and costs optimized.

On the other hand, after the 3 months blanking period [5, 6], patient's rhythm is evaluated and the therapy is modified in consequence. In those patients maintaining the NSR, the antiarrhythmic drugs are withdrawn whereas in patients relapsing to AF, ECV is proposed. Then after 6 months, the anticoagulant drugs are withdrawn in those patients maintaining the NSR. Thus, a preoperative prediction of patient's rhythm after 3 and 6 months could be useful. As the treatment before discharge, the patient's therapeutic treatment could be modulated depending on the risk of maintaining mid-term AF. Furthermore, the ECV could be planned in advance, reducing the postoperative AF duration and in that way, the arrhythmia perpetuation probability [15]. There are few studies aiming to predict patient's rhythm after 3 and 6 months using clinical information [13]. However, the obtained prediction capability was limited [13].

In conclusion, predicting short and mid term Cox-Maze surgery outcome would allow the customized modulation of the antiarrhythmic and anticoagulant drug treatments, as a function of the surgery outcome for each patient. To this respect, treatment personalization would allow to reach high efficacy and safety in AF management by applying specific therapies to each patient [32]. Furthermore, this kind of prognosis would also enable the anticipation of ECV-related decisions in those patients with bad outcome prediction. In this way, clinical costs could be reduced and the patient's quality of life could be improved.

5.1 ECG indices

5.1.1 AF organization

Regarding the ECG characterization, the AF organization has been related to the number of wavelets in the atria [158, 126], which, in turn, affects to the AF persistence [15]. These studies related a higher disorganization with a bigger number of wavelets through the atria. It is notable that the development of the surgical Maze procedure was predicated on this model of AF and the concept that maintenance of AF requires a critical number of circulating reentrant wavelets, each of which requires a critical mass of atrial tissue [159]. Thus, if the number of wavelets is high, the statistical probability of extinguishing all with the ablation will be lower than if only a small number of wavelets is present [15]. The number of wavelets at any point in time depends on the atrial conduction velocity, refractory period, and mass [14]. Thus, perpetuation of AF is favored by slowed conduction, shortened refractory periods, and increased atrial mass. Enhanced spatial dispersion of refractoriness promotes perpetuation by heterogeneous conduction delay and block [14]. In conclusion, the number of wavelets in the atria could be related to the electrical remodeling [15, 18].

Hence, AA organization could point the degree of electrical remodeling in the atria [137]. Furthermore, previous studies have shown that a high correlation exists between the refractory period as measured by programmed electrical stimulation and the average cycle length during fibrillation [15, 27]. Therefore, the DAF was computed to obtain the average cycle length. On the other hand, the SampEn measures the regularity in the AA signal and therefore, it is an estimation of the number of wavelets in the atria. In both cases, a higher value of these indices is related to a higher disorganization [29]. In agreement with those studies, in this paper, higher values of DAF and SampEn have been associated with AF recurrence, therefore a higher degree of disorganization would be related to a greater likelihood of AF recurrence after the Cox-Maze procedure. From this point of view, results suggest a higher probability of AF recurrence after surgery when the preoperative electrical remodeling is in a more advanced state.

With respect to the discrimination capability of both methods, SampEn obtained always statistically significant differences whereas DAF obtained them at 3, 6 and 12 months but not at discharge. Regarding the prediction capability, they obtained similar results being SampEn more accurate at discharge and 12 months whereas DAF was more accurate at 3 and 6 months. However, in this follow up, the DAF leave one out results were low and in consequence the accuracy is not completely reliable. Thus, in general, both indices show similar prediction capability but SampEn seems more reliable. These results are in agreement with previous works, which have reported that DAF and SampEn are metrics highly correlated, being the SampEn more accurate [29, 160].

Finally, the behaviour of these to indices with time is similar, adapting the

threshold to optimize the prediction capability. Furthermore, patients recovering NSR were patients with low DAF and SampEn values in the AF group. Thus, with the proper analysis, these indices could help to detect transient arrhythmyas after the Cox-Maze surgery during the blanking period.

5.1.2 Fibrillatory waves mean power

The f waves amplitude is the only ECG characterization used previously to predict long term Cox-Maze result, obtaining accurate results [24]. In agreement with these works, patients still in AF postoperatively showed lower fWP values than those in NSR [24]. In fact, low amplitude f waves is accepted as a risk factor of late AF recurrences after surgical treatment [106, 125]. The f waves amplitude represents the sum of local depolarization phenomena involving cardiac cells, which is related to the magnitude of the remaining viable atrial muscle[25]. Therefore, the f waves amplitude is mainly affected by the state of the atrium, such as atrial fibrosis and degeneration as well as the atrial size [24]. With the prolongation of AF, the atrial electric motive force is considered to decrease as a result of progression of atrial dilatation [98], loss of atrial muscle mass, and atrial fibrosis [24, 105], as well as degeneration of the atrial myocardium due to underlying disorders [15]. As a consequence, a low f waves amplitude could be associated with greater atrial fibrosis and degeneration resulting in a lower likelihood of NSR restoration [24].

Given that these characteristics have been used to determine the atrial structural remodeling [5, 18], the f waves amplitude could be considered as a concomitant estimator of the structural remodeling in AF [137]. However, most of the studies used a different method that the one used in this work. The method consists of measuring the greatest fibrillatory wave, with the aid of calipers, from the upper edge of the trough to the upper edge of the peak, and express it in millimeters [24]. This procedure is inaccurate and user-dependent, thus, this paper has proposed to study the f waves amplitude using the fWP, which is an automatic reliable method [161]. Analyzing the results, fWP showed statistical differences in every follow up. Moreover, fWP was one of the best predictors in every follow up. Therefore, in general, the fWP could be the best predictor between the studied. Furthermore, patients with postoperative AF shown lower fWP values than those in NSR, thus, the results obtained with the fWP are in agreement with previous studies using the traditional method [24]. In conclusion, given that f waves amplitude has been previously associated with structural parameters of the atria [24], this result suggests that the higher the preoperative atrial structural remodeling, the higher the probability of AF recurrence after the surgery.

On the other hand, the fWP threshold remained invariant with time, despite the changes in patients' rhythm. Indeed, the patients changing rhythm have fWP values along the AF range. In conclusion, the ROC and threshold computed for discharge analysis are robust, and not affected by time variations.

5.2 Clinical indices

5.2.1 AF duration

Regarding the clinical indices, previous studies have related AF duration with the shortening of atrial refractoriness period, which is a direct effect of the rate of electrical activation of the atrial cells [96]. Furthermore, AF duration also attenuates the physiological rate adaptation of the refractory period [162]. In the Wijffels studies [15, 96], the shortening of atrial refractoriness was accompanied by an increase in inducibility and stability of AF. In these studies, after cardioversion the atrial interval suddenly prolongs from about 100 to 150 ms during atrial fibrillation to about 1000 ms during sinus rhythm. When the atrial refractory period fails to adapt to such a sudden slowing in heart rate by a prolongation of the refractory period, or even worse, when it becomes shorter due to an inversed rate adaptation, after conversion to sinus rhythm the atria will be left with a dangerously short refractory period. Without the natural protection of a long refractory period, the atrial wavelength will be very short and on first occasion an atrial premature beat may start fibrillation again [15]. In conclusion, the shortening of the atrial refractory might explain the diminished success rate of the cardioversion and surgery attempts to restore NSR in patients with long-lasting AF.

Additionally, the finding that the shortening of atrial refractoriness needs a few days to revert completely could explain the early recurrences seen after cardioversion [15]. However, there are reasons to believe that besides the shortening of refractoriness also other factors may play a role in the development of chronic fibrillation. This is supported by the observation that the time course of changes in atrial refractoriness does not completely run parallel with the time course of development of sustained fibrillation [15]. In the Wijffels studies, it was observed that whereas the median fibrillation interval usually already reached a steady state within a couple of days, it often took an additional 1 to 2 weeks for atrial fibrillation to become persistent [15]. Therefore, although the AF duration is directly related with the likelihhof of relapsing to AF, it seems that there are additional changes in the atria requiring a longer time period to develop. In this study, AF duration has showed the best accuracy from clinical indices, and showing statistically significant differences in each follow up. Despite of these results, accuracy values are below the values yielded with the ECG indices.

With regards to the time evolution, this index improved significantly from discharge to 6 months follow up. And, although it decreased from 6 to 12 months follow up, the AUC increased in each follow up. Thus, AF duration is not a good predictor at discharge moment, but with time evolution its predictions are more accurate. However, in order to increase its prediction ability, the threshold is adapted in each follow up. On the other hand, AF duration could also help to identify those patients with transient arrhythmias during the blanking period, because, as with DAF and SampEn, patients recovering NSR were the ones with lower values in the AF group. This change also had an impact in the AF mean

value but not in the NSR group. Thus, patients changing rhythm are closer to NSR mean value than to the AF mean value.

Finally, in this index a "virtual" threshold can be observed. Over 6.5 years, any patient recovered NSR, while below that, the results are mixed. Hence, this index could provide an initial classification. Wether the patients AF lasts more than 6.5 years, Cox-Maze should not be applied and no further analyses are required. Below this value, another indices should be considered to make a decision.

5.2.2 LA size

With regard to the LA size, it is the most usual estimation of the atrial dilation [14], which promotes AF by increasing circuit path space so that larger reentry circuits can be supported and/or a larger number of circuits can be maintained [105]. The number of wavelets that can coexist in the atria is determined both by the atrial tissue mass (or surface area), and the wavelength of the atrial impulse. It is well known that in larger hearts atrial fibrillation is more stable and of longer duration, and that in humans atrial dilatation is an important risk factor for atrial fibrillation. This can be easily understood by realizing that the number of circuits in the atria increases with the square of the atrial diameter and that in larger mammals the wavelength of the atrial impulse does not increase proportionally to the size of the atria [15]. However, the results of these study related smaller LA size to AF. Analyzing Table 3.1, the LA size mean value and standar deviation is 47.6 mm $\pm$ 7. However, some studies have shown that LA size did not predict AF relapse when the diameter was below 55 mm [163], and the threshold to divide between AF relapse or not has been set around 65 mm [19]. In fact, many studies where the mean value was below 55 mm have not found statistically significant differences, and the mean values between NSR and AF groups was very similar [75, 164, 165].

LA size threshold was not affected by the patients' time evolution. Nevertheless, no significant differences were found in any follow up. Thus, further analysis should be performed before extracting conclusions.

5.2.3 Age

Regarding the age index, previous studies demonstrated that aging is associated with atrial remodeling characterized by: anatomical and structural changes, reductions in atrial voltage with discrete areas of low voltage, widespread conduction slowing as well as anatomically determined functional conduction delay and block, and sinus node dysfunction. These changes may, in part, be responsible for the increased propensity to atrial arrhythmias observed with increasing age [110]. Therefore, an older patient would have more likelihood to relapse to AF. However, many studies have shown that between 40 and 70 years old, age was not a relevant index to predict AF relapse [163, 164, 165]. Looking to the patients' age

included in this study, Table 3.1 shows that mean age and standard deviation is 67.1 $\pm$ 9.8 years. Therefore, the age of patients composing the database of this study is not in the interval that could provide significant results.

As with the LA size, no statistically significant differences were found. Thus, further analysis should be performed to extract conclusions. Nevertheless, regarding the time evolution, an interesting hypothesis could be state. Patients recovering NSR after the blanking period are the youngest ones of the AF group at discharge. Thus, age could also provide interesting information to predict transient arrythmias in patients.

5.2.4 Obesity

Finally, the last clinical indices analyzed were weight and BMI. The analysis of weight and BMI showed limited prediction capability and no statistically significant results. In this sense, similar results have been obtained previously when analyzing BMI as a risk factor of AF recurrence after catheter ablation [123]. Furthermore, in the Wanahita studies, although obesity increased the risk of new onset AF, in the postcardiac surgery population, obesity was not shown to increase the risk of developing AF [113]. However, other studies yielded the conclusion that obesity is an independent risk factor of AF recurrence after catheter ablation [119] and correlated it with LA size [118]. In conclusion, the mechanism by which BMI influences the perpetuation of AF resulting in higher arrhythmia recurrence is not completely understood [120] and is not always present. Nevertheless, it has been hypothesized that the association between high BMI and AF recurrence appears to be mediated by left atrial enlargement [120]. In this study neither BMI nor LA size was found as an independent risk factor of AF recurrence. However, computed crosscorrelation between weight and LA size yielded a 0.15 value, whereas cross correlation between LA size and BMI yielded 0.3. Thus, in this study, these indices are not strongly correlated.

Finally, regarding time evolution, weight index maintained its threshold invariant while BMI threshold changed from discharge to 6 months follow up and then, it remained invariant. In both cases, patients recovering NSR after the blanking period were patients with lower weight in the AF group, and, since in this study little weight has been associated to AF, the prediction capability of these indices worsened with time.

5.3 Prediction models development

The results showed by the prediction models showed the same tendency that the analysis performed to the indices separately, being better predictors the models using ECG indices that clinical indices. However, in all the cases, combination of both indices types improved the accuracy results and the Hosmer-Lemeshow

index for the logistic regression or the leave one out test for the classification tree. Therefore, combining indices provided greater accuracy and more robust prediction models.

Analyzing the leave one out results, they improved significantly with the different follow up periods, yielding 92.6% with the classification tree combining indices at 12 months. These results reinforce the clinicians theory that after Cox-Maze surgery postoperative AF may occur transiently after the procedure [5]. These transient arrhythmias may hinder the predictions performed at short and mid term.

5.4 Overall analysis

Analyzing the results, ECG indices seem to be better predictors than the clinical indices. To this respect, SampEn and fWP obtained statistically significant differences in every follow up. Additionally DAF was statistically significant at 3, 6 and 12 months follow up. On the other hand, regarding clinical indices, only AF duration showed statistically significant differences in every follow up. Furthermore, in general, the accuracy yielded with the ECG indices was bigger than the one obtained with the clinical indices. This result could be due to the fact that ECG indices analyze directly the effect of the AF over the heart electrical activity. On the other hand, clinical indices measure causes and likely effects produced by the AF [11, 21]. Thus, it is an indirect measure of the atrial remodeling. Furthermore, it could be a data bias related with the clinical indices. This bias is produced because clinicians decide to operate patients with greater likelihood to restore NSR and they assess this likelihood with the clinical information.

Regarding the time evolution effect on indices behavior: fWP, LA size and weight kept their threshold invariant, pointing that their ROC curves are robust to changes in patients. On the other hand, DAF, SampEn, AF time, age and BMI adapted their value. All these indices but BMI quantify directly or indirectly the atrial electrical remodelling. Since at 3 months follow up, 4 patients recovered NSR pointing they were at discharge due to the transient arrhythmias [75], the analysis of electrical remodelling could help to predict these transient arrhythmias and their causes. Additionally, in this work, all patients having arrhythmias were women. Thus, gender could also affect to the appareance of transient arrhythmias.

5.5 Limitations of the study

Finally, it is important to remark that despite showing auspicious results, this work present some limitations. Firstly, it has to be mentioned the relative low number of patients and, therefore, the presented results must be considered with

caution. Secondly, looking to the results it seems to be a selection bias regarding LA size and age. It is likely, that since these indices are accepted risk factors, old patients and patients with large LA size did not undergo surgery to avoid AF recurrence. Thirdly, only lead V1 has been studied to obtain information about the AA, thus ignoring the remaining ECG leads, which can contain significant information [166].

Chapter 6

Conclusions, Future Lines and Contributions

This final chapter contains the main conclusions derived from the research work carried out in this doctoral thesis. Furthermore, given that the accomplishment of a research work always suggests undertaking additional tasks, likely future lines of development are mentioned. FInally, the scientific contributions derived from this work are presented.

6.1 Global Conclusions

The present work has introduced, for the first time, a meticulous analysis of the ECG to predict preoperatively the outcome of the AF surgical ablation. This prediction has been performed at discharge, 3, 6 and 12 months after surgery using different ECG indices and traditional clinical indices. By gathering this information, this work intended to predict preoperatively the Cox-Maze surgery outcome.

In order to develop this goal, secondary objectives were presented and fulfilled: a comparison between clinical and ECG indices prediction capability was performed, to analyze patients evolution from discharge to 12 months follow up and to study a new way of quantifying the atrial remodelling by using the ECG information.

The results showed that the ECG analysis provided more accurate predictions than the traditional clinical analysis. In every follow up, ECG analysis showed statistically significant differences. On the other hand, from clinical indices, only AF duration obtained statistically significant results. Regarding the prediction capability, the ECG indices outperformed the clinical indices in any follow up period. On the other hand, the prediction models performed with ECG and clinical indices yielded similar results. However, this results are, in part, due to the fact that there were more clinical indices than ECG indices, and, therefore more information. In the classification trees, the leave one out test showed better results with the ECG indices. Nevertheless, since clinicians perform a previous analysis to decide which patients should undergo the surgery, is likely that a bias is present in the clinical indices. As a result, age and LA size showed no statistically differences between AF and NSR groups and were not useful to the predictions. Furthermore, weight and BMI, studied as risk factors, were not statistically significant neither. Hence, what can be affirmed is that, ECG analysis provide more detailed information and an additional tool to discriminate those patients that initially have been found suitable to undergo Cox-Maze surgery.

On the other hand, by analyzing ECGs, new approaches to quantify the atrial remodelling have been defined. In this sense, DAF and SampEn measure the AF organization, and, consequently, the electrical atrial remodelling. Thus, higher values of DAF and SampEn means that more wavelets are circulating through the atria and, in consequence, the higher DAF and SampEn, the higher the probability of relapsing to AF. Regarding the structural remodeling, it is related with atrial fibrosis, atrial dilatation and loss of atrial muscle mass. Thus, as the structural remodelling grows, the amplitude of the f waves decrease and, as a result, the fWP. Hence, lower values of fWP are related to greater structural remodelling and, therefore, lower fWP values point to greater probability of relapsing to AF.

In conclusion, new approaches to quantify the atrial remodelling have been proposed. These new approaches may help to understand several AF causes and mechanisms that are still unknown.

Finally, after analyzing the individual indices and the information contained, the main goal of the thesis was pursued by combining clinical and ECG indices to create different prediction models. Results confirmed that the information contained in the ECG is complementary to the clinical information and, consequently, the prediction capability improved. Furthermore, the prediction results with the classification trees generated exceeded 90% in all the follow up periods. However, the leave one out test decreased considerable the prediction capability at discharge, 3 and 6 months follow up. On the other hand, at 12 months after surgery, the leave one out test yielded 92.6% accuracy. Hence, prediction results at 12 months after surgery are auspicious and their robustness has been checked while, at short term, further analyses should be performed and new models must be generated to corroborate the results reliability.

6.2 Future Lines of Research

This work database consisted on only 27 patients, thus, the most important line would be to keep including patients to the database. In this way, further analysis could be done to better understand the AF mechanism and perform more accurate quantification of electrical and structural atrial remodelling. In addition, increasing the database will also lead to analyze the robustness of the results obtained in this work as well as could be helpful to develop and study better prediction models.

Once the database is increased and the robustness and repeteability of the results confirmed, it would be interesting to work in developing a classification tool able to predict *in situ* the surgery outcome, which should be readily usable by clinicians. In this way, the tool might contribute to differentiate patients which may restore NSR and also to personalize each postoperative treatment, avoiding innecesary drugs control and saving costs.

Additionally, the information analyzed to predict Cox-MAze surgery outcome could be studied to assess its prediction capability in other AF treatments such as rhythm control, ECV, catheter ablation, among others. Gathering all these data, a common prediction tool could be developed in such way that clinicians could analyze patients' information and receive a diagnosis that suggests the best strategy to treat the patient. In this way, the tool helps identifying patients expected to benefit most from rhythm control therapy, guides treatment choice (cardioversion, ablation, or drug therapy), and contributes to predict treatment outcome, ideally at the individual patient level.

Finally, given the behaviour observed in indices assessing electrical remodelling, more information could be gathered in order to understand and predict the appearrance of transient arrhythmias after surgical ablation of AF.

6.3 Scientific contributions

6.3.1 Main Thesis Publications

The work carried out in this thesis has been published in several scientific journals of international scope and has been presented in national and international conferences. Next these scientific contributions are enumerated.

An initial study assessing the ECG prediction capability of the Cox-Maze surgery outcome at discharge was published in the journal *Physiological Measurement*:

- A. Hernández, R. Alcaraz, F. Hornero, and J.J. Rieta. Preoperative study of the surface ECG for the prognosis of atrial fibrillation maze surgery outcome at discharge.*Physiological Measurement* 93, 2(2014), 1409-1423.

A study analyzing the atrial remodeling for long-term success prediction of concomitant surgical AF ablation has been published in the journal *Cirugía Cardiovascular*

- E.Martín, F. Hornero, J.J. Rieta, A. Hernández, F. Paredes, A. Mena, O. Gil, S. Cánovas, R. García, J. Martínez. Preoperative study of the surface ECG for the prognosis of atrial fibrillation maze surgery outcome at discharge.*Cirugía Cardiovascular* 23, 3(2016), 125-131.

A paper analyzing the ECG information to predict the outcome of AF surgery after the blanking period is currently under revision at the *Journal of Healthcare Engineering*:

- A. Hernández, R. Alcaraz, F. Hornero, and J.J. Rieta. Forecasting Cardiac Arrhythmias Surgery Outcome at Three Months Follow-up.*Journal of Healthcare Engineering*.

A paper comparing the clinical and ECG prediction capability after Cox-Maze surgery at different follow up periods has been submitted to the special issue *Entropy and Cardiac Physics II* published in the journal *Entropy*:

- A. Hernández, R. Alcaraz, F. Hornero, and J.J. Rieta. Atrial Substrate Remodeling Quantification for the Preoperative Envision of Atrial Fibrillation Surgical Ablation Outcome at Long Term Follow-Up.*Entropy*.

Currently, the development of a chapter for the book *Cardiac Surgery* is under process:

- A. Hernández, R. Alcaraz, F. Hornero, and J.J. Rieta. Application of Signal Analysis to Cardiac Surgery of Atrial Fibrillation.*Cardiac Surgery*.

In addition, some of the main contributions of this thesis have been presented in international conferences:

- A. Hernández, R. Alcaraz, F. Hornero, and J.J. Rieta. Role of Fibrillatory Waves Amplitude as Predictors of Immediate Arrhythmia Termination After Maze Surgery of Atrial Fibrillation.*Computing in Cardiology (CinC)* (2012), vol. 39, p. 661-664.

- A. Hernández, R. Alcaraz, F. Hornero, and J.J. Rieta. Combination of Clinical and Electrocardiographic Indices to Predict Cox-Maze Surgery Outcome at Discharge.*Computing in Cardiology (CinC)* (2013), vol. 40, p. 727-730.

- A. Hernández, R. Alcaraz, F. Hornero, and J.J. Rieta. Application of the Preoperative ECG to Predict Cox-Maze Surgery Mid-term Outcome.*Computing in Cardiology (CinC)* (2013), vol. 40, p. 723-726.

- A. Hernández, R. Alcaraz, F. Hornero, and J.J. Rieta. Preoperative Prognosis of Atrial Fibrillation Concomitant Surgery Outcome after the Blanking Period.*Mediterranean Conference on Medical and Biological Engineering and Computing* (2013), vol. 13, p. 1879-1882.

- A. Hernández, R. Alcaraz, F. Hornero, and J.J. Rieta. Relevance of the Atrial Substrate Remodeling During Follow-Up to Predict Preoperatively Atrial Fibrillation Cox-Maze Surgery Outcome.*Mediterranean Conference on Medical and Biological Engineering and Computing* (2013), vol. 13, p. 1005-1008.

and also in national conferences:

- A. Hernández, R. Alcaraz, F. Hornero, and J.J. Rieta. Predictores Preoperatorios de Terminación Inmediata de la Fibrilación Auricular tras Cirugía Cardíaca.*Congreso anual de la Sociedad Española de Ingeniería Biomédica (CASEIB)* (2012), vol. 30.

- A. Hernández, R. Alcaraz, F. Hornero, and J.J. Rieta. Predictores Electrocardiográficos del Éxito de la Cirugía Maze en el Momento del Alta.*Congreso anual de la Sociedad Catalana de Cirugía Cardíaca* (2013), vol. 16.
  - Best oral communication award.

- A. Hernández, R. Alcaraz, F. Hornero, and J.J. Rieta. Amplitud de las Ondas Fibrilatorias como Predictor Relevante del Resultado de la Cirugía de Fibrilación Auricular.*Congreso de las Enfermedades Cardiovasculares (SEC)* (2013).

- A. Hernández, R. Alcaraz, F. Hornero, and J.J. Rieta. ndicadores Electrocardiográficos Preoperatorios del Ritmo Tras el Período de Enmascaramiento en Cirugía Cox-Maze de Fibrilación Auricular Concomitante.*Congreso de las Enfermedades Cardiovasculares (SEC)* (2013).

6.4 Funding

This work has been supported by the projects TEC2010–20633 from the Spanish Ministry of Science and Innovation, TEC2013–41428–R from the Spanish Ministry of Economy and Competitiveness and PPII11–0194–8121 from Junta de Comunidades de Castilla La Mancha.

Bibliography

[1] D. A. Fitzmaurice, F. D. R. Hobbs, S. Jowett, J. Mant, E. T. Murray, R. Holder, J. P. Raftery, S. Bryan, M. Davies, G. Y. H. Lip, and T. F. Allan. Screening versus routine practice in detection of atrial fibrillation in patients aged 65 or over: cluster randomised controlled trial. *BMJ*, 335(7616):383, Aug 2007.

[2] S. Stewart, C. L. Hart, D. J. Hole, and J. J. McMurray. Population prevalence, incidence, and predictors of atrial fibrillation in the renfrew/paisley study. *Heart*, 86(5):516–521, Nov 2001.

[3] H. V. Bhatt and G. W. Fischer. Atrial Fibrillation: Pathophysiology and Therapeutic Options. *Journal of Cardiothoracic and Vascular Anesthesia*, 29(5):1333–1340, October 2015.

[4] A. S. Go, E. M. Hylek, K. A. Phillips, Y. Chang, L. E. Henault, J. V. Selby, and D. E. Singer. Prevalence of diagnosed atrial fibrillation in adults: national implications for rhythm management and stroke prevention: the anticoagulation and risk factors in atrial fibrillation (atria) study. *JAMA*, 285(18):2370–2375, May 2001.

[5] C. T. January, L. S. Wann, J. S. Alpert, H. Calkins, J. E. Cigarroa, and American College of Cardiology/American Heart Association Task Force on Practice Guidelines. 2014 AHA/ACC/HRS guideline for the management of patients with atrial fibrillation: a report of the American College of Cardiology/American Heart Association Task Force on Practice Guidelines and the Heart Rhythm Society. *Journal of the American College of Cardiology*, 64(21):e1–76, December 2014.

[6] P. Kirchhof, S. Benussi, D. Kotecha, A. Ahlsson, D. Atar, and B. Casadei. 2016 ESC Guidelines for the management of atrial fibrillation developed in collaboration with EACTS. *European Heart Journal*, 37(38):2893–2962, 2016.

[7] D. B. Doty. Surgical treatment of atrial fibrillation. *Heart Lung Circ*, 13(3):280–287, Sep 2004.

[8] J. Dunning, M. Nagendran, O. R. Alfieri, S. Elia, A. P. Kappetein, U. Lockowandt, G. E. Sarris, P. H. Kolh, and E. A. C. T. S. Clinical Guidelines Com-

mittee. Guideline for the surgical treatment of atrial fibrillation. *Eur J Cardiothorac Surg*, 44(5):777–791, Nov 2013.

[9] N. Ad, S. Barnett, E. A. Lefrak, A. Korach, A. Pollak, D. Gilon, and A. Elami. Impact of follow-up on the success rate of the cryosurgical maze procedure in patients with rheumatic heart disease and enlarged atria. *J Thorac Cardiovasc Surg*, 131(5):1073–1079, May 2006.

[10] S. M. Prasad, H. S. Maniar, C. J. Camillo, R. B. Schuessler, J. P. Boineau, T. M. Sundt, J. L. Cox, and R. J Damiano. The Cox-Maze III procedure for atrial fibrillation: long-term efficacy in patients undergoing lone versus concomitant procedures. *J Thorac Cardiovasc Surg*, 126(6):1822–1828, Dec 2003.

[11] N. Ad. The Cox-Maze procedure: history, results, and predictors for failure. *J Interv Card Electrophysiol*, 20(3):65–71, Dec 2007.

[12] F. Hornero, J. A. Montero, S. Cánovas, and M. Bueno. Biatrial radiofrequency ablation for atrial fibrillation: epicardial and endocardial surgical approach. *Interact Cardiovasc Thorac Surg*, 1(2):72–77, Dec 2002.

[13] R. J. Damiano, F. H. Schwartz, M. S. Bailey, H. S. Maniar, N. A. Munfakh, M. R. Moon, and R. B. Schuessler. The Cox-Maze IV procedure: predictors of late recurrence. *J Thorac Cardiovasc Surg*, 141(1):113–121, Jan 2011.

[14] H. Calkins, K. H. Kuck, R. Cappato, J. Brugada, A. J. Camm, and S. A. Chen. 2012 HRS/EHRA/ECAS Expert Consensus Statement on Catheter and Surgical Ablation of Atrial Fibrillation: recommendations for patient selection, procedural techniques, patient management and follow-up, definitions, endpoints, and research trial design. *Europace*, 14(4):528–606, Apr 2012.

[15] M. C. Wijffels, C. J. Kirchhof, R. Dorland, and M. A. Allessie. Atrial fibrillation begets atrial fibrillation. a study in awake chronically instrumented goats. *Circulation*, 92(7):1954–1968, Oct 1995.

[16] S. Petrutiu, J. Ng, G. M. Nijm, H. Al-Angari, S. Swiryn, and A. V. Sahakian. Atrial fibrillation and waveform characterization. A time domain perspective in the surface ECG. *IEEE Eng Med Biol Mag*, 25(6):24–30, 2006.

[17] J. L. Cox, R. B. Schuessler, H. J. D'Agostino, C. M. Stone, B. C. Chang, M. E. Cain, P. B. Corr, and J. P. Boineau. The surgical treatment of atrial fibrillation. III. Development of a definitive surgical procedure. *J Thorac Cardiovasc Surg*, 101(4):569–583, Apr 1991.

[18] M. Allessie, J. Ausma, and U. Schotten. Electrical, contractile and structural remodeling during atrial fibrillation. *Cardiovasc Res*, 54(2):230–246, May 2002.

[19] S. L. Gaynor, R. B. Schuessler, M. S. Bailey, Y. Ishii, J. P. Boineau, M. J. Gleva, J. L. Cox, and R. J. Damiano. Surgical treatment of atrial fibrillation: predictors of late recurrence. *J Thorac Cardiovasc Surg*, 129(1):104–111, Jan 2005.

[20] H. G. Je, J. W. Lee, S. H. Jung, S. J. Choo, H. Song, S. C. Yun, and C. H. Chung. Risk factors analysis on failure of maze procedure: mid-term results. *Eur J Cardiothorac Surg*, 36(2):272–8; discussion 278–9, Aug 2009.

[21] L. Kappenberger. A new look at atrial fibrillation: lessons learned from drugs, pacing, and ablation therapies. *European Heart Journal*, July 2013.

[22] M. Thurmann and J. G. Janney. The diagnostic importance of fibrillatory wave size. *Circulation*, 25:991–994, Jun 1962.

[23] R. H. Peter, J. J. Morris, and H. D. McIntosh. Relationship of fibrillatory waves and P waves in the electrocardiogram. *Circulation*, 33(4):599–606, Apr 1966.

[24] J. Kamata, K. Kawazoe, H. Izumoto, H. Kitahara, Y. Shiina, Y. Sato, K. Nakai, T. Ohkubo, I. Tsuji, and K. Hiramori. Predictors of sinus rhythm restoration after Cox maze procedure concomitant with other cardiac operations. *Ann Thorac Surg*, 64(2):394–398, Aug 1997.

[25] I. Nault, N. Lellouche, S. Matsuo, S. Knecht, M. Wright, K. Lim, F. Sacher, P. Platonov, A. Deplagne, P. Bordachar, N. Derval, M. D. O'Neill, G. J. Klein, M. Hocini, P. Jaïs, J. Clémenty, and M. Haïssaguerre. Clinical value of fibrillatory wave amplitude on surface ECG in patients with persistent atrial fibrillation. *J Interv Card Electrophysiol*, 26(1):11–19, Oct 2009.

[26] J. Slocum, A. Sahakian, and S. Swiryn. Diagnosis of atrial fibrillation from surface electrocardiograms based on computer-detected atrial activity. *J Electrocardiol*, 25(1):1–8, Jan 1992.

[27] M. Holm, S. Pehrson, M. Ingemansson, L. Sörnmo, R. Johansson, L. Sandhall, M. Sunemark, B. Smideberg, C. Olsson, and S. B. Olsson. Non-invasive assessment of the atrial cycle length during atrial fibrillation in man: introducing, validating and illustrating a new ECG method. *Cardiovasc Res*, 38(1):69–81, Apr 1998.

[28] F. Chiarugi, M. Varanini, F. Cantini, F. Conforti, and G. Vrouchos. Noninvasive ECG as a tool for predicting termination of paroxysmal atrial fibrillation. *IEEE Trans Biomed Eng*, 54(8):1399–1406, Aug 2007.

[29] R. Alcaraz and J. J. Rieta. A review on sample entropy applications for the non-invasive analysis of atrial fibrillation electrocardiograms. *Biomedical Signal Processing and Control*, 5(1):1 – 14, 2010.

[30] A. Bollmann, D. Husser, M. Stridh, L. Sörnmo, M. Majic, H. U. Klein, and S. B. Olsson. Frequency measures obtained from the surface electrocardiogram in atrial fibrillation research and clinical decision-making. *J Cardiovasc Electrophysiol*, 14(10 Suppl):S154–S161, Oct 2003.

[31] H. J. Sih, D. P. Zipes, E. J. Berbari, and J. E. Olgin. A high-temporal resolution algorithm for quantifying organization during atrial fibrillation. *IEEE Trans Biomed Eng*, 46(4):440–450, Apr 1999.

[32] A. M. Gillis, A. D. Krahn, A. C. Skanes, and S. Nattel. Management of atrial fibrillation in the year 2033: new concepts, tools, and applications leading to personalized medicine. *Can J Cardiol*, 29(10):1141–1146, Oct 2013.

[33] U. R. Acharya, S. M. Krishnan, J. A. E. Spaan, and J. S. Suri. *Advances in Cardiac Signal Processing*. Springer, 2007.

[34] P.A. Iaizzo. *Handbook of Cardiac Anatomy, Physiology, and Devices*. Current clinical oncology. Humana Press, 2009.

[35] R. Klabunde. *Cardiovascular Physiology Concepts*. M - Medicine Series. Wolters Kluwer Health, 2011.

[36] J. Malmivuo and R. Plonsey. *Bioelectromagnetism: Principles and Applications of Bioelectric and Biomagnetic Fields*. Oxford University Press, USA, 1 edition, July 1995.

[37] A. M. Katz. *Physiology of the heart*. Lippincott Williams & Wilkins, Philadelphia, 4th ed edition, 2006.

[38] B. R. Wilcox, A. C. Cook, and R. H. Anderson. *Surgical anatomy of the heart*. Cambridge University Press, Cambridge, UK, 3rd ed edition, 2004.

[39] R. Plonsey and R.C. Barr. *Bioelectricity: A Quantitative Approach. Third Ed.* Springer, 2007.

[40] Robert Paine. *Generation and interpretation of the electrocardiogram*. Lea & Febiger, Philadelphia, 1988.

[41] D. B. Geselowitz. On the theory of the electrocardiogram. *Proceedings of the IEEE*, 77(6):857–876, 1989.

[42] J. Thomas. *The electrocardiogram and clinical correlations*. AMEC Sunday School Union/Legacy Pub., Nashville, TN, 1995.

[43] V. Fuster, L. E. Rydén, D. S. Cannom, H. J. Crijns, A. B. Curtis, K. A. Ellenbogen, J. L. Halperin, G. N. Kay, J. Y. Le Huezey, J. E. Lowe, S. B. Olsson, E. N. Prystowsky, J. L. Tamargo, and L. S. Wann. 2011 ACCF/AHA/HRS focused updates incorporated into the ACC/AHA/ESC 2006 Guidelines for the management of patients with atrial fibrillation: a report of the American College of Cardiology Foundation/American Heart Association Task Force on Practice Guidelines developed in partnership with the European Society of Cardiology and in collaboration with the European Heart Rhythm Association and the Heart Rhythm Society. *J Am Coll Cardiol*, 57(11):e101–e198, Mar 2011.

[44] P. A. Wolf, R. D. Abbott, and W. B. Kannel. Atrial fibrillation as an independent risk factor for stroke: The Framingham Study. *Stroke*, 22(8):983–988, Aug 1991.

[45] W. B. Kannel, R. D. Abbott, D. D. Savage, and P. M. McNamara. Epidemiologic features of chronic atrial fibrillation: The Framingham Study. *N Engl J Med*, 306(17):1018–1022, Apr 1982.

[46] C. D. Furberg, B. M. Psaty, T. A. Manolio, J. M. Gardin, V. E. Smith, and P. M. Rautaharju. Prevalence of atrial fibrillation in elderly subjects (The Cardiovascular Health Study). *Am J Cardiol*, 74(3):236–241, Aug 1994.

[47] E. J. Benjamin, P. A. Wolf, R. B. D'Agostino, H. Silbershatz, W. B. Kannel, and D. Levy. Impact of atrial fibrillation on the risk of death: the framingham heart study. *Circulation*, 98(10):946–952, Sep 1998.

[48] A. S. Go, D. Mozaffarian, V. L. Roger, E. J. Benjamin, J. D. Berry, W. B. Borden, D. M. Bravata, S. Dai, American Heart Association Statistics Committee, and Stroke Statistics Subcommittee. Heart disease and stroke statistics–2013 update: a report from the american heart association. *Circulation*, 127(1):e6–e245, Jan 2013.

[49] S. L. Kopecky, B. J. Gersh, M. D. McGoon, J. P. Whisnant, D. R. Holmes, D. M. Ilstrup, and R. L. Frye. The natural history of lone atrial fibrillation. a population-based study over three decades. *N Engl J Med*, 317(11):669–674, Sep 1987.

[50] C. F. Tsai, C. T. Tai, M. H. Hsieh, W. S. Lin, W. C. Yu, K. C. Ueng, Y. A. Ding, M. S. Chang, and S. A. Chen. Initiation of atrial fibrillation by ectopic beats originating from the superior vena cava: electrophysiological characteristics and results of radiofrequency ablation. *Circulation*, 102(1):67–74, Jul 2000.

[51] P. Jaïs, M. Haïssaguerre, D. C. Shah, S. Chouairi, L. Gencel, M. Hocini, and J. Clémenty. A focal source of atrial fibrillation treated by discrete radiofrequency ablation. *Circulation*, 95(3):572–576, Feb 1997.

[52] R. Peinado, J. L. Merino, J. A. Gómez, and J. A. Sobrino. Focal auricular fibrillation: catheter ablation with radiofrequency. *Rev Esp Cardiol*, 51(6):494–497, Jun 1998.

[53] G. K. Moe. On multiple wavelet hypothesis of atrial fibrillation. *Archives Internationales de Pharmacodynamie et de Therapie*, 140:1–2, 1962.

[54] S. Lévy. Epidemiology and classification of atrial fibrillation. *J Cardiovasc Electrophysiol*, 9(8 Suppl):S78–S82, Aug 1998.

[55] J. M. Miller, R. C. Kowal, V. Swarup, J. P. Daubert, E. G. Daoud, J. D. Day, K. A. Ellenbogen, and J. D. Hummel. Initial independent outcomes from focal impulse and rotor modulation ablation for atrial fibrillation: Multicenter firm registry.

[56] J. Jalife, O. Berenfeld, and M. Mansour. Mother rotors and fibrillatory conduction: a mechanism of atrial fibrillation. *Cardiovascular Research*, 54(2):204, 2002.

[57] S. V. Pandit and J. Jalife. Rotors and the dynamics of cardiac fibrillation. *Circulation Research*, 112(5):849–862, 2013.

[58] G. G. Lalani, R. Trikha, D. E. Krummen, and S. M. Narayan. Rotors and focal sources for human atrial fibrillation. *Circulation Journal*, 78(10):2357–2366, 2014.

[59] D. E. Krummen, V. Swarup, and S. M. Narayan. The role of rotors in atrial fibrillation. *Journal of Thoracic Disease*, 7(2), 2015.

[60] U. Schotten, D. Dobrev, P. G. Platonov, H. Kottkamp, and G. Hindricks. Current controversies in determining the main mechanisms of atrial fibrillation. *Journal of Internal Medicine*, 279(5):428–438, 2016.

[61] C. R Barbhayia, S. Kumar, and G. F. Michaud. Mapping atrial fibrillation: 2015 update.

[62] S. Verheule, J. Eckstein, D. Linz, B. Maesen, E. Bidar, A. Gharaviri, and U. Schotten. Role of endo-epicardial dissociation of electrical activity and transmural conduction in the development of persistent atrial fibrillation. *Progress in Biophysics and Molecular Biology*, 115(2):173 – 185, 2014. Novel Technologies as Drivers of Progress in Cardiac Biophysics.

[63] J. Eckstein, S. Zeemering, D. Linz, B. Maesen, S. Verheule, A. van Hunnik, H. Crijns, M. A. Allessie, and Ul. Schotten. Transmural conduction is the predominant mechanism of breakthrough during atrial fibrillationclinical perspective. *Circulation: Arrhythmia and Electrophysiology*, 6(2):334–341, 2013.

[64] S. Verheule, E. Tuyls, A. Gharaviri, S. Hulsmans, A. van Hunnik, M. Kuiper, J. Serroyen, S. Zeemering, N. H.L. Kuijpers, and U. Schotten. Loss of continuity in the thin epicardial layer because of endomysial fibrosis increases the complexity of atrial fibrillatory conductionclinical perspective. *Circulation: Arrhythmia and Electrophysiology*, 6(1):202–211, 2013.

[65] E. N. Prystowsky. The history of atrial fibrillation: the last 100 years. *J Cardiovasc Electrophysiol*, 19(6):575–582, Jun 2008.

[66] A. Bollmann, D. Husser, L. Mainardi, F. Lombardi, P. Langley, A. Murray, J. J. Rieta, J. Millet, S. B. Olsson, M. Stridh, and L. Sörnmo. Analysis of surface electrocardiograms in atrial fibrillation: Techniques, research, and clinical applications. *Europace*, 8(11):911–926, Nov 2006.

[67] L. Sörnmo, M. Stridh, D. Husser, A. Bollmann, and S. B. Olsson. Analysis of atrial fibrillation: from electrocardiogram signal processing to clinical management. *Philos Trans A Math Phys Eng Sci*, 367(1887):235–253, Jan 2009.

[68] Tong Liu, editor. *Atrial Fibrillation - Mechanisms and Treatment*. InTech, February 2013.

[69] S. J. Melby, A. Zierer, M. S. Bailey, J. L. Cox, J. S. Lawton, N. Munfakh, T. D .Crabtree, N. Moazami, C. B. Huddleston, M. R. Moon, and R. J. Damiano. A new era in the surgical treatment of atrial fibrillation: the impact of ablation technology and lesion set on procedural efficacy. *Ann Surg*, 244(4):583–592, Oct 2006.

[70] J. L. Cox. The surgical treatment of atrial fibrillation. IV. Surgical technique. *J Thorac Cardiovasc Surg*, 101(4):584–592, Apr 1991.

[71] J. L. Cox, J. P. Boineau, R. B. Schuessler, R. D. Jaquiss, and D. G. Lappas. Modification of the Maze procedure for atrial flutter and atrial fibrillation. I. Rationale and surgical results. *J Thorac Cardiovasc Surg*, 110(2):473–484, Aug 1995.

[72] S. L. Gaynor, M. D. Diodato, S. M. Prasad, Y. Ishii, R. B. Schuessler, M. S. Bailey, N. R. Damiano, J. B. Bloch, M. R. Moon, and R. J. Damiano. A prospective, single-center clinical trial of a modified Cox-Maze procedure with bipolar radiofrequency ablation. *J Thorac Cardiovasc Surg*, 128(4):535–542, Oct 2004.

[73] R. J. Damiano and M. Bailey. The Cox-Maze IV procedure for lone atrial fibrillation. *Multimed Man Cardiothorac Surg*, 2007(723):mmcts.2007.002758, Jan 2007.

[74] A. T. Kawaguchi, Y. Kosakai, Y. Sasako, K. Eishi, K. Nakano, and Y. Kawashima. Risks and benefits of combined maze procedure for atrial fibrillation associated with organic heart disease. *J Am Coll Cardiol*, 28(4):985–990, Oct 1996.

[75] L. C. Maroto, M. Carnero, J. A. Silva, J. Cobiella, N. Pérez-Castellano, F. Reguillo, J. Pérez-Villacastín, and J. E. Rodríguez. Early recurrence is a predictor of late failure in surgical ablation of atrial fibrillation. *Interact Cardiovasc Thorac Surg*, 12(5):681–686, May 2011.

[76] L. Sörnmo and P. Laguna. *Bioelectrical Signal Processing in Cardiac and Neurological Applications*. Elsevier Academic Press, June 2005.

[77] S. Luo and P. Johnston. A review of electrocardiogram filtering. *J Electrocardiol*, 43(6):486–496, 2010.

[78] J. C. Huhta and J.G. Webster. 60-hz interference in electrocardiography. *Biomedical Engineering, IEEE Transactions on*, BME-20(2):91–101, 1973.

[79] S. M. M. Martens, M. Mischi, S. G. Oei, and J. W. M. Bergmans. An improved adaptive power line interference canceller for electrocardiography. *IEEE Trans Biomed Eng*, 53(11):2220–2231, Nov 2006.

[80] E. Erçelebi. Electrocardiogram signals de-noising using lifting-based discrete wavelet transform. *Comput Biol Med*, 34(6):479–493, Sep 2004.

[81] H. Yang, S. T. Bukkapatnam, and R. Komanduri. Nonlinear adaptive wavelet analysis of electrocardiogram signals. *Phys Rev E Stat Nonlin Soft Matter Phys*, 76(2 Pt 2):026214, Aug 2007.

[82] B. N. Singh and A. K. Tiwari. Optimal selection of wavelet basis function applied to ECG signal denoising. *Digital Signal Processing*, 16(3):275–287, May 2006.

[83] J. M. Leski and N. Henzel. EcG baseline wander and powerline interference reduction using nonlinear filter bank. *Signal Processing*, 85(4):781–793, April 2005.

[84] I. Dotsinsky and T. Stoyanov. Optimization of bi-directional digital filtering for drift suppression in electrocardiogram signals. *J Med Eng Technol*, 28(4):178–180, 2004.

[85] L. Mainardi, L. Sörnmo, and S. Cerutti. Understanding Atrial Fibrillation: The Signal Processing Contribution, Part I. *Synthesis Lectures on Biomedical Engineering*, 3(1):1–129, 2008.

[86] R. Alcaraz and J. J. Rieta. Adaptive singular value cancelation of ventricular activity in single-lead atrial fibrillation electrocardiograms. *Physiol Meas*, 29(12):1351–1369, Dec 2008.

[87] P. Langley, J. J. Rieta, M. Stridh, J. Millet, L. Sörnmo, and A. Murray. Comparison of atrial signal extraction algorithms in 12-lead ECGs with atrial fibrillation. *IEEE Trans Biomed Eng*, 53(2):343–346, Feb 2006.

[88] J. J. Rieta, F. Castells, C. Sánchez, V. Zarzoso, and J. Millet. Atrial activity extraction for atrial fibrillation analysis using blind source separation. *IEEE Trans Biomed Eng*, 51(7):1176–1186, Jul 2004.

[89] M. Stridh and L. Sörnmo. Spatiotemporal qrst cancellation techniques for analysis of atrial fibrillation. *IEEE Trans Biomed Eng*, 48(1):105–111, Jan 2001.

[90] J. Slocum, E. Byrom, L. McCarthy, A. Sahakian, and S. Swiryn. Computer detection of atrioventricular dissociation from surface electrocardiograms during wide qrs complex tachycardias. *Circulation*, 72(5):1028–1036, Nov 1985.

[91] S. Shkurovich, A. V. Sahakian, and S. Swiryn. Detection of atrial activity from high-voltage leads of implantable ventricular defibrillators using a cancellation technique. *IEEE Trans Biomed Eng*, 45(2):229–234, Feb 1998.

[92] J. Pan and W. J. Tompkins. A real-time qrs detection algorithm. *IEEE Trans Biomed Eng*, 32(3):230–236, Mar 1985.

[93] M. Stridh, L. Sörnmo, C. J. Meurling, and S. B. Olsson. Characterization of atrial fibrillation using the surface ECG: Time-dependent spectral properties. *IEEE Trans Biomed Eng*, 48(1):19–27, Jan 2001.

[94] Z. Lu, B. J. Scherlag, J. Lin, G. Niu, K. A. Fung, L. Zhao, M. Ghias, W. M. Jackman, R. Lazzara, H. Jiang, and S. S. Po. Atrial fibrillation begets atrial fibrillation: autonomic mechanism for atrial electrical remodeling induced by short-term rapid atrial pacing. *Circ Arrhythm Electrophysiol*, 1(3):184–192, Aug 2008.

[95] S. Kumar, A. W. Teh, C. Medi, P. M. Kistler, J. B. Morton, and J. M. Kalman. Atrial remodeling in varying clinical substrates within beating human hearts: relevance to atrial fibrillation. *Prog Biophys Mol Biol*, 110(2-3):278–294, 2012.

[96] M. C. Wijffels, C. J. Kirchhof, R. Dorland, J. Power, and M. A. Allessie. Electrical remodeling due to atrial fibrillation in chronically instrumented conscious goats: roles of neurohumoral changes, ischemia, atrial stretch, and high rate of electrical activation. *Circulation*, 96(10):3710–3720, Nov 1997.

[97] M. J. Davies and A. Pomerance. Pathology of atrial fibrillation in man. *Br Heart J*, 34(5):520–525, May 1972.

[98] C. A. Morillo, G. J. Klein, D. L. Jones, and C. M. Guiraudon. Chronic rapid atrial pacing. structural, functional, and electrophysiological characteristics of a new model of sustained atrial fibrillation. *Circulation*, 91(5):1588–1595, Mar 1995.

[99] M. Chen, J. Chang, H. Chang, C. Chen, C. Yang, Y. Chen, and M. Fu. Clinical determinants of sinus conversion by radiofrequency maze procedure for persistent atrial fibrillation in patients undergoing concomitant mitral valvular surgery. *Am J Cardiol*, 96(11):1553–1557, Dec 2005.

[100] F. Solti, T. Vecsey, V. Kékesi, and A. Juhász-Nagy. The effect of atrial dilatation on the genesis of atrial arrhythmias. *Cardiovasc Res*, 23(10):882–886, Oct 1989.

[101] F. Ravelli and M. Allessie. Effects of atrial dilatation on refractory period and vulnerability to atrial fibrillation in the isolated langendorff-perfused rabbit heart. *Circulation*, 96(5):1686–1695, Sep 1997.

[102] I. C. Van Gelder, H. J. Crijns, W. H. Van Gilst, H. P. Hamer, and K. I. Lie. Decrease of right and left atrial sizes after direct-current electrical cardioversion in chronic atrial fibrillation. *Am J Cardiol*, 67(1):93–95, Jan 1991.

[103] A. T. Gosselink, H. J. Crijns, H. P. Hamer, H. Hillege, and K. I. Lie. Changes in left and right atrial size after cardioversion of atrial fibrillation: role of mitral valve disease. *J Am Coll Cardiol*, 22(6):1666–1672, Nov 1993.

[104] A. Elvan, A. Adiyaman, R. J. Beukema, H. T. Sie, and M. A. Allessie. Electrophysiological effects of acute atrial stretch on persistent atrial fibrillation in patients undergoing open heart surgery. *Heart Rhythm*, 10(3):322–330, Mar 2013.

[105] S. Nattel, B. Burstein, and D. Dobrev. Atrial remodeling and atrial fibrillation: mechanisms and implications. *Circ Arrhythm Electrophysiol*, 1(1):62–73, Apr 2008.

[106] M. A. Romano, D. S. Bach, F. D. Pagani, R. L. Prager, G. M. Deeb, and S. F. Bolling. Atrial reduction plasty Cox-Maze procedure: extended indications for atrial fibrillation surgery. *Ann Thorac Surg*, 77(4):1282–7; discussion 1287, Apr 2004.

[107] W. L. Henry, J. Morganroth, A. S. Pearlman, C. E. Clark, D. R. Redwood, S. B. Itscoitz, and S. E. Epstein. Relation between echocardiographically determined left atrial size and atrial fibrillation. *Circulation*, 53(2):273–279, Feb 1976.

[108] K. C. Kim, K. R. Cho, Y. Kim, D. Sohn, and K. Kim. Long-term results of the Cox-Maze III procedure for persistent atrial fibrillation associated with rheumatic mitral valve disease: 10-year experience. *Eur J Cardiothorac Surg*, 31(2):261–266, Feb 2007.

[109] M. S. Spach and P. C. Dolber. Relating extracellular potentials and their derivatives to anisotropic propagation at a microscopic level in human cardiac muscle. evidence for electrical uncoupling of side-to-side fiber connections with increasing age. *Circ Res*, 58(3):356–371, Mar 1986.

[110] P. M. Kistler, P. Sanders, S. P. Fynn, I. H. Stevenson, S. J. Spence, J. K. Vohra, P. B. Sparks, and J. M. Kalman. Electrophysiologic and electroanatomic changes in the human atrium associated with age. *J Am Coll Cardiol*, 44(1):109–116, Jul 2004.

[111] E. P. Anyukhovsky, E. A. Sosunov, P. C., T. S. Rosen, P. A. Boyden, P. Danilo, and M. R. Rosen. Age-associated changes in electrophysiologic remodeling: a potential contributor to initiation of atrial fibrillation. *Cardiovasc Res*, 66(2):353–363, May 2005.

[112] T. J. Wang, H. Parise, D. Levy, R. B. D'Agostino, P. A. Wolf, R. S. Vasan, and E. J. Benjamin. Obesity and the risk of new-onset atrial fibrillation. *JAMA*, 292(20):2471–2477, Nov 2004.

[113] N. Wanahita, F. H. Messerli, S. Bangalore, A. S. Gami, V. K. Somers, and J. S. Steinberg. Atrial fibrillation and obesity–results of a meta-analysis. *Am Heart J*, 155(2):310–315, Feb 2008.

[114] T. S. M. Tsang, M. E. Barnes, Y. Miyasaka, S. S. Cha, K. R. Bailey, G. C. Verzosa, J. B. Seward, and B. J. Gersh. Obesity as a risk factor for the progression of paroxysmal to permanent atrial fibrillation: a longitudinal cohort study of 21 years. *Eur Heart J*, 29(18):2227–2233, Sep 2008.

[115] A. O. Badheka, A. Rathod, M. A. Kizilbash, N. Garg, T. Mohamad, L. Afonso, and S. Jacob. Influence of obesity on outcomes in atrial fibrillation: yet another obesity paradox. *Am J Med*, 123(7):646–651, Jul 2010.

[116] A. Ardestani, H. J. Hoffman, and H. A. Cooper. Obesity and outcomes among patients with established atrial fibrillation. *Am J Cardiol*, 106(3):369–373, Aug 2010.

[117] P. M. Kistler, P. Sanders, J. B. Morton, J. K. Vohra, J. M. Kalman, and P. B. Sparks. Effect of body mass index on defibrillation thresholds for internal cardioversion in patients with atrial fibrillation. *Am J Cardiol*, 94(3):370–372, Aug 2004.

[118] M. Guglin, K. Maradia, R. Chen, and A. B. Curtis. Relation of obesity to recurrence rate and burden of atrial fibrillation. *Am J Cardiol*, 107(4):579–582, Feb 2011.

[119] L. Cai, Y. Yin, Z. Ling, L. Su, Z. Liu, J. Wu, H. Du, X. Lan, J. Fan, W. Chen, Y. Xu, P. Zhou, J. Zhu, and B. Zrenner. Predictors of late recurrence of atrial fibrillation after catheter ablation. *Int J Cardiol*, 164(1):82–87, Mar 2013.

[120] L. Guijian, Y. Jinchuan, D. Rongzeng, Q. Jun, W. Jun, and Z. Wenqing. Impact of body mass index on atrial fibrillation recurrence: a meta-analysis of observational studies. *Pacing Clin Electrophysiol*, 36(6):748–756, Jun 2013.

[121] K. Jongnarangsin, A. Chugh, E. Good, S. Mukerji, S. Dey, T. Crawford, J. F. Sarrazin, M. Kuhne, N. Chalfoun, D. Wells, W. Boonyapisit, F. Pelosi, F. Bogun, F. Morady, and H. Oral. Body mass index, obstructive sleep apnea, and outcomes of catheter ablation of atrial fibrillation. *J Cardiovasc Electrophysiol*, 19(7):668–672, Jul 2008.

[122] Y. M. Cha, P. A. Friedman, S. J. Asirvatham, W. K. Shen, T. M. Munger, R. F. Rea, P. A. Brady, A. Jahangir, K. H. Monahan, D. O. Hodge, R. A. Meverden, B. J. Gersh, S. C. Hammill, and D. L. Packer. Catheter ablation for atrial fibrillation in patients with obesity. *Circulation*, 117(20):2583–2590, May 2008.

[123] K. P. Letsas, C. H. Sikl'ody, P. Korantzopoulos, R. Weber, G. Bürkle, C. C. Mihas, D. Kalusche, and T. Arentz. The impact of body mass index on the efficacy and safety of catheter ablation of atrial fibrillation. *Int J Cardiol*, 164(1):94–98, Mar 2013.

[124] J. S. Richman and J. R. Moorman. Physiological time-series analysis using approximate entropy and sample entropy. *Am J Physiol Heart Circ Physiol*, 278(6):H2039–H2049, Jun 2000.

[125] H. Nakajima, J. Kobayashi, K. Bando, Y. Yasumura, S. Nakatani, K. Kimura, K. Niwaya, O. Tagusari, and S. Kitamura. Consequence of atrial fibrillation and the risk of embolism after percutaneous mitral commissurotomy: the necessity of the maze procedure. *Ann Thorac Surg*, 78(3):800–5; discussion 805–6, Sep 2004.

[126] T. H. Everett, L. C. Kok, R. H. Vaughn, J. R. Moorman, and D. E. Haines. Frequency domain algorithm for quantifying atrial fibrillation organization to increase defibrillation efficacy. *IEEE Trans Biomed Eng*, 48(9):969–978, Sep 2001.

[127] A. Bollmann, K. Sonne, H. D. Esperer, I. Toepffer, J. J. Langberg, and H. U. Klein. Non-invasive assessment of fibrillatory activity in patients with paroxysmal and persistent atrial fibrillation using the holter ecg. *Cardiovasc Res*, 44(1):60–66, Oct 1999.

[128] V. D.A. Corino, R. Sassi, L. T. Mainardi, and S. Cerutti. Signal processing methods for information enhancement in atrial fibrillation: Spectral analysis and non-linear parameters. *Biomedical Signal Processing and Control*, 1(4):271 – 281, 2006.

[129] Y. Asano, J. Saito, K. Matsumoto, K. Kaneko, T. Yamamoto, and M. Uchida. On the mechanism of termination and perpetuation of atrial fibrillation. *Am J Cardiol*, 69(12):1033–1038, Apr 1992.

[130] A. Capucci, M. Biffi, G. Boriani, F. Ravelli, G. Nollo, P. Sabbatani, C. Orsi, and B. Magnani. Dynamic electrophysiological behavior of human atria during paroxysmal atrial fibrillation. *Circulation*, 92(5):1193–1202, Sep 1995.

[131] A. Bollmann, N. K. Kanuru, K. K. McTeague, P. F. Walter, D. B. DeLurgio, and J. J. Langberg. Frequency analysis of human atrial fibrillation using the surface electrocardiogram and its response to ibutilide. *Am J Cardiol*, 81(12):1439–1445, Jun 1998.

[132] D. Husser, M. Stridh, D. S. Cannom, A. K. Bhandari, M. J. Girsky, S. Kang, L. Sörnmo, S. B. Olsson, and A. Bollmann. Validation and clinical application of time-frequency analysis of atrial fibrillation electrocardiograms. *J Cardiovasc Electrophysiol*, 18(1):41–46, Jan 2007.

[133] R. Alcaraz and J. Rieta. Time and frequency recurrence analysis of persistent atrial fibrillation after electrical cardioversion. *Physiol Meas*, 30(5):479–489, May 2009.

[134] P. D. Welch. Use of Fast Fourier Transform for estimation of power spectra: A method based on time averaging over short modified periodograms. *IEEE Trans. Audio and Electroacustics*, 15(2):70–73, 1967.

[135] R. Alcaraz and J. Rieta. Non-invasive organization variation assessment in the onset and termination of paroxysmal atrial fibrillation. *Comput Methods Programs Biomed*, 93(2):148–154, Feb 2009.

[136] A. Bollmann. Quantification of electrical remodeling in human atrial fibrillation. *Cardiovasc Res*, 47(2):207–209, Aug 2000.

[137] R. Alcaraz, F. Hornero, and J. J. Rieta. Noninvasive time and frequency predictors of long-standing atrial fibrillation early recurrence after electrical cardioversion. *Pacing Clin Electrophysiol*, 34(10):1241–1250, Oct 2011.

[138] S. M. Pincus. Approximate entropy as a measure of system complexity. *Proc Natl Acad Sci U S A*, 88(6):2297–2301, Mar 1991.

[139] R. Alcaraz, D. Abásolo, R. Hornero, and J. J. Rieta. Optimal parameters study for sample entropy-based atrial fibrillation organization analysis. *Comput Methods Programs Biomed*, 99(1):124–132, Jul 2010.

[140] W. Chen, J. Zhuang, W. Yu, and Z. Wang. Measuring complexity using FuzzyEn, ApEn, and SampEn. *Med Eng Phys*, 31(1):61–68, Jan 2009.

[141] R. Alcaraz and J. J. Rieta. Sample entropy of the main atrial wave predicts spontaneous termination of paroxysmal atrial fibrillation. *Med Eng Phys*, 31(8):917–922, Oct 2009.

[142] L. R. Rabiner, J. H. McClellan, and T. W. Parks. FIR digital filter design techniques using weighted chebyshev approximation. *Proc. IEEE*, 63:595–610, 1975.

[143] J. Theiler, S. Eubank, A. Longtin, B. Galdrikian, and J. D. Farmer. Testing for nonlinearity in time series: The method of surrogate data. *Physica D*, 58:77–94, 1992.

[144] M. Palus and D. Hoyer. Detecting nonlinearity and phase synchronization with surrogate data. *IEEE Eng Med Biol Mag*, 17(6):40–45, 1998.

[145] T. Schreiber. Surrogate time series. *Physica D: Nonlinear Phenomena*, 142(3-4):346–382, August 2000.

[146] Q. Xi, A. V. Sahakian, T. G. Frohlich, J. Ng, and S. Swiryn. Relationship between pattern of occurrence of atrial fibrillation and surface electrocardiographic fibrillatory wave characteristics. *Heart Rhythm*, 1(6):656–663, Dec 2004.

[147] I. H. Witten and E. Frank. *Data Mining: Practical Machine Learning Tools and Techniques with Java Implementations (The Morgan Kaufmann Series in Data Management Systems)*. Morgan Kaufmann, 1st edition, October 1999.

[148] R. J. Lewis. *An Introduction to Classification and Regression Tree (CART) Analysis*. 2000.

[149] D. Coppersmith, S. Hong, and J. R. M. Hosking. Partitioning nominal attributes in decision trees. *Data Mining and Knowledge Discovery*, 3(2):197–217, 1999.

[150] L. Breiman, J. Friedman, C. J. Stone, and R. A. Olshen. *Classification and Regression Trees*. Chapman & Hall/CRC, 1984.

[151] J. R. Quinlan. Improved use of continuous attributes in c4.5. *Journal of Artificial Intelligence Research*, 4:77–90, 1996.

[152] A. J. Dobson. *An Introduction to Generalized Linear Models*. Chapman and Hall/CRC, second edition, 2002.

[153] C. M. Bishop. *Pattern Recognition and Machine Learning*. Springer-Verlag New York, Inc., Secaucus, NJ, USA, 2006.

[154] D. W. Hosmer and S. Lemeshow. *Applied logistic regression (Wiley Series in probability and statistics)*. Wiley-Interscience Publication, 2 edition, September 2000.

[155] In J. Myung. Tutorial on maximum likelihood estimation. *Journal of Mathematical Psychology*, 47(1):90–100, February 2003.

[156] C.B. Boyer and U.C. Merzbach. *A history of mathematics*. Wiley, 1991.

[157] W. Gould, J. Pitblado, W. Sribney, and Stata Corporation. *Maximum Likelihood Estimation with Stata, Third Edition*. Taylor & Francis, 2006.

[158] L. Faes, G. Nollo, R. Antolini, F. Gaita, and F. Ravelli. A method for quantifying atrial fibrillation organization based on wave-morphology similarity. *IEEE Trans Biomed Eng*, 49(12 Pt 2):1504–1513, Dec 2002.

[159] J. L. Cox, T. E. Canavan, R. B. Schuessler, M. E. Cain, B. D. Lindsay, C. Stone, P. K. Smith, P. B. Corr, and J. P. Boineau. The surgical treatment of atrial fibrillation. ii. intraoperative electrophysiologic mapping and description of the electrophysiologic basis of atrial flutter and atrial fibrillation. *J Thorac Cardiovasc Surg*, 101(3):406–426, Mar 1991.

[160] R. Alcaraz, F. Sandberg, L. S´ornmo, and J. J. Rieta. Classification of paroxysmal and persistent atrial fibrillation in ambulatory ECG recordings. *IEEE Transactions on Biomedical Engineering*, 58(5):1441–1449, May 2011.

[161] R. Alcaraz and J. J. Rieta. The application of nonlinear metrics to assess organization differences in short recordings of paroxysmal and persistent atrial fibrillation. *Physiol Meas*, 31(1):115–130, Jan 2010.

[162] M. J. Janse. Why does atrial fibrillation occur? *Eur Heart J*, 18 Suppl C:C12–C18, May 1997.

[163] E. M. Balk, A. C. Garlitski, A. A. Alsheikh-Ali, T. Terasawa, M. Chung, and S. IP. Predictors of atrial fibrillation recurrence after radiofrequency catheter ablation: A systematic review. *Journal of Cardiovascular Electrophysiology*, 21(11):1208–1216, 2010.

[164] P. Osmancik, P. Budera, Z. Straka, and P. Widimsky. Predictors of complete arrhythmia free survival in patients undergoing surgical ablation for atrial fibrillation. PRAGUE-12 randomized study sub-analysis. *International journal of cardiology*, 172(2):419–422, March 2014.

[165] C. Loardi, F. Alamanni, F. Veglia, C. Galli, A. Parolari, and M. Zanobini. Modified Maze Procedure for Atrial Fibrillation as an Adjunct to Elective Cardiac Surgery: Predictors of Mid-Term Recurrence and Echocardiographic Follow-Up. *Texas Heart Institute Journal*, 42(4):341–347, August 2015.

[166] M. Meo, V. Zarzoso, O. Meste, D. G. Latcu, and N. Saoudi. Spatial variability of the 12-lead surface ecg as a tool for noninvasive prediction of catheter ablation outcome in persistent atrial fibrillation. *IEEE Trans Biomed Eng*, 60(1):20–27, Jan 2013.

List of Figures

List of Tables

List of Acronyms

AA	Atrial Activity
ABS	Average Beat Subtraction
AF	Atrial Fibrillation
ASVC	Adaptive Singular Value Cancellation
BMI	Body Mass Index
DAF	Dominant Atrial Frequency
ECG	Electrocardiogram
ECV	Electrocardioversion
f waves	Fibrillatory waves
FFT	Fast Fourier Transform
FIR	Finite impulse response
fWP	Fibrillatory Waves Power
HF	Heart failure
IIR	Infinite impulse response
LA	Left atrium
MAW	Main Atrial Wave
NSR	Normal sinus rhythm
PSD	Power spectral density
PV	Pulmonary vein
QRST	QRS complex and T wave
RA	Right atrium
ROC	Receiver Operative Characteristic
SampEn	Sample Entropy
SA	Sinoatrial
SCV	Superior vena cava
WCT	Wilson Central Terminal